SMC-TR-97-18

AEROSPACE REPORT NO.
TR-97(1410)-5

Ground Cloud Dispersion Measurements During The Titan IV Mission #K22 (12 May 1996) at Vandenberg Air Force Base

Volume 1—Test Overview and Data Summary

30 June 1997

Assembled by

Environmental Systems Directorate
Systems Engineering
Space Launch Operations

Prepared for

Launch Programs
SPACE AND MISSILE SYSTEMS CENTER
AIR FORCE MATERIEL COMMAND
2430 E. El Segundo Boulevard
Los Angeles Air Force Base, CA 90245

Space Systems Group

THE AEROSPACE CORPORATION
El Segundo, California

This report was submitted by The Aerospace Corporation, El Segundo, CA 90245-4691, under Contract No. F04701-93-C-0094 with the Space and Missile Systems Center, 2430 E. El Segundo Blvd., Los Angeles Air Force Base, CA 90245. It was reviewed and approved for The Aerospace Corporation by N. F. Dowling, Systems Director, Environmental Systems, Systems Engineering Directorate.*

This report has been reviewed by the Public Affairs Office (PAS) and is releasable to the National Technical Information Service (NTIS). At NTIS, it will be available to the general public, including foreign nationals.

This technical report has been reviewed and is approved for publication. Publication of this report does not constitute Air Force approval of the report's findings or conclusions. It is published only for the exchange and stimulation of ideas.

R. Reiner, Maj, USAF
SMC/CLN

REPORT DOCUMENTATION PAGE

Form Approved
OMB No. 0704-0188

1. AGENCY USE ONLY (*Leave blank*)	2. REPORT DATE	3. REPORT TYPE AND DATES COVERED
	30 June 1997	

4. TITLE AND SUBTITLE
Ground Cloud Dispersion Measurements During The Titan IV Mission #K22 (12 May 1996) at Vandenberg Air Force Base — Vol. 1 Test Overview and Data Summary

5. FUNDING NUMBERS
F04701-93-C-0094

6. AUTHOR(S)
Environmental Systems Directorate

7. PERFORMING ORGANIZATION NAME(S) AND ADDRESS(ES)
The Aerospace Corporation
Technology Operations
El Segundo, CA 90245-4691

8. PERFORMING ORGANIZATION REPORT NUMBER
TR-97(1410)-5

9. SPONSORING/MONITORING AGENCY NAME(S) AND ADDRESS(ES)
Space and Missile Systems Center
Air Force Materiel Command
2430 E. El Segundo Boulevard
Los Angeles Air Force Base, CA 90245

10. SPONSORING/MONITORING AGENCY REPORT NUMBER
SMC-TR-97-18

11. SUPPLEMENTARY NOTES

12a. DISTRIBUTION/AVAILABILITY STATEMENT
Approved for public release; distribution unlimited

12b. DISTRIBUTION CODE

13. ABSTRACT (*Maximum 200 words*)

Launch plume imagery, ground and aircraft HCl measurements and FTIR temperature measurements were accomplished during the launch of Titan IV Mission #K-22 at Vandenberg Air Force Base on 12 May 1996. These data will be used to improve the accuracy of the Rocket Exhaust Effluent Diffusion Model. The imagery from five sites (two IR and three visible) showed a cloud stabilization height of 702 m (66% higher than predicted), reached in 4–7 min (100% to 250% longer than predicted). The cloud trajectory of 340° was more southerly than the 330° predicted by REEDM, and the 6.8 m/s speed exceeds the predicted 3 m/s. Aircraft HCl measurements with the Geomet instrument were as high as 45 ppm, and ground dosimeters measured dosages as high as 389 ppm min. The FTIR spectroscopy at 2.9 mi from the cloud indicated much cooler temperatures than expected, and the cloud became optically thin within about two minutes. Thirty-seven minutes of calibrated data was obtained; however, extraction of true cloud temperatures will require sophisticated modeling of the radiance contributions from the atmosphere.

14. SUBJECT TERMS
Toxic launch cloud, Toxic hazard corridors, Atmospheric dispersion models, Launch cloud development and dispersion, Launch cloud imagery, HCl monitoring

15. NUMBER OF PAGES
96

16. PRICE CODE

17. SECURITY CLASSIFICATION OF REPORT	18. SECURITY CLASSIFICATION OF THIS PAGE	19. SECURITY CLASSIFICATION OF ABSTRACT	20. LIMITATION OF ABSTRACT
UNCLASSIFIED	UNCLASSIFIED	UNCLASSIFIED	

Preface

The Air Force Space and Missile Systems Center's Launch Programs Office (SMC/CL) is sponsoring the Atmospheric Dispersion Model Validation Program (MVP). This program is collecting launch cloud dispersion data that will be used to determine the accuracy of atmospheric dispersion models, such as REEDM, in predicting toxic hazard corridors at the launch ranges. This report presents launch cloud dispersion and meteorological measurements performed during the #K22 Titan IV launch at Vandenberg Air Force Base on 12 May 1996.

An MVP Integrated Product Team (IPT) led by Capt. Brian Laine (SMC/CLNM) is directing the MVP effort. Dr. Bart Lundblad of The Aerospace Corporation's Environmental Systems Directorate (ESD) is the MVP technical manager. This report was prepared by Mr. Norm Keegan (ESD) and Dr. Lundblad from materials contributed by personnel participating in the #K22 launch cloud dispersion measurements.

Visible and infrared imagery measurements and FTIR spectrometry measurements were made of the launch cloud by Dr. Robert Abernathy, Mr. Jeff Hall, Mr. Bob Klingberg, Mr. Tom Knudtson, Dr. George Scherer, Mr. Don Stone, and Mr. Jess Valero of The Aerospace Corporation's Environmental Monitoring and Technology Department (EMTD). Mr. Jim Kephart of Aerospace's Western Range Directorate coordinated camera site selection and logistical support. Ms. Foster digitized the imagery data for analysis by Dr. Abernathy. The description of the cloud imagery results was prepared by Dr. Abernathy. The FTIR spectrometry data was analyzed and reported by Mr. Jeff Hall.

The aircraft-based HCl measurement effort was managed by Mr. Marv Becker and Mr. Pete Mazur of SRS Technologies. The Piper Seminole sampling aircraft was owned and operated by the Florida Institute of Technology. The aircraft was outfitted with a Geomet HCl detector that was modified and calibrated for airborne sampling by Mr. Paul Yocom of the NASA Toxic Vapor Detection/Contamination Monitoring Laboratory. Ms. Jeanne Hawkins of the 45th Medical Group Bioenvironmental Engineering Services (45 AMDS/SGPB) was on-board the aircraft during the sampling measurements to monitor Geomet performance and cockpit contamination. The on-board data logger and GPS system was provided and installed by Mr. Shane Beard of NOAA's Environmental Research Laboratories. The raw aircraft sampling data was processed and analyzed by Dr. Abernathy.

The ground-level HCl measurement effort was managed by Lt. Col. Kent Stringham of the 30th Medical Group Bioenvironmental Engineering Services organization (30 AMDS/SGPB). The HCl dosimeters were provided by and later analyzed by the NASA Toxic Vapor Detection/Contamination Monitoring Laboratory.

The meteorological data displayed in this report was provided by Mr. Steve Sambol of the VAFB Weather Squadron (30WS/DOS). The REEDM launch cloud dispersion prediction was provided by Mr. Darryl Dargitz of the VAFB Range Safety Office (30 SW/SEY).

The #K22 mission was the seventh Titan IV launch for which usable launch cloud dispersion data was collected by MVP. The previous missions were #K7, #K23, #K19, #K21, #K15, and #K16. It was the fourth Titan IV launch to employ an aircraft to collect HCl dispersion data. The previous airborne sampling activities were following the #K23, #K15, and #K16 launches.

Contents

Figures

Tables

Executive Summary

This report presents plume imagery and aircraft– and ground-based hydrogen chloride (HCl) sampling data documenting the development and dispersion of the Titan IV #K22 launch ground cloud at Vandenberg Air Force Base (VAFB). The report also presents pertinent meteorological data taken from towers and rawinsonde balloons.

The imaging team successfully tracked the trajectory and time evolution of the vehicle's exhaust ground cloud for 32 min following launch using two infrared and three visible light camera systems. A twin-engine Piper Seminole aircraft, equipped with a Geomet total HCl analyzer, was used to measure HCl concentrations within and below the ground cloud as a function of time for approximately 100 min following launch. An FTIR spectrometer was used to measure the cloud's infrared spectrum. In addition, HCl dosimeters were deployed downwind of the launch pad to determine ground-level HCl dosages.

Meteorological data were collected to improve understanding of cloud dispersion and to use as input during model simulations and evaluations. Rawinsonde balloon data from shortly before launch and meteorological tower data from shortly before and after launch were collected and archived. These data and similar data on other Titan IV launches (past and future) will be used to determine the accuracy of atmospheric dispersion models such as the Rocket Exhaust Effluent Diffusion Model (REEDM) in predicting toxic hazard corridors (THCs) at the USAF Eastern and Western Ranges. These THCs assess the risk of exposing the public to HCl exhaust from solid rocket motors or hypergolic propellant vapors accidentally released during launch operations.

The #K22 launch occurred on 5 May 1996 at 2132 Zulu time. The sampling aircraft entered the ground cloud approximately 8 min after launch and made 44 passes through and below the cloud. Peak HCl concentrations from 2 to 42 ppm were measured during these passes.

Reduction of imagery data from the first 32 min following launch yielded the stabilization height, rise time, ground track, and speed of the ground cloud. Comparison to REEDM 7.07 predictions show that the imagery-derived stabilization height (702 m) is 66% higher than predicted by REEDM (424 m), and that the imagery-derived time to stabilization (4–7 min) is 100–250% longer than the REEDM-predicted stabilization time (2 min). The imagery-derived ground track of the cloud (340¡) is 10° more clockwise than predicted by REEDM (330°), and the imagery-derived velocity of the cloud (6.8 m/s) is 127% greater than predicted by REEDM (3 m/s). The imagery analysis suggests that an improved prediction of stabilization height by REEDM would result in improved predictions of cloud direction and speed.

Forty-seven HCl dosimeters were deployed along the projected cloud track at heights of five feet above ground. The dosimeters were arranged in four arcs to the south of the launch site, with the closest arc at a range of 700–1600 ft, and the farthest arc at a range of 10,500–13,500 ft from the launch site. Dosimeters in all four arcs showed exposure to HCl with peak doses ranging from 390 ppm-min in the closest arc to 5.4 ppm-min in the farthest arc.

1. Introduction

Launch vehicles that employ solid propellant rocket motors release exhaust ground clouds containing large quantities of hydrogen chloride (HCl) into the launch areas at Cape Canaveral Air Station (CCAS) and Vandenberg Air Force Base (VAFB). Large quantities of hazardous liquid fuels and oxidizers could also be released as a result of propellant transfer accidents or launch vehicle failures. The Air Force uses atmospheric dispersion models to predict the downwind diffusion and concentration of toxic launch clouds. There exists a strong need to collect launch cloud data that can be used to test and validate the performance of these dispersion models.

The Air Force range safety organizations at Patrick Air Force Base (45 SW/SE) and VAFB (30 SW/SE) are responsible for assuring that launches occur only when meteorological conditions will not expose nearby public areas to hazardous levels of launch exhausts and propellant vapors. Predictions of toxic hazard corridors that extend into public areas can lead to costly launch delays. The present use of non-validated models requires the use of conservative launch criteria. The development and validation of accurate atmospheric dispersion models are expected to increase launch opportunities and significantly reduce launch costs. The Space and Missile Systems Center's Launch Programs Office (SMC/CL) established the Atmospheric Dispersion Model Validation Program (MVP) to collect launch cloud data and to use the data to test and validate current and future atmospheric dispersion models at the ranges.

The MVP effort involves the collection of data during Titan IV launches at CCAS and VAFB to characterize HCl launch cloud rise, growth, and stabilization, as well as launch cloud transport and diffusion. These data, along with data collected during tracer gas releases, will be used to determine the capability of the Rocket Exhaust Effluent Diffusion Model (REEDM) for predicting toxic hazard corridors at the ranges. REEDM is used at CCAS and VAFB to predict the locations of toxic hazard corridors in support of launch operations. It is applied to large heated sources of toxic air emissions such as nominal launches, catastrophic failure fireballs, and inadvertent ignitions of solid rocket motors. It uses launch vehicle and meteorological data to generate ground-level concentration isopleths of HCl, hydrazine fuels, nitrogen dioxide, and other toxic launch emissions. Launch holds may occur when REEDM toxic concentration predictions exceed adopted exposure standards. REEDM is a unique and complex model based on relatively simple modeling physics. It has a long development history with the Air Force and NASA, but has never been fully validated. Validation of REEDM has been identified as a range safety priority.

The MVP has been organized and is being directed by the MVP Integrated Product Team (IPT). SMC/CL is serving as the IPT leader, while The Aerospace Corporation's Environmental Systems Directorate serves as the IPT technical manager. The IPT consists of personnel with expertise in atmospheric dispersion modeling, meteorology, and atmospheric dispersion field studies. MVP participants include personnel from SMC, 30 SW, 45 SW, Armstrong Laboratory, The Aerospace Corporation, NASA, NOAA, and contractors. Key functions include program planning, field data collection, data review and compilation, range coordination, and model validation.

This report presents the results of measurements performed at VAFB during the Titan IV #K22 launch on 5 May 1996. Visible and infrared measurements were made on the ground cloud to

monitor its growth, stabilization, and trajectory. An aircraft equipped with an HCl detector was flown through and below the visible cloud to measure HCl concentrations. An FTIR spectrometer was used to measure the infrared spectrum radiated by the ground cloud. Ground-level HCl doses were measured at selected locations downwind of the launch site. The imagery results are presented in Section 2, and the aircraft HCl sampling results are presented in Section 3. Section 4 summarizes FTIR spectrometer measurements, and Section 5 describes the ground-level HCl measurements. REEDM predictions of ground-cloud stabilization heights and surface concentrations are presented in Appendix A. Measurements of meteorological data are tabulated in Appendix B. A description of the cloud sampling aircraft is provided in Appendix C.

The imagery data obtained show that the T–0.25 hour REEDM 7.07 calculation underestimates cloud stabilization height (702 m vs. 424 m predicted), underestimates cloud stabilization time (4–7 min vs. 2 min predicted), and underestimates cloud speed (6.8 m/s vs. 3 m/s predicted). The imagery and HCl concentration results presented in this, as well as other MVP reports, will allow the accuracy of REEDM and other launch range atmospheric dispersion models to be determined over the range of possible meteorological conditions.

2. Imagery of the Titan IV #K22 Ground Cloud

[The material in this section was contributed by R. N. Abernathy, K. L. Foster, and B. P. Kasper of the Environmental Monitoring and Technology Department of The Aerospace Corporation's Space and Environment Technology Center.]

2.1 Background

The Aerospace Corporation has been deploying visible and/or infrared imaging systems to Titan IV launches since the #K10 Launch on 07 February 1994. These deployments include Titan IV missions #K02, #K07, #K09, #K10, #K13, #K14, #K15, #K16, #K19, #K21, #K22, and #K23. Typically, two-dimensional cloud images are recorded at each of two to three imaging sites and are combined in a pairwise fashion to produce stereoscopic 3-D information about the exhaust cloud. When atmospheric conditions were favorable and two (or more) imagery sites were manned (i.e., #K02, #K07, #K13, #K15, #K16, #K19, #K21, #K22, and #K23), the analysis of these data yields the ground cloud's rise time, stabilization height, dimensions, ground track, and ground speed. These imagery data and the resulting cloud characteristics are available to modelers as part of the model validation program (MVP).

For #K22, all three selected imagery sites yielded data useful for tracking the cloud. The analysis of the first 32 min of the imagery data yields the ground cloud's rise time, stabilization height, ground track, and speed. The raw infrared imagery data for the #K22 mission were recorded digitally using AGEMA Thermovision 900's. The raw visible imagery data were recorded by a VCR. A PC-based image-capture board allowed the digitization of selected images from the VCR tapes. Subsequently, all of the imagery data that were processed for this report were archived on magneto-optical disks as digital image files.

2.2 Introduction

On 12 May 1996, the Titan IV #K22 mission was successfully launched from VAFB SLC-4E at 1432 PDT (2132 GMT). This section describes the exhaust cloud imagery data collected by three imagery sites during the 37 min immediately following the launch. It also briefly describes the data acquisition hardware and analysis software. Analysis of the first 32 min of this imagery yields the stabilization time, the stabilization height, the ground track, and the speed of the ground cloud without recourse to additional data sources. Rudimentary knowledge of the rawinsonde wind data is needed for more quantitative interpretation of the imagery data reported in this section. The pre-launch rawinsonde data are documented in Appendix B and referenced in this section. REEDM predictions are documented in Appendix A and referenced in this section. An Aircraft sampled the HCl in the exhaust cloud, and that data is documented in section 3. A Fourier-Transform Infrared (FTIR) recorded the spectra of the exhaust cloud, and that data is documented in Section 4.

2.3 Field Deployment

2.3.1 Planning

The Aerospace Corporation's participants are listed in various subteams below (members of the imaging teams for #K22 are indicated with asterisks and paired with the imagery sites they supported):

Technology Operations
Space and Environment Technology Center
Environmental Monitoring and Technology Department

R. N. Abernathy*	J. T. Valero*	*(Block Wall)*
R. A. Klingberg*	J. T. Knudtson*	*(Tetra Tech)*
D. K. Stone* (Agema & Visible Imagers)		*(Bldg 900)*
G. J. Scherer*	J. L. Hall* (FTIR)	*(Bldg 900)*
K. L. Foster	B. P. Kasper	

Space Launch Operations
Systems Engineering Directorate
Environmental Systems
N. F. Dowling, Systems Director
H. L. Lundblad
Western Range
Systems Engineering Directorate
E. J. Tomei, Systems Director
J. F. Kephart

2.3.2 Equipment

The equipment at each site included all the hardware and software necessary to record and document the launch, to communicate between sites, and to supply backup power in case of a power outage. The Building 900 site used fixed power from the building, while both Tetra Tech and Block Wall Sites used gasoline-powered generators. The launch of #K22 marked the sixth opportunity to deploy the Titan IV-dedicated Visible and Infrared Imaging System (VIRIS) hardware.

The VIRIS consists of an array of four cloud tracking systems and was designed and fabricated at the request of Space Launch Operations, Systems Engineering Directorate, at The Aerospace Corporation. Three of the tracking systems include coaligned visible and infrared (IR) (8–12 μm) imagers, mounted on an azimuth- and elevation-encoding tripod, with an associated data acquisition and display console. The fourth tracking system does not include an infrared imager. The combination of visible and IR imagers permits cloud tracking in both daylight and darkness. The #K22 launch represented a daylight launch. The unique capabilities built into the VIRIS hardware include digital insertion of imager azimuth (Az) and elevation (El), GPS-derived time, and GPS-derived location into the VCR recording of the imagery. The system electronics are integrated in a single package, which has been ruggedized for field use. Pre-wiring of this package makes deployment of these imagery systems straightforward, usually requiring less than 45 min for instrumentation at a site to become fully operational. For the Titan IV #K22 mission, the operators at all sites set the FOVs of the IR and the visible imagers to their maximum values using

fixed FOV and adjustable FOV lenses, respectively. Table 1 summarizes the FOVs of the imagery sites for the #K22 launch.

The imaging systems deployed for the Titan IV #K22 mission were capable of total autonomy. At VAFB, the VIRIS's builtin GPS receivers did not receive differential correction broadcasts. Therefore, we rented a Sokkia differential GPS receiver to document each imager's position to a 2-m precision in the horizontal plane. Typically, 35 m is the precision in the horizontal plane for the VIRIS's differentially corrected data (i.e., for Cape Canaveral Air Station). Gasoline-powered AC generators (Honda Ex1000) are insurance against loss of fixed power and were used as the sole source of power at Tetra Tech and Block Wall Sites. The Stirling cooler option for the AGEMA 900 series IR imagers was chosen so that liquid nitrogen would not be required at the sites. Each unit was transported in a van.

The tripod's Az/El angle encoder for each imagery site was calibrated using reference objects (e.g., SLC-4E) within the field of view of the imagers. Typically, the position of the reference object is derived from the Department of Defense Geodetic Coordinates Database (WGS 1984 datum). Since the imagery sites used for the #K22 mission were surveyed using 2-m resolution differential GPS service, the accuracy (3 m standard error) of the reference object's location is a more significant term in determining the calibration accuracy. Imagery pixelation and operator error in edge detection contribute as well to the error in defining the cloud boundary. Step-size in the tripod angle encoders is a third and the most significant source of error. Therefore, the accuracy of the VIRIS system is usually determined by the availability of optimal references for Az/El calibration or by the encoder step size. A 0.07° accuracy applies to the Az/El calibrations used for the #K22 analysis and is equivalent to the encoder step size.

Table 2 documents the imagery site locations (based upon the 2-m precision GPS survey) and their angles to the SLC-4E pad (34.632039° N, 120.610629° W, 153 m MSL from June 1993 DOD Geodetic Coordinates Manual using WGS 1984 Datum).

Table 1. Field of View (FOV) for Imagery Sites during #K22 Mission

Imagery Site	Imager Type (Visible or IR)	FOV (horizontal) (deg)	FOV (vertical) (deg)
Block Wall	Visible CCD	31.74	24.14
Block Wall	AGEMA Infrared	40.528	20.536
Building 900	Visible CCD	31.74	24.14
Building 900	AGEMA Infrared	40.827	20.998
Tetra Tech	Visible CCD	31.62	24.14

Table 2. Imagery Site Positions and Angles to SLC-4E Pad.

Imagery Site	Latitude (deg)	Longitude (deg)	Altitude (MSL) (m)	AZ (SLC-4E) (deg)	EL (SLC-4E) (deg)
Block Wall	34.706202	-120.600496	5	186.41	1.02
Building 900	34.663684	-120.578843	114	219.57	0.48
Tetra Tech	34.692873	-120.537945	108	224.50	0.27

2.4 Processing of Imagery Data

The processing of the imagery data requires several transformations that are performed upon return to The Aerospace Corporation:

1. Digitizing frames of visible imagery from the VCR tapes.

2. Measuring the pixel locations of the reference sites within each image (i.e., FOV and angular calibration).

3. Measuring the pixel locations of exhaust cloud features in digitized images.

4. Converting pixel locations to azimuth and elevation readings.

5. Calculating cloud characteristics (i.e., position in Cartesian coordinates relative to the launch pad and MSL).

The processing requires the use of specialized hardware and software. Time, Az, and El are tabulated for each digitized image. Sets of digitized images exist for selected times following the launch. A setup file is created for each pair of images and contains all relevant information necessary to compute the cloud geometry from the imagery. The Aerospace program **PLMTRACK** is run to digitize the x, y, and z coordinates of cloud features.

PLMTRACK is a software program developed in the Environmental Monitoring and Technology Department (EMTD) of The Aerospace Corporation by Brian P. Kasper. It is designed to analyze pairs of cloud images synchronized in time. The operator selects the location of a particular cloud feature in the images from the two imagery sites by moving a screen pointer over the desired point in each image and clicking a mouse button. **PLMTRACK** then calculates the three-dimensional location of this point and writes the information to a data file.

Another implementation of **PLMTRACK** is the "box method," illustrated in Figure 1. The operator draws a rectangle about a cloud feature in the images from the two imagery sites by moving a screen pointer to the extreme corners of the rectangles and clicking a mouse button. **PLMTRACK** then calculates the closest approach for various rays, as illustrated in Figure 1 and described below. The top of the cloud is defined by rays determining T1 and T2 (i.e., T1 $\times$ T2); the bottom is determined by rays defining B1 and B2 (i.e., B1 $\times$ B2); and the middle is defined by the geometric mean of top and bottom (i.e., M1 $\times$ M2). To define the "faces" of the polygon surrounding the cloud, the points of closest approach for ray M1 with L2 and R2 (the left and right tangents to the cloud from Imager 2) are defined (i.e., M1 $\times$ L2 and M1 $\times$ R2). A

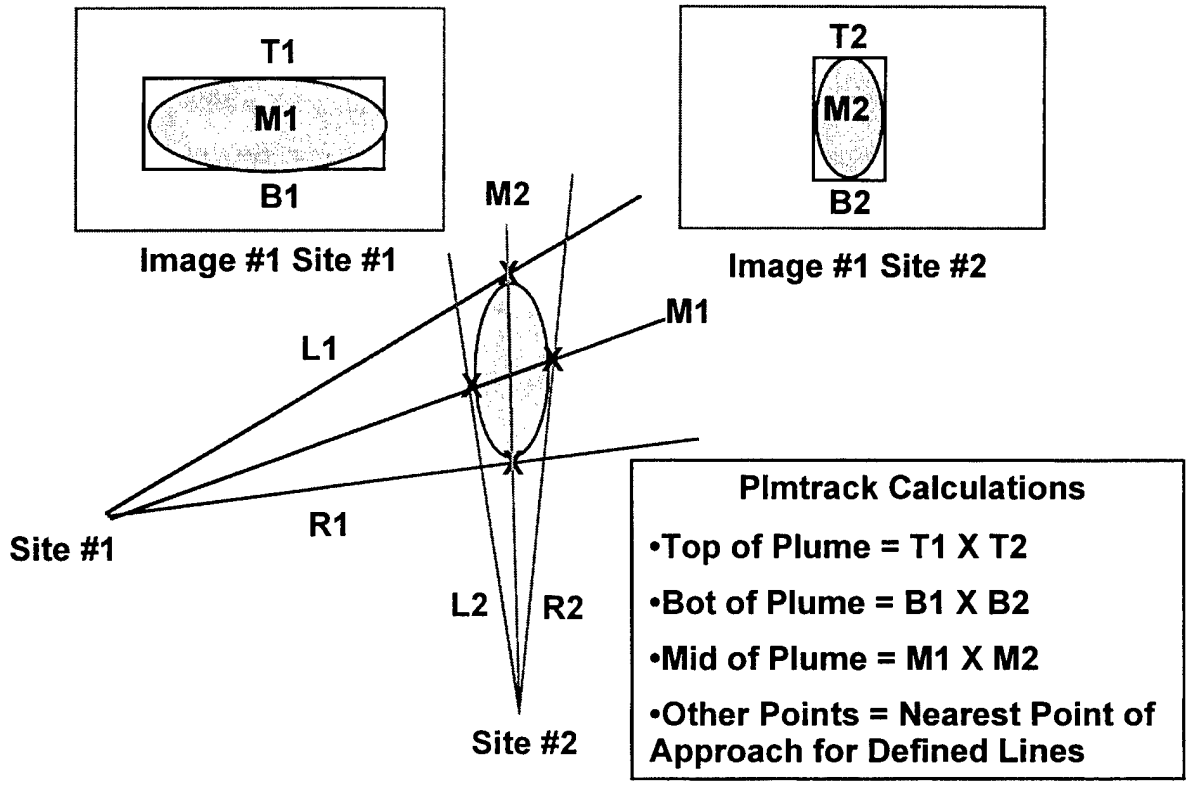

Figure 1. Implementation of the "box" method with two imagers.

similar procedure is used to define the points of closest approach for M2 with L1 and R1, yielding M2 × R1 and M2 × L1. Thus, seven points are defined for the "cell" surrounding the cloud (a point in the center of each of the six faces, plus a middle point). Four additional points are calculated by **PLMTRACK** (L1 × L2, L1 × R2, R1 × L2, and R1 × R2), and they define the extreme vertices of a polygon projected onto the ground plane and surrounding the observable cloud. All eleven points are written to a comma-separated-variable (csv) file.

When three (or more) imagers are viewing the cloud simultaneously (as accomplished for #K02, #K13, #K15, #K16, #K19, #K22, and #K23), a six-sided polygon method (documented in Figure 2 for the #K22 mission) can been employed as an initial step to determine cloud volume as a function of time. With three imagers, there is a triply redundant determination of the top, middle, and bottom of the cloud by **PLMTRACK**. The horizontal extent of the cloud is determined by defining the rays from each imager that are tangential to the widest part of the cloud as seen from that site. Projection of these extreme rays for each imager on the x-y ground plane forms a six-sided polygon (for three sites) that bounds all material in the ground cloud at all altitudes, as shown in Figure 2. When the polygon area is combined with the mean cloud height (i.e., the difference between the top and the bottom) of the cloud, one can obtain an upper bound for cloud volume. This upper bound volume may *significantly* overestimate the volume of the cloud as illustrated by Figure 2 by the relative areas of the polygon and of the cloud outline.

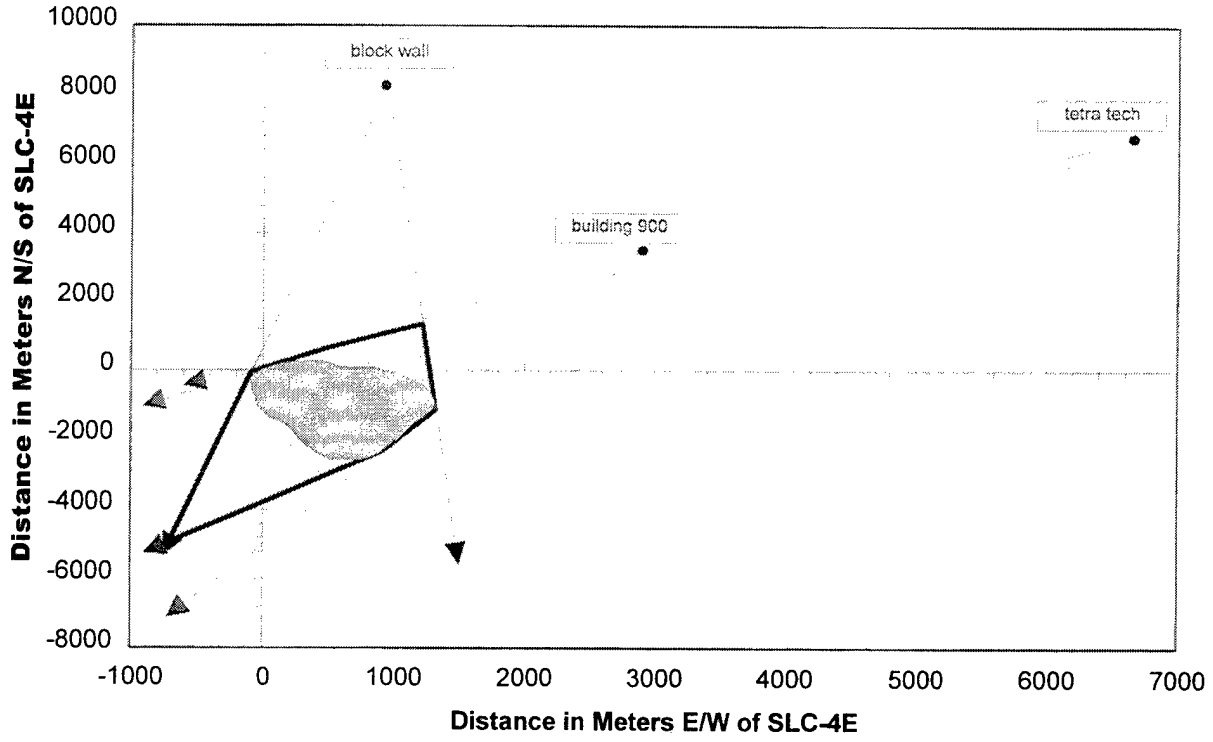

Figure 2. Implementation of the six-sided polygon method for three imagers. The imager positions and rays are actual #K22 data for imagery collected 4 min after launch. The cartoon of the cloud was synthesized for heuristic purposes to illustrate the potential for overestimation of the cloud's size by the polygon method.

Examination of Figure 2 reveals that all three imagery sites were in the northeast quadrant relative to the SLC-4E pad. One would obtain better triangulation of the cloud's position and closer estimates of its volume if one could find three imagery sites more evenly distributed about the launch pad. Unfortunately, there is a mountain to the east of the pad. As illustrated by the imagery included in this report, it is easier to image the cloud against the sky than against the terrain. Therefore, one prefers sites at or below the pad's altitude. We were not able to deploy south of the pad because of exclusion zones (chemistry and debris). The ocean is to the west of the pad. For future launches, we are investigating potential imagery sites to the east (in spite of the hill) and to the west (i.e., possibly an oil derrick) of the pad.

2.5 Results and Discussion

2.5.1. Correlation of Ground Cloud Trajectory with Wind Direction

Various wind and cloud bearings are plotted in Figure 3 using the rawinsonde convention (defined fully in Subsection 2.5.5). Briefly, all angles are reported as the angle (clockwise from north) from which the wind would blow to move the cloud along the predicted or measured bearing. The cloud trajectories are anchored to SLC-4E on the map. The heaviest arrow (i.e., thickest linewidth) is used to plot the 340° cloud direction derived from visible and infrared imagery using the **PLMTRACK** Box Method. Three additional cloud vectors are included to document the REEDM output that applies to the predicted exhaust cloud trajectory: (1) the 321° bearing of the cloud during rise; (2) the 324° bearing to maximum concentration at 424 m (i.e., REEDM's T–0.25h prediction for the stabilization height); and (3) the 330° average wind bear-

ing for the second mixing layer (i.e., this dominates the vector of the stabilized cloud at later times). Since the #K22 imagery data extends to 32 min, well after stabilization, we will use the 330° REEDM prediction for the cloud trajectory after stabilization when comparing trajectories. To the far right of the map in Figure 3, three wind vectors document the rawinsonde-derived wind directions associated with the bottom (345°), middle (333°), and top (351°) of the imagery-derived cloud heights. Although the rawinsonde originated from building 1764 (see Figure 3), the wind directions are anchored to the right of the map to avoid clutter. Figure 3 also documents the locations of the three imagery sites chosen by The Aerospace Corporation for the #K22 imagery.

It is evident from examination of Figure 3 and from the discussion in the preceding paragraph that REEDM predicts a cloud track (330° based upon the wind for the second mixing layer) that is rotated only 10° from the imaged cloud track (340°). Likewise, it is evident from examination of Figure 3 that the imagery-derived southeasterly cloud direction and speed (340° at 6.8 m/s) is consistent with the T–0.25h wind direction and speed (333° at 6.9 m/s) measured at a height equivalent to the middle of the stabilized ground cloud. As illustrated by the imagery-derived cloud track in Figure 3 and discussed in the next section, the imagery documented that the ground cloud rises and stabilizes to the south-southeast of the pad. The T–0.25h rawinsonde data in Figure 3 are documented in Appendix B. The REEDM predictions in Figure 3 are documented in Appendix A.

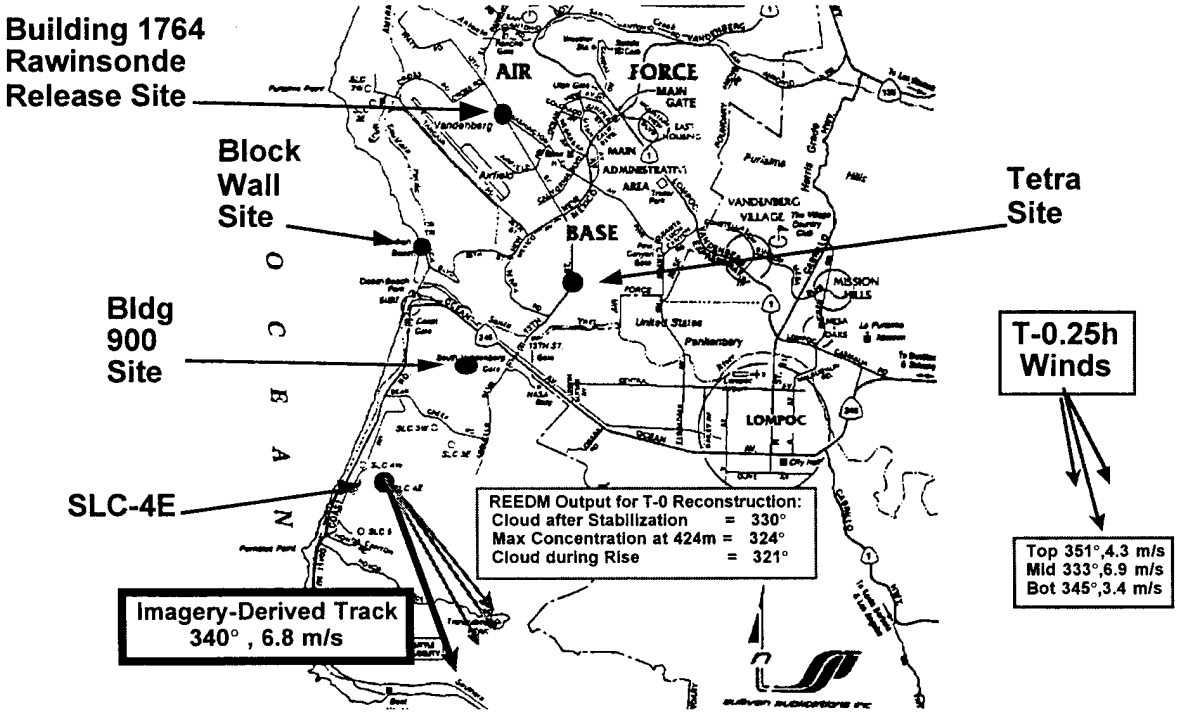

Figure 3. A map documenting the locations of the three imagery sites, the observed #K22 ground cloud's track (340°), the REEDM predictions for the #K22 exhaust cloud (321° during rise, 324° to maximum concentration at the stabilization height, and 330° for the cloud after stabilization), and the rawinsonde wind directions for the top (351°), middle (333°), and bottom (345°) altitudes for the imaged cloud. The rawinsonde sounding was at 2117 GMT (T–0.25h) from building 1764 site and was modified using DAS data to synthesize the T–0h reconstruction for REEDM runs.

2.5.2. Images of the Titan IV #K22 Exhaust Cloud

As discussed in the previous section, the imagery data is consistent with the T–0.25h rawinsonde wind directions. The imagery documents a more southerly cloud track than predicted by REEDM. Figures 4 through 8 are infrared and visible images of the Titan IV #K22 exhaust cloud as seen from the imagery sites at the specified times after launch. For clarity, boxes have been drawn about the "ground cloud," and arrows are used to identify the launch complex structures. It is immediately obvious that the cloud is not spherically symmetric in any of these images.

Figure 4 documents (a) visible and (b) infrared imagery of the exhaust cloud at 1 min after launch as observed from building 900 site. In these images, the analyst identified the ground cloud as the wide portion of the cloud, with the launch column extending upward from its middle. The analyst used the width of the ground cloud to differentiate it from the launch column during the first several minutes after launch. Comparison of the visible to the infrared imagery illustrates the complimentary nature of the techniques. The IR sees the hot exhaust cloud in emission against the background (i.e., the cool sky and warm ground) while the visible imagery sees the cloud as illuminated by the sun (i.e., reflection and shadows depending upon the illumination angle). The background for the visible imagery is dominated by scatter from the clouds as well as from aerosols in the lower atmosphere. Since the high-altitude atmospheric clouds are cooler than the ground cloud and the launch column, they do not contribute significantly to the IR background. However, the warmer low-altitude atmosphere and the warm hillside do contribute to the IR background. Hence, the signal-to-noise ratio for the IR image increases with elevation, as evidenced by the dark background at the top of the IR images and the bright background at the bottom of the IR images. It is apparent in Figure 4, that the visible camera was tilted on its platform (i.e., the Titan IV trajectory was not normal to the ground). Therefore, PLMTRACK was not used to process the visible imagery from building 900 site. However, the imagery from building 900 (the closest site) provides the best comparison of IR-to-visible imagery for qualitative purposes and, hence, is included in this section.

Figure 5 documents the ground cloud at 2 min after launch as observed from building 900. Figure 6 documents the ground cloud at 4 min from building 900. Figure 7 documents the ground cloud at 6 min from wall beach site. Figure 8 documents the view from Tetra Tech site at 4 and 6 minutes after launch. It is apparent in these images that the signal-to-noise changes with elevation, with distance from the cloud, and with time. As illustrated in Figures 2 and 3, building 900 is much closer to the pad than either Tetra Tech or wall beach sites. Likewise, Figure 3 reveals that the cloud moves away from all of these sites with time. The top and bottom of the "ground cloud" are defined by the analyst after careful review of previous and subsequent imagery from all imagery sites. The analyst draws his "box" about the mass of the cloud that contributes to the stabilized ground cloud.

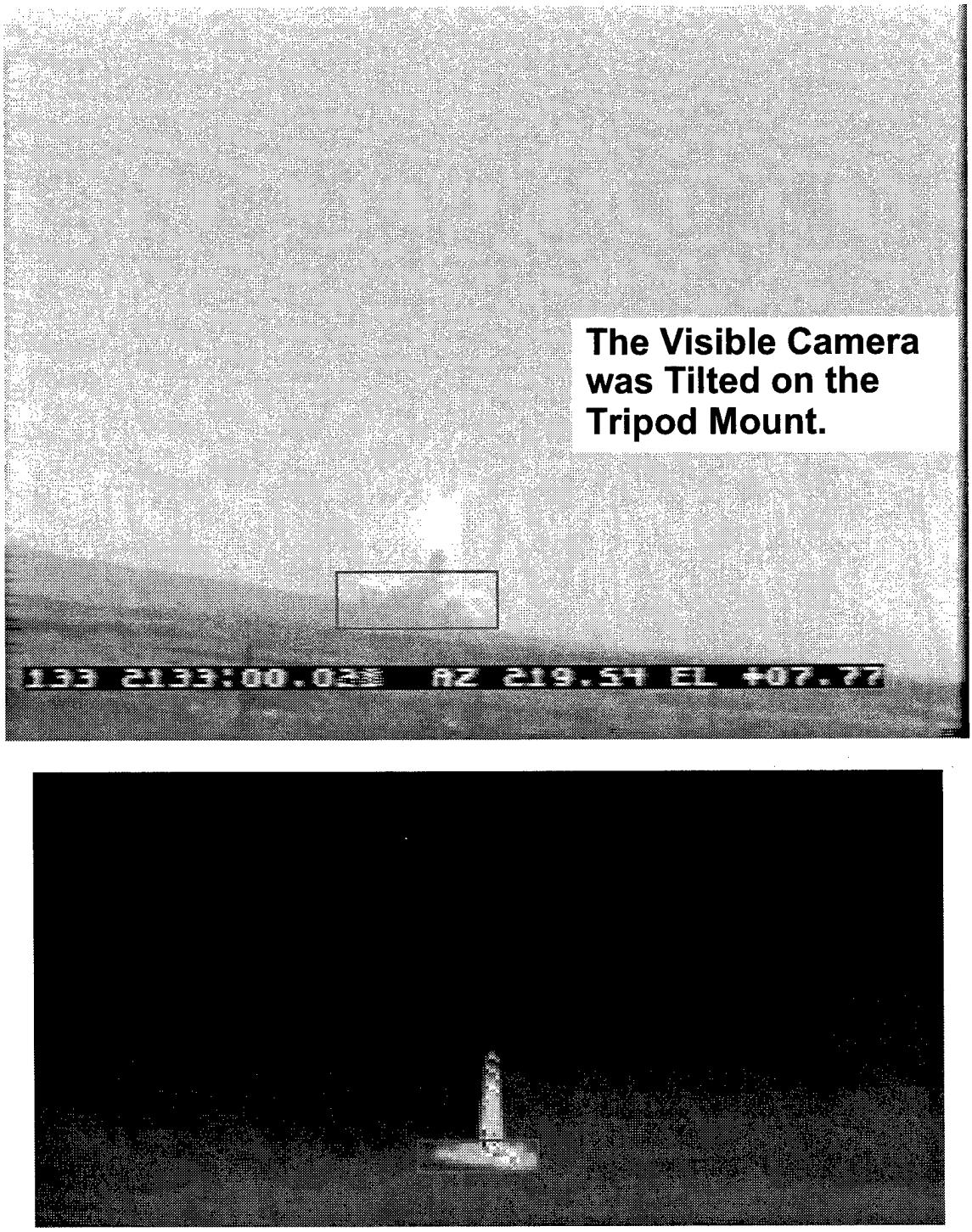

Figure 4. #K22 Ground Cloud, Launch Column, and Titan IV as Observed from Bldg 900 at 01:00 (mm:ss) after Launch: (a) Visible Imagery and (b) Infrared Imagery.

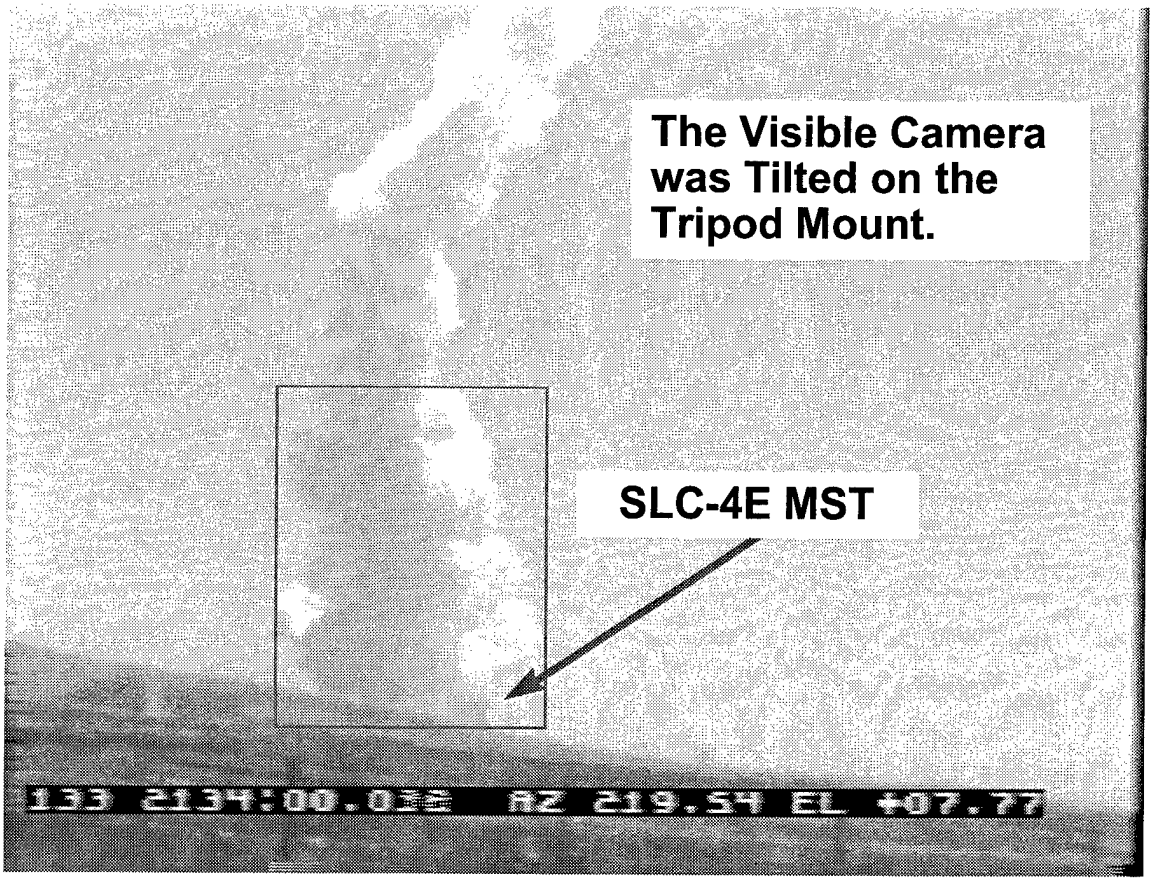

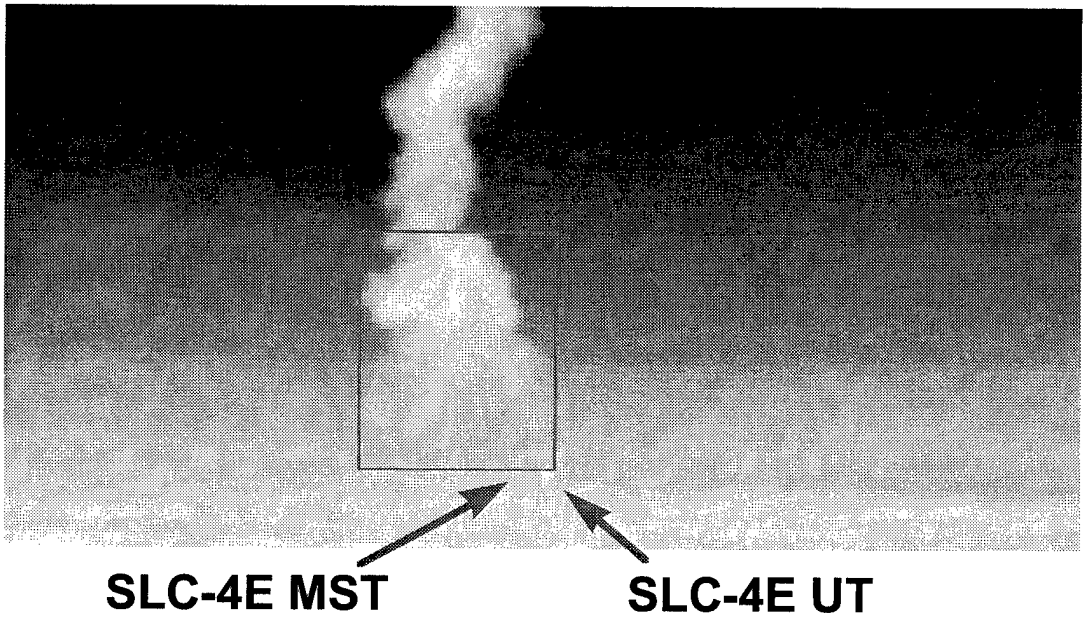

Figure 5. #K22 Ground Cloud with Attached Launch Column as Observed from Bldg 900 at 02:00 (mm:ss) after Launch: (a) Visible Imagery and (b) Infrared Imagery.

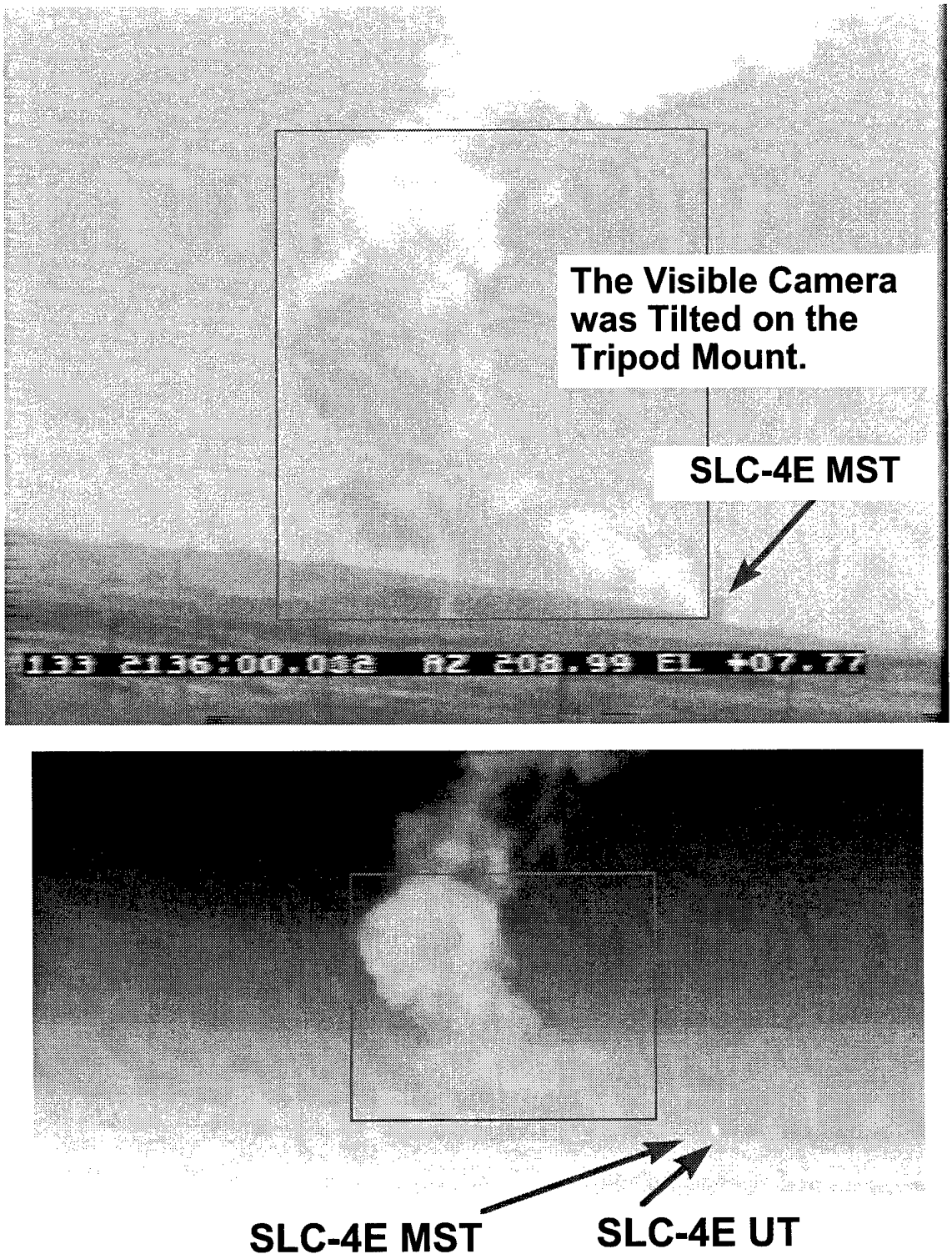

Figure 6. #K22 Ground Cloud with Attached Launch Column as Observed from Bldg 900 at 04:00 (mm:ss) after Launch: (a) Visible Imagery and (b) Infrared Imagery.

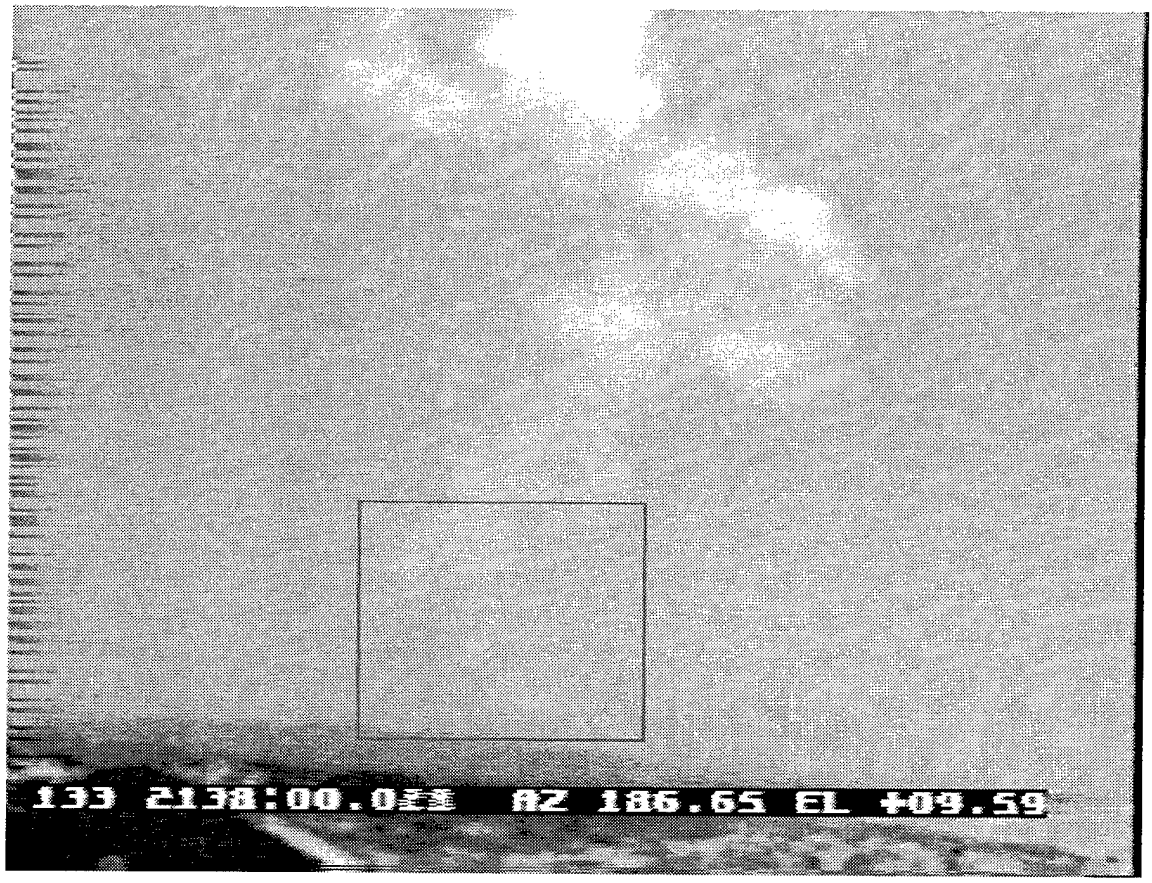

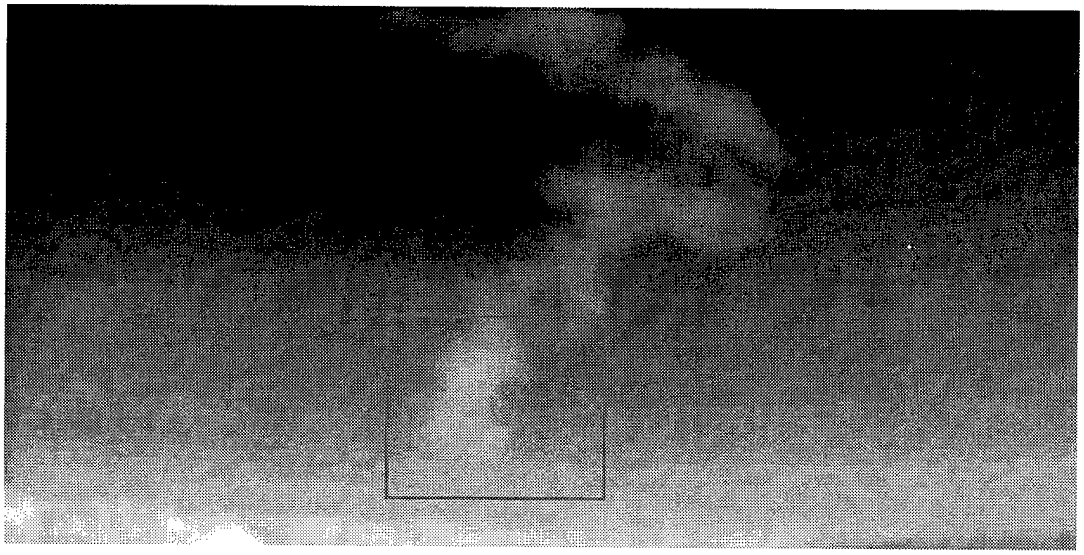

Figure 7. #K22 Ground Cloud with Attached Launch Column as Observed from Block Wall Site at 06:00 (mm:ss) after Launch: (a) Visible Imagery and (b) Infrared Imagery.

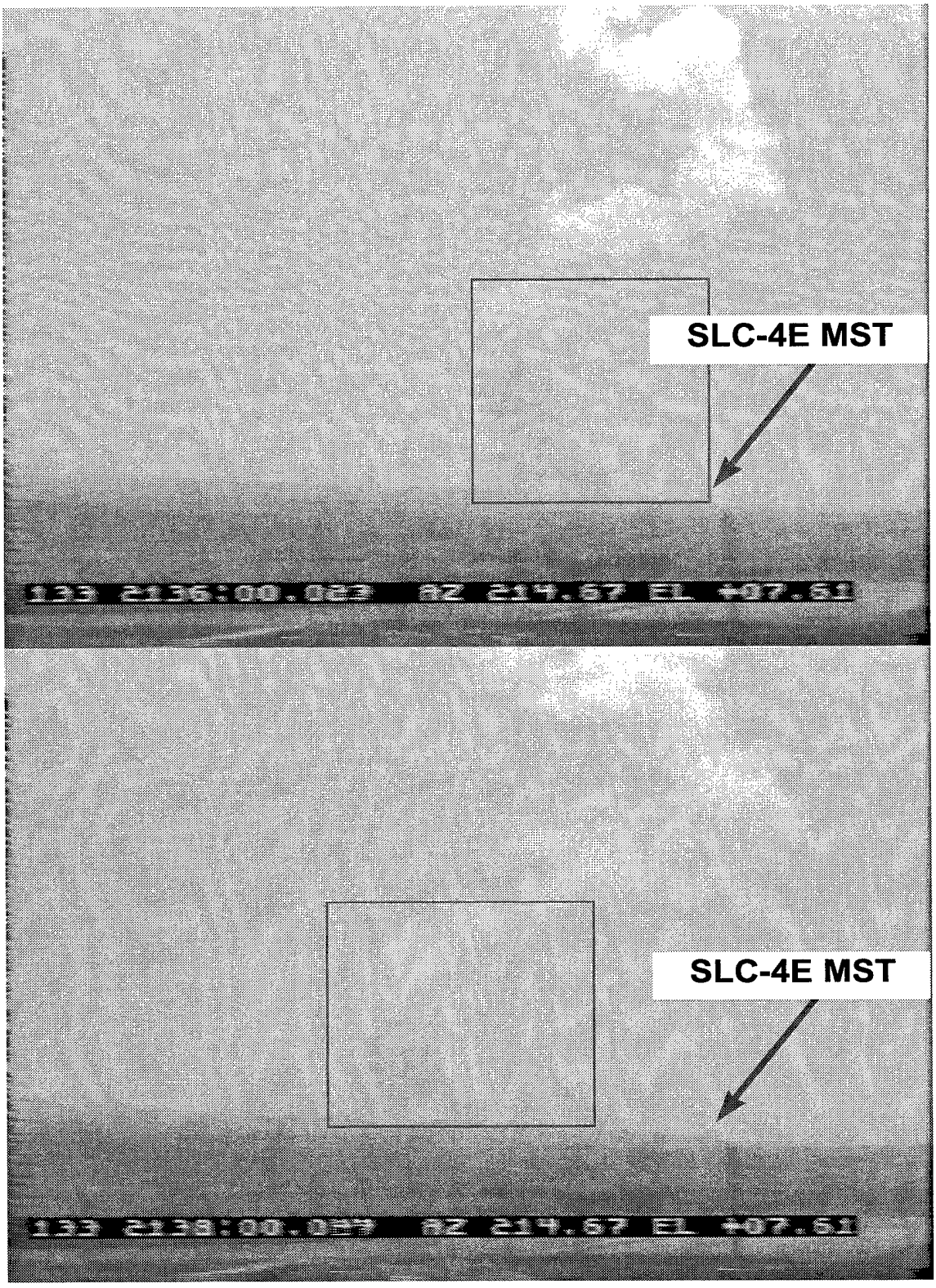

Figure 8. #K22 Ground Cloud with Attached Launch Column as Observed by Visible Imagery from Tetra Tech Site: (a) at 04:00 (mm:ss) after Launch, and (b) at 06:00 (mm:ss) after Launch.

2.5.3. Cloud Rise Times and Stabilization Heights

The plots presented in Figures 9–11 show the time-dependent altitude (meters above SLC-4E = m AS4E) of the "bottom," the "middle," and the "top" of the ground cloud as documented by the imagery from the three camera sites. The "a" plots label the data according to the type of imagery and the camera site for pairs of images as follows:

b9ibwi	infrared imagery from building 900 and infrared from Block Wall site
b9ibwv	infrared imagery from building 900 and visible from Block Wall site
tevb9i	visible imagery from Tetra site Tech and infrared from building 900 site
tevbwi	visible imagery from Tetra Tech site and infrared from Block Wall site
tevbwv	visible imagery from Tetra Tech site and visible from Block Wall site

The labels on the "a" plots not only allow one to look for trends associated with certain combinations of imagery sites but also allow direct comparison of infrared to visible imagery for identical camera sites. Review of the "a" plots reveals that no single combination of sites or cameras produces systematically different results when compared to the other data over the entire monitoring time. Certainly the "a" plots support the treatment of the imagery data as one set as done in the "b" plots. The "b" plots include a polynomial fit to the combined data and horizontal lines, illustrating the stabilization height as well as the $\pm 3\sigma$ error levels.

It is evident from review of Figures 9–11 that the shapes of the cloud rise curves for the top, middle, and bottom of the ground cloud are dramatically different. The top of the cloud reaches its stabilization height within 4–7 min. The bottom of the cloud is detected for the first 7 min after launch with acceptable signal-to-noise ratios. As the cloud dissipates and moves away from the imagery sites, the bottom of the cloud is difficult to detect due to a decreasing signal-to-noise for the remote cloud at low elevation (as revealed by the imagery in the previous section). Therefore, after reaching an apparent plateau between 5–7 min after launch, the bottom of the cloud appears to rise at times greater than 7 min (as a result of poor signal-to-noise at low elevation). In contrast, the imagery had much better signal-to-noise for the top of the cloud throughout the 32 min of tracking, as evidenced by its almost constant elevation after stabilization and by the imagery in the previous section. The middle of the cloud is calculated from the top and bottom and, therefore, presents an intermediate behavior. The cloud's characteristic rise times and stabilization heights are compared to REEDM predictions in the next section.

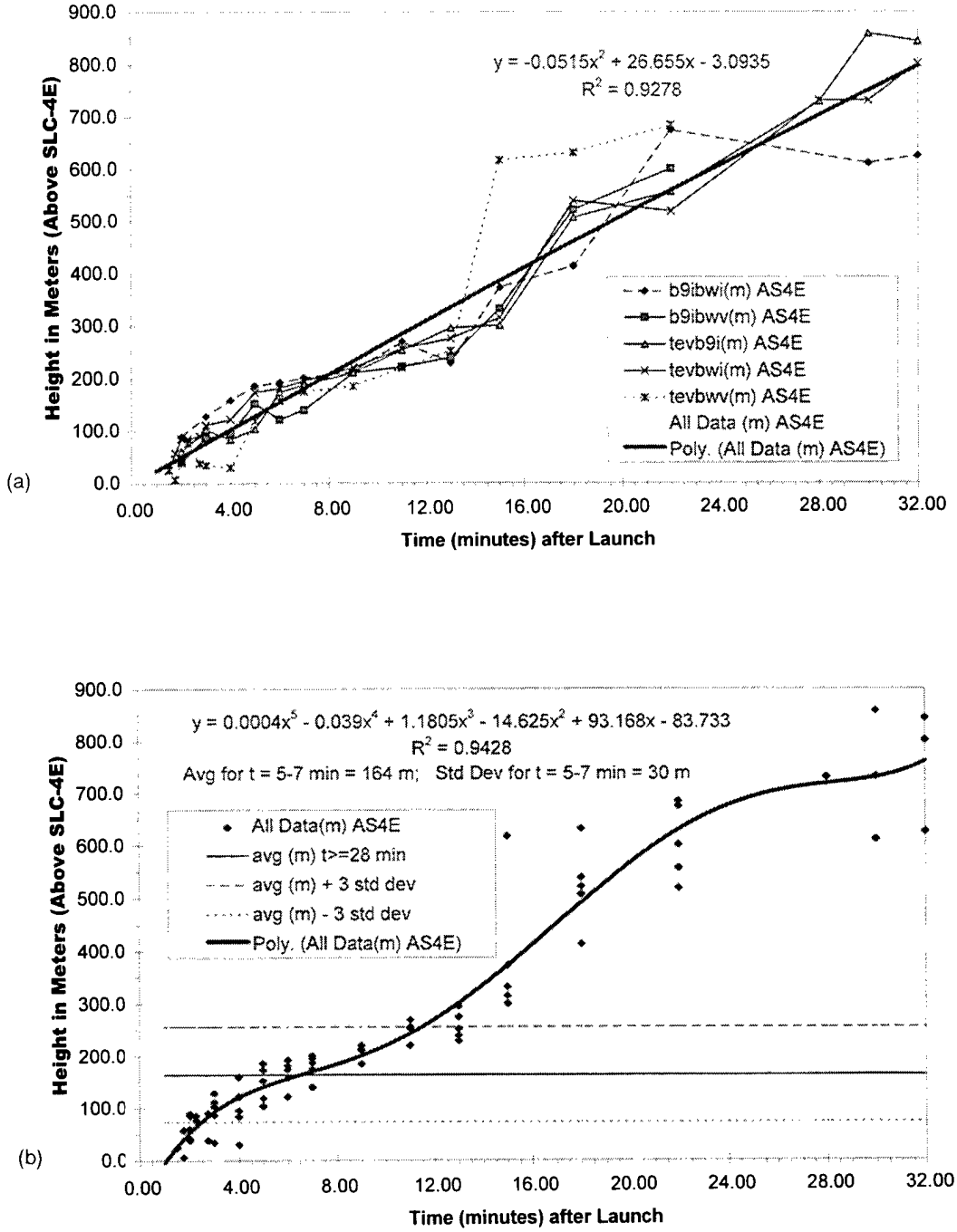

Figure 9. Cloud rise plot for the bottom of the #K22 cloud with data labeled by imagery pairs (a). (b) The values of Height (m) vs t (min) are displayed with the fifth-order polynomial fits to all data and lines documenting the 3s error bands as well as the stabilization height (164 m [538 ft] above SLC-4E). The variance (R2) of 0.9428 indicates the quality of the fit. After 7 min, poor signal-to-noise at low elevations results in continued rise of the "observable bottom" of the cloud.

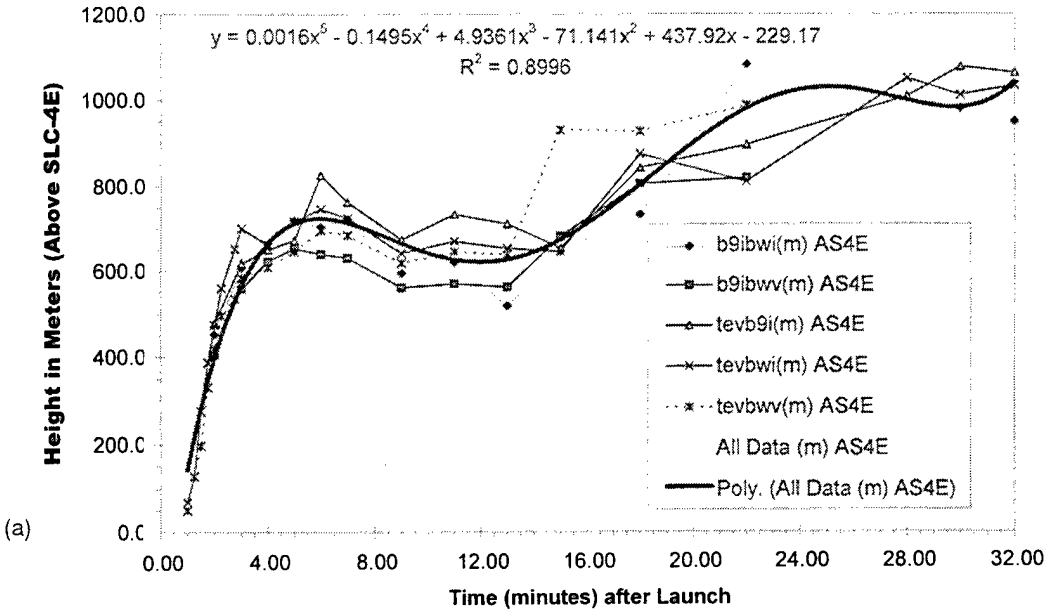

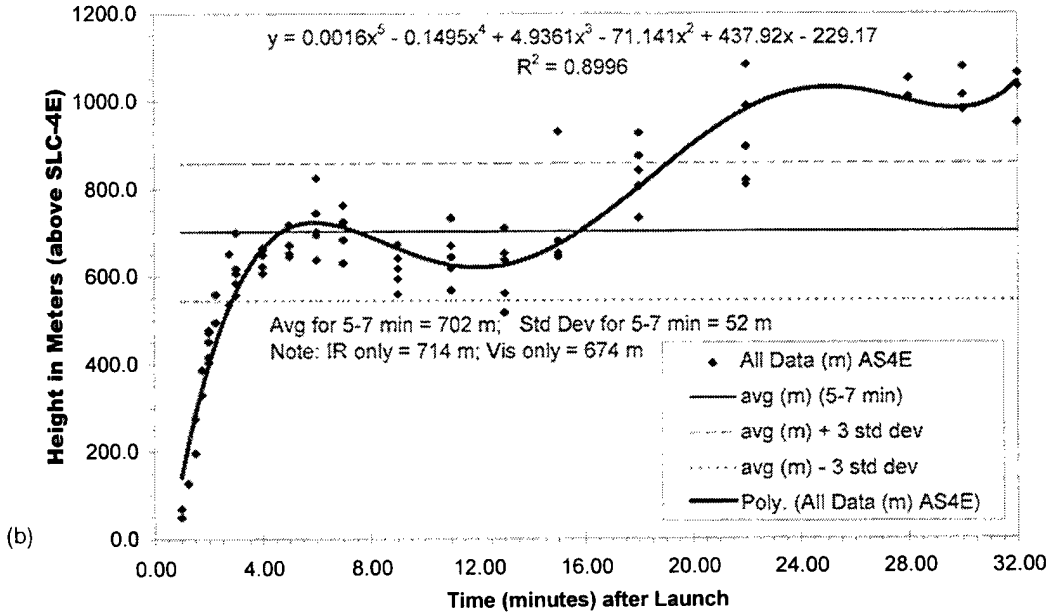

Figure 10. Cloud rise plot for the middle of the #K22 cloud with data labeled by imagery pairs (a). (b) The values of Height (m) vs t (min) are displayed with the fifth-order polynomial fits to all data and lines documenting the 3σ error bands as well as the stabilization height (702 m [2303 ft] above SLC-4E). The variance (R^2) of 0.8996 indicates the quality of the fit.

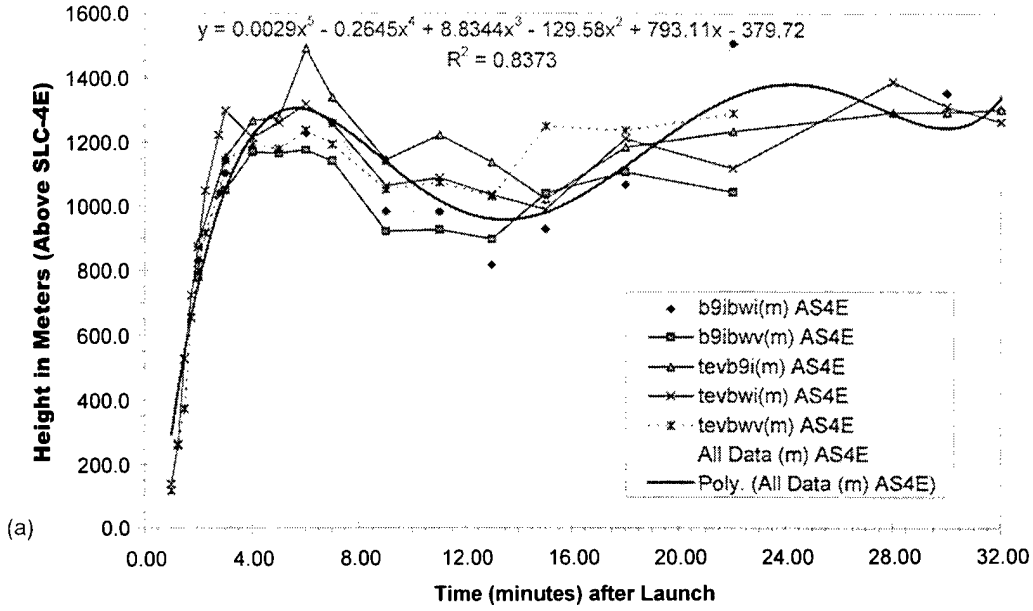

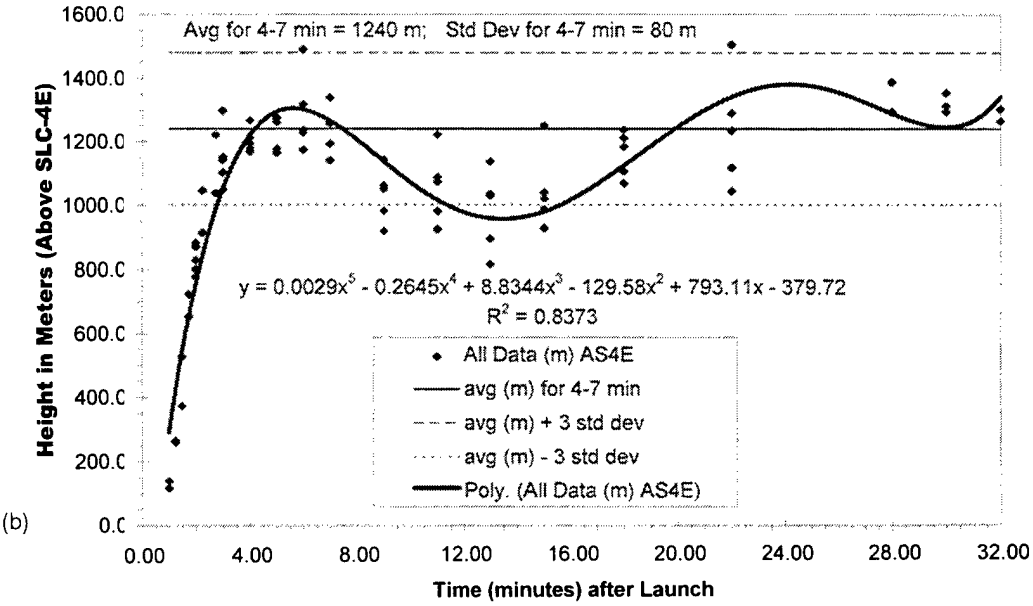

Figure 11. Cloud rise plot for the top of the #K22 cloud with data labeled by imagery pairs (a). (b) The values of Height (m) vs t (min) are displayed with the fifth-order polynomial fits to all data and lines documenting the 3s error bands as well as the stabilization height (1240 m [4068 ft] above SLC-4E). The variance (R^2) of 0.8373 indicates the quality of the fit.

2.5.4. Comparison of REEDM Prediction to Imagery Data: Rise Rate and Height

In Figure 12, the imagery-derived heights for the cloud's top, middle, and bottom are plotted with the T–0.25h REEDM prediction of the height for the cloud's middle against time. It can be seen that the measured stabilization height of the cloud's center (702 ± 52 m above SLC-4E) is 66% higher than the value predicted by REEDM (424 m in Appendix A) using pre-launch rawinsonde data (Appendix B). The amount of time required to reach the stabilization height (approximately 4–7 min from the imagery) is 100 to 250% longer than the 2 min predicted by REEDM. This is evident from comparison of the shapes of the "middle" curves in Figure 12. As mentioned previously, the signal-to-noise ratio decreased rapidly at low elevation as the cloud dispersed and moved away from the imagery sites. Therefore, the bottom of the cloud appears to rise at times greater than 7 min as a result of poor signal-to-noise at low elevation. In contrast, the imagery had much better signal-to-noise for the top of the cloud throughout the 32 min of tracking, as evidenced by its almost constant elevation after stabilization.

The variances (R^2) of the polynomial fits to the data (i.e., Figures 9–11) indicate that the fits are reasonably good. A polynomial fit was used in those figures as a convenient method to permit the representation of cloud overshoot and subsequent damped oscillation around the stabilization height. To be consistent with REEDM, stabilization time and height refer to the first maximum in

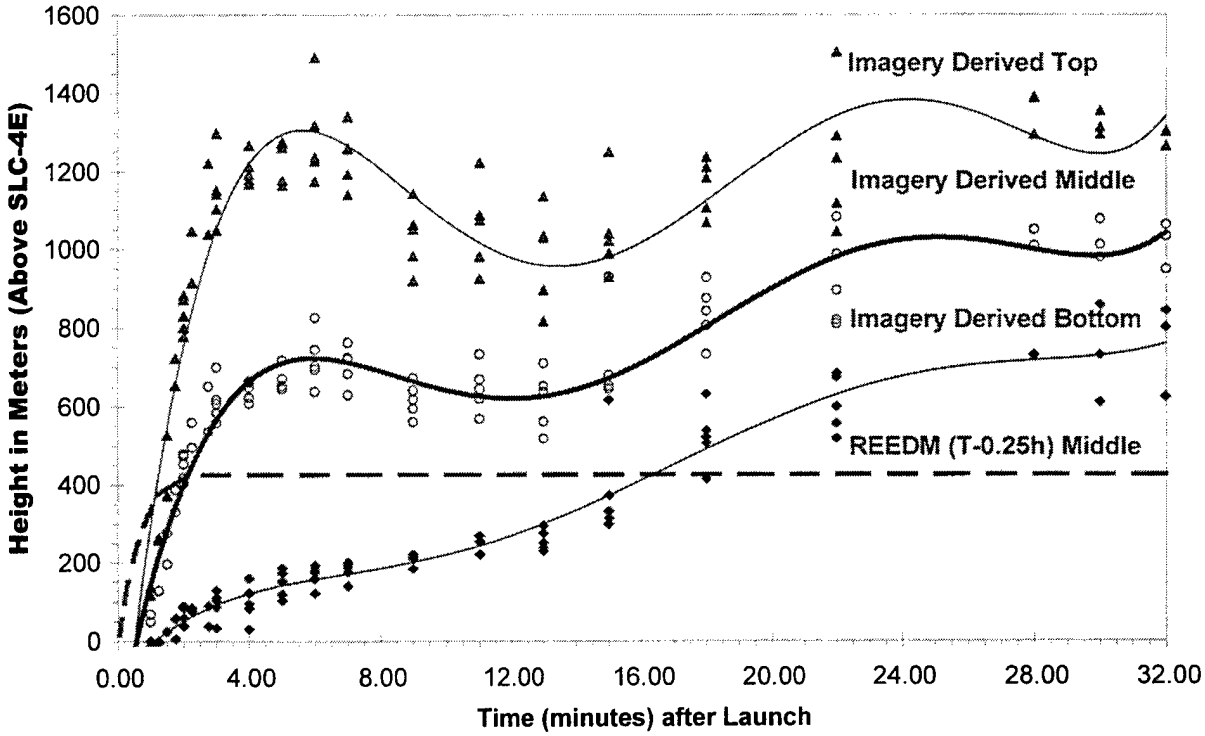

Figure 12. The imagery-derived heights for the top, middle, and bottom of the ground cloud (Figures 9–11) are plotted as H(t) vs t. The T–0.25h REEDM modeling run predictions for the cloud middle (424 m after stabilization) are presented for comparison to the middle curve derived from the imagery (702 m to first maximum), which is 66% higher than the REEDM prediction.

these fits. REEDM predicts that the cloud goes through damped oscillatory motion with a period of $2\pi/S^{1/2}$, where S is the static stability parameter [Ref. 1, Eq. (7)].[1] Sensitivity of REEDM predictions to input parameters has been examined by Womack.[2] Careful imaging of launch ground clouds under a variety of meteorological conditions is a vital element in REEDM evaluation.

2.5.5. Comparison of REEDM Prediction to Imagery Data: Trajectory and Speed

Figures 13 and 14 present data for the ground track and for the displacement of the cloud from the launch pad as determined by imagery. The "box" method of analysis for the imagery data does not yield independent values of the cloud track for the top, middle, and bottom of the cloud. We have chosen to present data for the middle of the cloud as defined by **PLMTRACK**.

To be precise, the ground track in Figure 13 represents the ground-plane projection of the trajectory of the middle of the cloud as a function of time. An "average" ground track is computed as a linear fit to the position data using the following formula:

$$Y = mX + b, \tag{1}$$

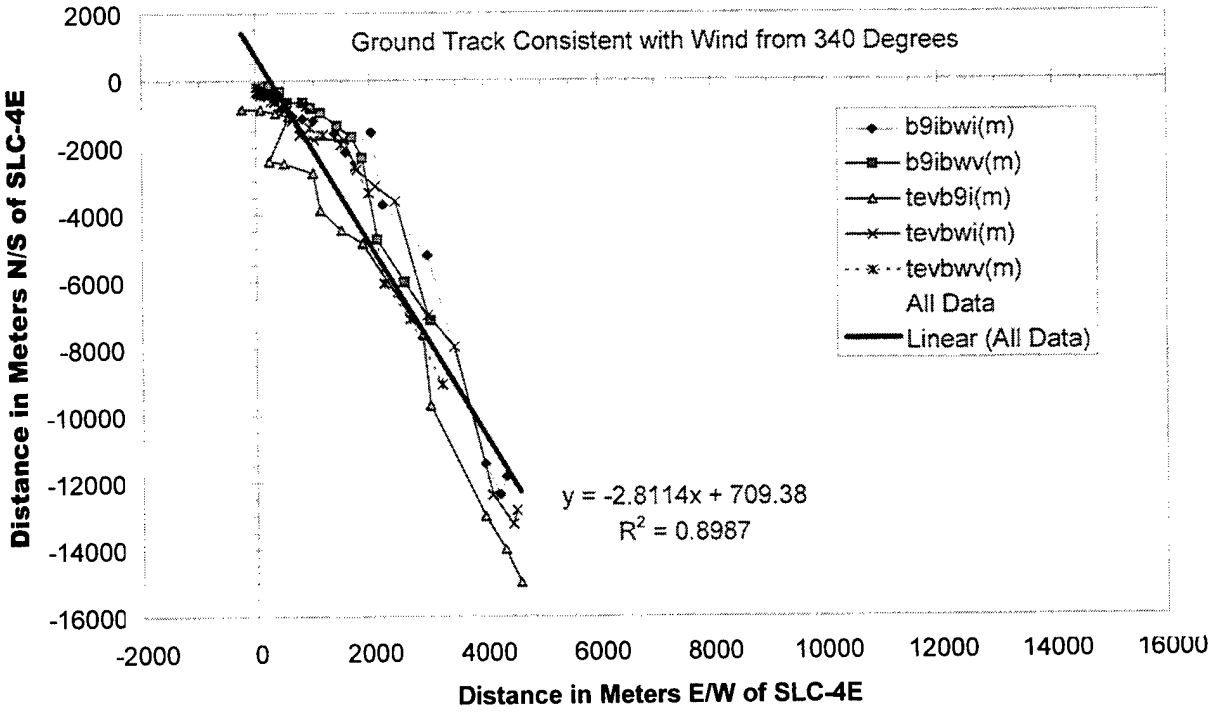

Figure 13. Ground track for the middle of the #K22 launch cloud. The cloud followed a southeasterly path as illustrated by fitting all of the data to a line using linear regression. This 340° bearing is more southerly than the vectors reported by REEDM: (1) the 321° trajectory during rise, (2) the 324° bearing to maximum concentration at the 424 m (the predicted stabilization height), and (3) the 330° wind for the second mixing layer (affecting the cloud at later times). In contrast, the rawinsonde winds at the top (351°), middle (333°), and bottom (345°) of the imaged cloud are consistent with the observed cloud trajectory (340°).

where Y is the distance in meters along the north-south axis, m is the slope of the fit, X is the distance in meters along the eastwest axis, and b is the intercept for the fit. We normally permit the intercept (b) to be nonzero since the cloud origin may differ from the location of the launch complex due to low-altitude winds and exhaust duct geometry. That displacement can also be modeled within the REEDM code.

In this report, the angles will conform to the convention of rawinsonde wind vectors (the angle (clockwise from north) from which the wind originates that would push the cloud to its imaged position). Thus, the angles are related by

$$J = 180 + F, \tag{2}$$

where ϑ is the equivalent rawinsonde wind angle, and Φ is the measured polar angle of the cloud relative to SLC-4E and clockwise of true north. For example, when the cloud is due east of SLC-4E, Φ is 90°, and ϑ is 270°. The slope (m) of the fitted line is determined by the angle θ, where $\theta = \tan^{-1} m$, and therefore $\Phi = 90° - \theta$.

Figure 14 presents the ground distance of the cloud from the launch pad as derived from analysis of pairs of imagery. The distance from SLC-4E increases with time. A linear fit to this trend

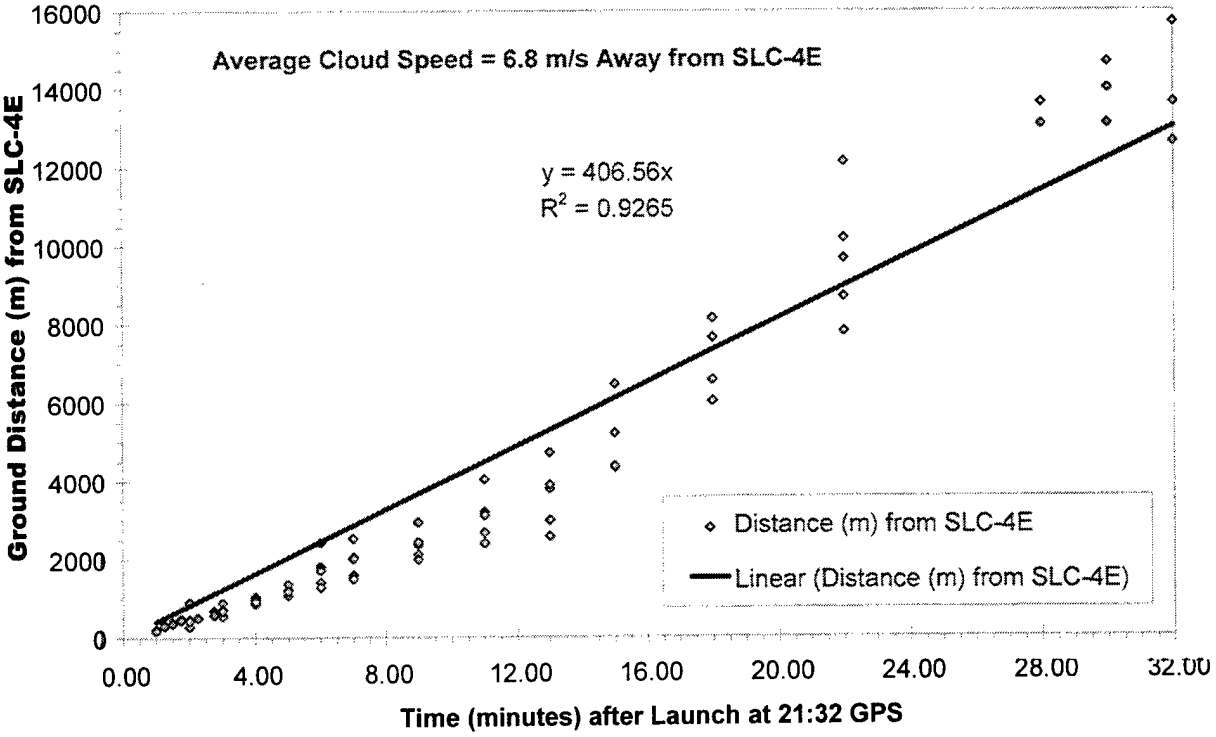

Figure 14. Time plot of ground distance for the middle of the #K22 ground cloud from the launch pad. The slope yields a speed of 6.8 m/s away from SLC-4E. The high value for the variance (R^2 = 0.9265) indicates the quality of this linear fit to these data. For comparison, REEDM predicts 3 m/s (during rise), while the rawinsonde sounding (T–0.25h) documents 6.9 m/s at the height of the middle of imaged cloud. The rawinsonde was launched from Building 1764 (i.e., north-northeast of the pad).

provides the average velocity of the ground cloud (6.8 m/s cloud velocity away from SLC-4E). The high value for the variance for this linear fit (i.e., R^2 =0.9265) illustrates the quality of these data. As with the cloud trajectory, the speed varies slightly as the cloud rises. REEDM (T–0.25h) predicts a cloud speed of 3 m/s, which is significantly lower than the observed speed. However, the T–0.25h rawinsonde sounding (Appendix B) documents a wind speed of 6.9 m/s at the height of the middle of the imaged cloud, which is in excellent agreement with the imagery-derived 6.8 m/s. The winds at the height of the stabilized cloud are derived from rawinsonde measurements at T–0.25h from building 1764 area (i.e., north-northeast of the pad). Therefore, there are offsets both in time and distance between the rawinsonde sounding and the exhaust cloud rise.

2.5.6. Comparison of REEDM Prediction to Imagery Data: Summary Table

Table 3 summarizes the imagery-derived, rawinsonde-measured (T–0.25h), and REEDM-predicted (T–0h reconstruction based upon the T–0.25h rawinsonde sounding and T–0h DASS profiles) data for the #K22 launch cloud. Several conclusions are derived from review of the contents of this table:

(1) the imagery-derived direction and speed of the cloud are similar to the T–0.25h rawinsonde data at the imagery-derived stabilization height of the cloud;

(2) the imagery-derived stabilization height (702 m) is 66% higher than predicted by REEDM (424 m);

(3) the imagery-derived stabilization time (4–7 min) is 100% to 250% longer than predicted by REEDM (2 min);

(4) the imagery-derived velocity (6.8 m/s) of the ground cloud is 127% faster than predicted by REEDM (3 m/s); and

(5) the imagery-derived cloud track (340°) is 10° more clockwise than predicted by REEDM (330°).

These data suggest that better prediction of stabilization height by REEDM might provide better direction and speed predictions if they are biased by the rawinsonde data near the stabilization height.

Table 3. Summary for #K22 Launch Cloud Data Derived from Visible and Infrared Imagery, T–0.25h Rawinsonde Sounding Data, and T–0.25h REEDM Predictions.

Attribute	Feature	Imagery (IR only)	Imagery (Vis only)	Imagery (Mixed)	Rawinsonde (T–0.25h)	REEDM 7.07 (T–0.25h)
Height (m)	Top	#N/A	#N/A	1240	1264	#N/A
Above SLC-4E	Middle	714	674	702	723	424
(SLC-4E = 153 m MSL	Bottom	#N/A	#N/A	164	153	#N/A
Time (min)	Top	#N/A	#N/A	4–7	#N/A	#N/A
After Launch	Middle	5–7	5–7	5–7	#N/A	2
	Bottom	#N/A	#N/A	5–7	#N/A	#N/A
Bearing (deg)	Top	#N/A	#N/A	#N/A	351	#N/A
(Rawinsonde)	Middle	#N/A	#N/A	340	333	330 (layer #2)
	Bottom	#N/A	#N/A	#N/A	345	#N/A
Speed (m/s)	Top	#N/A	#N/A	#N/A	4.3	#N/A
Away From	Middle	#N/A	#N/A	6.8	6.9	3 (layer #2)
SLC-4E	Bottom	#N/A	#N/A	#N/A	3.4	#N/A

2.6 Summary and Conclusions

The Titan IV #K22 mission was launched successfully from the Eastern Range (SLC-4E) at 1432 PDT (2132 GMT) on 12 May 1996. Personnel from The Aerospace Corporation deployed two IR imaging systems and three visible imagery systems to monitor this daylight launch and to track the time evolution and the ground trajectory of the solid rocket motor exhaust cloud. The three imagery sites were located to the northeast, north-northeast, and north relative to launch complex SLC-4E. Imagery data were recorded for 37 min and the cloud was tracked for 32 min. When combined with the Az/El readings and the IRIG-B time data, the imagery was used to quantify movement, rise, and speed of the cloud for 32 min after the launch. The launch of #K22 marked the sixth deployment of the VIRIS imaging platforms to a Titan IV launch and the first VIRIS deployment for VAFB launch.

The definition of exhaust cloud geometric features was complicated by multiple contributions to the complex shape of the evolving cloud (i.e., rapid rise of the hot ground cloud and shearing of the high-altitude launch column). The analyst included only the portions of the exhaust cloud that became incorporated into the stabilized ground cloud.

Analysis of the imagery data presented in this report has focused on determining parameters that are directly comparable to REEDM predictions. The most accurately determined quantities by imagery are the cloud rise time, its stabilization height, cloud speed, and ground track. Using the T–0.25h rawinsonde data, REEDM predicted a stabilization height of 424 m above ground level and a stabilization time of 2 min while the imagery yielded values of 702 m above SLC-4E and 4–7 min. The imagery-derived cloud trajectory was 340°, and the cloud's ground speed was 6.8 m/s away from SLC-4E. This compares to 330° and 3 m/s predicted by REEDM (T–0.25h). Therefore, the imaged cloud stabilized at a height that was 66% higher than predicted by REEDM (T–0.25h), traveled at a speed 127% faster than predicted by REEDM (T–0.25h), and headed in a direction 10° more clockwise than predicted by REEDM (T–0.25h).

3. Aircraft Elevated HCl Measurements

[The material in this section was contributed by Dr. R. N. Abernathy and Karen L. Foster of the Environmental Monitoring and Technology Department of The Aerospace Corporation's Space and Environment Technology Center.]

3.1 Background

On 12 May 1996, the Titan IV #K22 mission was successfully launched from VAFB at 1432 PDT (2132 GMT). This section describes the hydrochloric acid (HCl) concentration data collected by an aircraft that sampled that portion of the exhaust cloud known as the ground cloud. The aircraft used a modified Geomet total HCl detector to measure the HCl concentrations within the ground cloud for 100 min subsequent to the launch. This aircraft sampling campaign involved Air Force, NASA, NOAA, and contractor (I-NET and SRS) organizations. The Aerospace Corporation analyzed the aircraft's HCl concentration data as described in this section.

The aircraft sampled at altitudes ranging from 450 to 1350 m MSL. Based upon sampling at altitudes ranging from slightly below to slightly above the imagery-derived center of the cloud, the aircraft's HCl concentration data document the rapid (i.e., 8.3 m/s) movement of the ground cloud along a 344° bearing at early times. At later times while sampling at altitudes at and slightly below the imagery-derived center of the cloud, the aircraft's HCl data document a 331° bearing and a 7.7 m/s speed for the ground cloud. The aircraft's altitude was measured using a Global Positioning System (GPS) receiver with regular service (±100 m in latitude and in longitude and ±250 m in altitude). Differential GPS service was not available for this mission at VAFB.

The aircraft's Geomet data (i.e., total HCl concentration measurements) are reported here in several graphical formats to facilitate comparison with REEDM predictions (Appendix A), rawinsonde sounding data (Appendix B), quantitative imagery data (Section 2), FTIR spectroscopy of the exhaust cloud (Section 4), and ground-based HCl measurements (Section 5). The aircraft's setup is described in Appendix C. For clarity, this section includes some data from other sections in its figures, tables, and text. It is apparent from review of this section, that these data will be useful for validating current and future dispersion models.

The purpose of this report is to document the quality and quantity of the aircraft data available from the #K22 mission for validating dispersion models. However, it is difficult to extract the data for a single pass through the cloud from summary plots that contain 44 passes through the cloud. Therefore, in order to facilitate the comparison of these data to individual dispersion model runs, two subsequent reports will provide: (1) a detailed correlation between imagery and aircraft data for the first 32 min after launch and (2) a detailed graphical analysis of the aircraft's HCl concentration profiles using polar and Cartesian coordinates for each 10-min time window throughout the 100-min flight time. These subsequent detailed analyses will provide the data in a format that will allow direct comparison to model runs for specific times, altitudes, and distances

from the release site. The aircraft data are also available as comma-separated-variable files providing time, latitude, longitude, altitude, Geomet response, and HCl concentration.

3.2 Introduction

I-NET, a NASA contractor, modified a Geomet for mounting in the nose of a Piper (PA-44-180) Seminole (a twin-engine, four-seat aircraft). The Geomet is a total HCl monitor that produces a response proportional to the combined HCl present in both the vapor and the aerosol phases. It reports the HCl concentration as parts-per-million (ppm) by volume (i.e., V_{HCl} 10^6/ V_{total}). This instrument sampled the air through a horizontal 4-ft–long ceramic inlet wetted with a bromate/bromide-containing reagent. The HCl diffuses to the wetted walls of the ceramic tube and produces bromine vapor through reactions with the reagent. The bromine vapor is swept into a buffered hydrogen peroxide/Luminol solution resulting in photoluminescence detected by a filtered photometric detector. The Geomet provides a millivolt response that is proportional to the combined HCl vapor and aerosol concentration entering the inlet. I-NET calibrated the Geomet against HCl vapor before and after the #K22 mission, as discussed in this section.

SRS Technologies Inc., a contractor, provided an interface between the I-NET laboratory and the Florida Institute of Technology (FIT) flight crew. NASA, NOAA/Air Resources Laboratory/Field Research Division, I-NET, SRS, and FIT cooperated in the integration of the NOAA data system, the FIT aircraft, and the Air Force Geomet into an airborne sampling and data logging system. FIT personnel piloted the aircraft during the #K22 mission while 45th AMDS/SGPB personnel operated the NOAA data system and the Geomet detector. The NOAA data system logged GPS time and position as well as Geomet response every 0.25 s during the flight. NOAA provided a comma-separated-variable (csv) data file to the Aerospace Corporation.

The Aerospace Corporation processed the aircraft's HCl data as presented in this section. In addition, the Aerospace Corporation imaged the rise, movement, and growth of the ground cloud for the first 32 min subsequent to the #K22 launch as documented in Section 2. This quantitative imagery documented the stabilization height (above SLC-4E) and the bearing (relative to SLC-4E) of the ground cloud. Rudimentary knowledge of the rawinsonde wind data (Appendix B), REEDM predictions (Appendix A), and the imagery data (Section 2) was required for the interpretation of the aircraft's HCl sampling data as reported in this section.

As stated previously, the aircraft's altitude was measured using a GPS receiver using regular service (no differential corrections were available for the VAFB area during this mission). The GPS altitude data were recorded as meters relative to mean sea level (MSL).

When comparing the aircraft's GPS-derived altitude to the imagery, rawinsonde, and REEDM data, it is essential to use the same frame of reference for measuring the height. REEDM reports the predicted height of the exhaust cloud relative to MSL and relative to ground level but incorrectly assumes that the altitude of the rawinsonde release site (building 1764 for the #K22 mission) is the same as the height of the launch pad (SLC-4E for the #K22 mission). This is the case at Cape Canaveral, but is not the case at VAFB, and results in a significant error in REEDM's output. We assert that REEDM's predicted height above ground level (AGL) was intended to be height above origin, which, for a launch, is height above the launch pad NOT above the rawin-

sonde release site. Therefore, in Section 2, the observed height of the imaged cloud and the predicted height for the stabilized cloud were reported in meters above SLC-4E (i.e., above the launch pad). For this conversion, we assumed the height AGL reported by REEDM was the same as the height above SLC-4E. Since SLC-4E is 153 m (501 ft) above MSL, height relative to SLC-4E is converted to height MSL by adding 153 m (501 ft). Since REEDM incorrectly uses the height of the rawinsonde release site (100 m, 328 ft) rather than the height of the launch pad (153m, 501 ft) for its conversion of height AGL to height MSL, the height MSL reported by REEDM in Appendix A is low by 53 m (173 ft). The magnitude of this correction will vary for each mission since the rawinsonde release site can vary (i.e., the #K15 rawinsonde was launched from building 900 while the #K22 rawinsonde was launched from building 1764). Table 4 provides the imaged and the predicted (i.e., by REEDM) heights relative to MSL and to SLC-4E by correctly using the SLC-4E pad as the origin for the #K22 launch.

Table 4. Imagery-Derived Stabilization Heights and REEDM's Predicted Stabilization Height Expressed Relative to MSL (comparable to the aircraft's GPS data) and Relative to SLC-4E (as reported in Section 2). Note that SLC-4E is 501 ft (153 m) above mean sea level (MSL).

Stabilized Exhaust Cloud Characteristic	H (m MSL) (comparable to the aircraft's GPS data)	H (ft MSL) (501 + H (ft SLC-4E)	H (m SLC-4E) (as reported in Chapter 2)	H (ft SLC-4E) (unit conversion from H (m SLC-4E)
Imaged Bottom	317	1039	164	538
Imaged Middle	855	2804	702	2303
Imaged Top	1393	4569	1240	4068
REEDM's Middle	577	1892	424	1391

3.3 Results and Discussion

The aircraft's exhaust cloud data are most easily interpreted with knowledge of the rawinsonde and imagery results. Figure 15 plots various wind and cloud bearings using the rawinsonde convention [defined fully in Subsection 3.3.2]. Briefly, we report the angle (clockwise from north) from which the wind originates that would push the cloud to the sampled position.

Six cloud bearings (represented as arrows) are anchored to SLC-4E on the map in Figure 155. The two shortest arrows with the largest arrowheads represent the aircraft-derived bearings for the ground cloud: (1) 344° at 8.3 m/s measured at early times while sampling at higher-altitudes (700 to 1350 m MSL) and (2) 331° at 7.7 m/s measured at later times while sampling at lower altitudes (450 to 850 m MSL). The single long arrow with a thick shaft represents the imagery-derived ground cloud bearing of 340° at 6.8 m/s measured during the first 32 min after launch (Section 2). The imagery also quantified the ground cloud's stabilization height as 855m MSL (702 m AGL). Therefore, at early times, the aircraft sampled the cloud at altitudes slightly higher than the middle of the stabilized cloud. At later times, the aircraft sampled the cloud at altitudes lower than the middle of the stabilized cloud. The three additional arrows with the thin shafts document the REEDM predictions for the ground cloud bearing: (1) the 324° bearing to maximum concentration at 577m MSL (or 424 m AGL, which was REEDM's T–0.25h prediction for the stabilization height); (2) the 321° bearing of the ground cloud at stabilization time; and (3) the 330° average wind bearing for the second mixing layer (i.e., this dominates the bearing for the stabilized cloud at later times).

Figure 15 also includes three arrows located to the right of the map that document the T–0.25h rawinsonde-derived wind directions measured at altitudes corresponding to the imagery-derived bottom, middle, and top of the stabilized ground cloud. Although the rawinsonde launch originated from Building 1764 (located on North VAFB as illustrated in Figure 15), the arrows that document the rawinsonde wind directions are anchored to the right of the map to avoid clutter. Lastly, Figure 15 documents the locations of the rawinsonde release site and the three imagery sites used by The Aerospace Corporation.

It is evident from examination of Figure 15 and from the discussion in the preceding paragraph that REEDM cloud bearing predictions could be interpreted as a 324° bearing during rise, a 321° bearing at stabilization, and a 330° bearing after stabilization at 577m MSL (424m AGL). These predictions are significantly different from the imagery-derived cloud bearing of 340° with a stabilization height of 855m MSL (702 m AGL). The aircraft-derived cloud bearing of 344° (measured at early times and higher altitudes) is closer to the imagery-derived 340° than the REEDM-predicted 330°. In contrast, the aircraft-derived cloud bearing of 331° (measured at later times and lower altitudes) is almost identical to REEDM's predicted 330°. The pre-launch

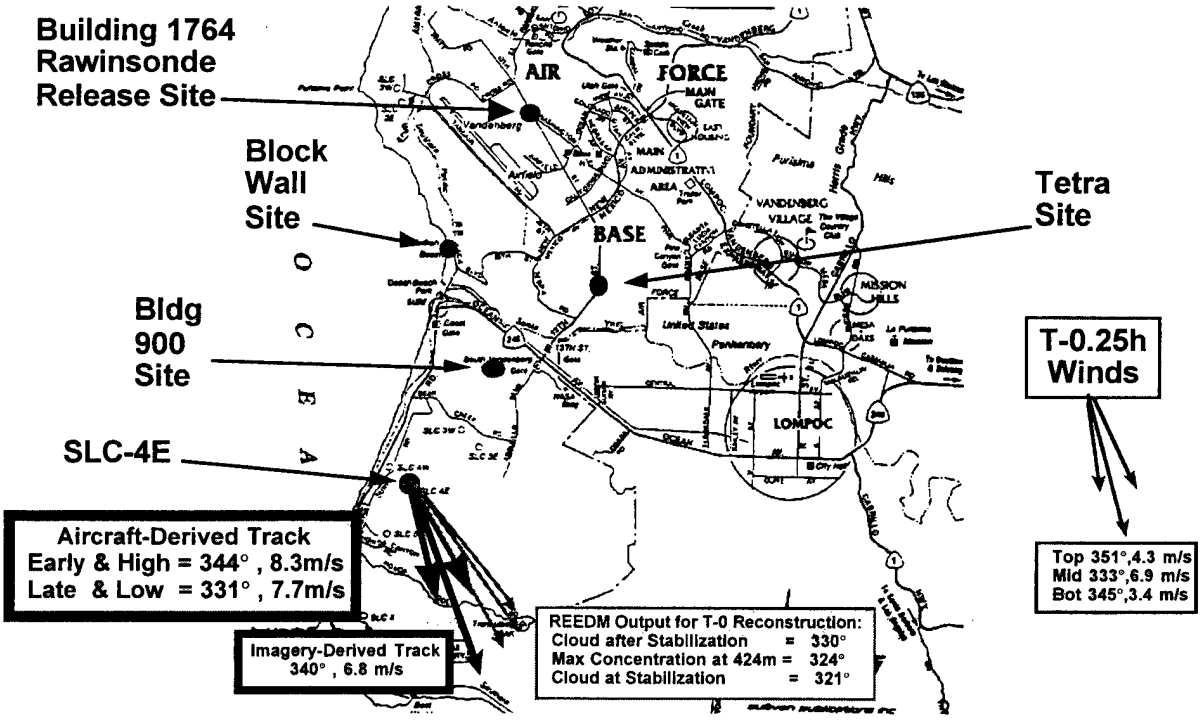

Figure 15. Partial map of VAFB documenting the locations of the rawinsonde release site, the three imagery sites, and the available #K22 ground cloud data. The #K22 ground cloud data includes: the aircraft-derived ground cloud bearings, the imagery-derived ground cloud bearing, the REEDM predictions for the ground cloud bearing, and the wind directions measured at the imagery-derived altitudes corresponding to the top, middle, and bottom of the stabilized ground cloud. The rawinsonde sounding was at 2117 GMT (T–0.25h) from Building 1764 and was modified using Doppler acoustic sounder data to synthesize the T–0h reconstruction. The ground cloud bearings are anchored to SLC-4E pad, and the rawinsonde winds to the right of the map.

wind directions (351, 330, and 345° measured at heights equivalent to the top, middle, and bottom of the stabilized ground cloud, respectively) bracket not only the cloud bearings measured by the aircraft (early and late data) and by the imagery (early data) but also those predicted by REEDM.

The following sections of this report will document the aircraft's HCl concentration measurements and, when useful, will compare them to REEDM, rawinsonde, and imagery-derived data. It is important to remember that REEDM predicts the dispersion of the cloud using a single rawinsonde sounding from a site that is remote from the launch pad. The winds can vary with time and over terrain. The rawinsonde data document that the winds vary with altitude. Therefore validation of REEDM is necessary.

3.3.1. Overview of Aircraft Sampling Data

3.3.1.1 Raw Aircraft Data

Table 5 presents a sample of the aircraft's data as delivered to The Aerospace Corporation with added headings. The headings are as follows: Log (mission log number assigned by NOAA); yr (year); d (Julian day of the year); hm (local time by inaccurate data logger clock in hour and minutes, two digits each); s (seconds by the data logger); ppm (raw HCl concentration based upon single-point calibration and mV response from the Geomet); rng (range of the Geomet); mV

Table 5. Five Seconds from the Aircraft's Data File as Provided to The Aerospace Corporation by NOAA. These data include the aircraft's first detection of the Titan IV #K22 ground cloud. Note that the "hm" column does not agree with the "tGPS" column. The Aerospace Corporation registered all data to the GPS time using the seconds from the "s" column. When "tGPS" was not available, the computer time ("hm" column) was used to interpolate the time between valid "tGPS" entries.

Log	yr	d	hm	s	ppm	rng	mV	tGPS	lat	N/S	lon	E/W	diff	# Sat	HDOP	alt	units
113	1996	133	1440	21	0.07	193	1753	214033	3436.5518	N	12035.7345	W	1	6	1.2	790	M
113	1996	133	1440	21.25	0.07	193	1760	214033	3436.5518	N	12035.7345	W	1	6	1.2	790	M
113	1996	133	1440	21.5	0.892	1813	22.29	214033	3436.5518	N	12035.7345	W	1	6	1.2	790	M
113	1996	133	1440	21.75	0.486	825	1216	214034	3436.5129	N	12035.7397	W	1	6	1.2	791	M
113	1996	133	1440	22	5.67	1379	1418	214034	3436.5129	N	12035.7397	W	1	6	1.2	791	M
113	1996	133	1440	22.25	9.89	1479	2473	214034	3436.5129	N	12035.7397	W	1	6	1.2	791	M
113	1996	133	1440	22.5	30.09	1816	752	214034	3436.5129	N	12035.7397	W	1	6	1.2	791	M
113	1996	133	1440	22.75	25.75	1816	643.8	214035	3436.474	N	12035.7451	W	1	6	1.2	791	M
113	1996	133	1440	23	12.03	1816	300.8	214035	3436.474	N	12035.7451	W	1	6	1.2	791	M
113	1996	133	1440	23.25	38.9	1816	972	214035	3436.474	N	12035.7451	W	1	6	1.2	791	M
113	1996	133	1440	23.5	41.73	1815	1043	214035	3436.474	N	12035.7451	W	1	6	1.2	791	M
113	1996	133	1440	23.75	40.62	1815	1015	214036	3436.4354	N	12035.7511	W	1	6	1.2	791	M
113	1996	133	1440	24	45.22	1816	1131	214036	3436.4354	N	12035.7511	W	1	6	1.2	791	M
113	1996	133	1440	24.25	45.46	1816	1136	214036	3436.4354	N	12035.7511	W	1	6	1.2	791	M
113	1996	133	1440	24.5	43.77	1815	1094	214036	3436.4354	N	12035.7511	W	1	6	1.2	791	M
113	1996	133	1440	24.75	42.35	1815	1059	214037	3436.3969	N	12035.7573	W	1	6	1.2	791	M
113	1996	133	1440	25	43.65	1815	1091	214037	3436.3969	N	12035.7573	W	1	6	1.2	791	M
113	1996	133	1440	25.25	43.92	1815	1098	214037	3436.3969	N	12035.7573	W	1	6	1.2	791	M
113	1996	133	1440	25.5	39.27	1815	982	214037	3436.3969	N	12035.7573	W	1	6	1.2	791	M
113	1996	133	1440	25.75	32.88	1815	822	214038	3436.3586	N	12035.7634	W	1	6	1.2	793	M
113	1996	133	1440	26	29.54	1815	739	214038	3436.3586	N	12035.7634	W	1	6	1.2	793	M

(Geomet response in millivolts); tGPS (GPS receiver GM time in hhmmss [documenting hours minutes seconds as six digits without separation]); lat (latitude, ddmm.mmmm, in degrees and decimal minutes); N/S (label for latitude, North/South); lon (longitude, ddmm.mmmm, in degrees and decimal minutes); E/W (label for longitude, East/West); diff (differential, 2, or normal, 1, GPS mode); # Sat (number of GPS Satellites); HDOP (horizontal dilution of precision [measure of GPS accuracy]); alt (altitude reported from GPS receiver); and units (M, meters for alt). The hm column is local and inaccurate computer time. Therefore, tGPS was used to interpret the aircraft data (using the "s" column to bin data reproducibly). The hm data were only used to interpolate between valid tGPS entries when the GPS failed to log time. Personnel from The Aerospace Corporation have reviewed these data in 10-min increments and applied baseline corrections to eliminate negative HCl concentrations. Personnel from The Aerospace Corporation have also performed the conversions necessary to report distance, polar angles, and Cartesian position in meters relative to SLC-4E.

3.3.1.2 Cartesian Plot of the Aircraft's Data

Figure 16 plots the spatial extent of aircraft's sampling during 100 min following the #K22 launch. It represents conversion of the latitude and the longitude of the aircraft's position to Cartesian coordinates centered on the SLC-4E space launch complex. The aircraft's position is labeled with HCl concentration at each sampling position by the use of different plot symbols.

Figure 16 documents that the aircraft's flight pattern was confined to a 20 km × 40 km rectangle to the southeast of the launch complex. The aircraft flew predominantly cross-wind sampling

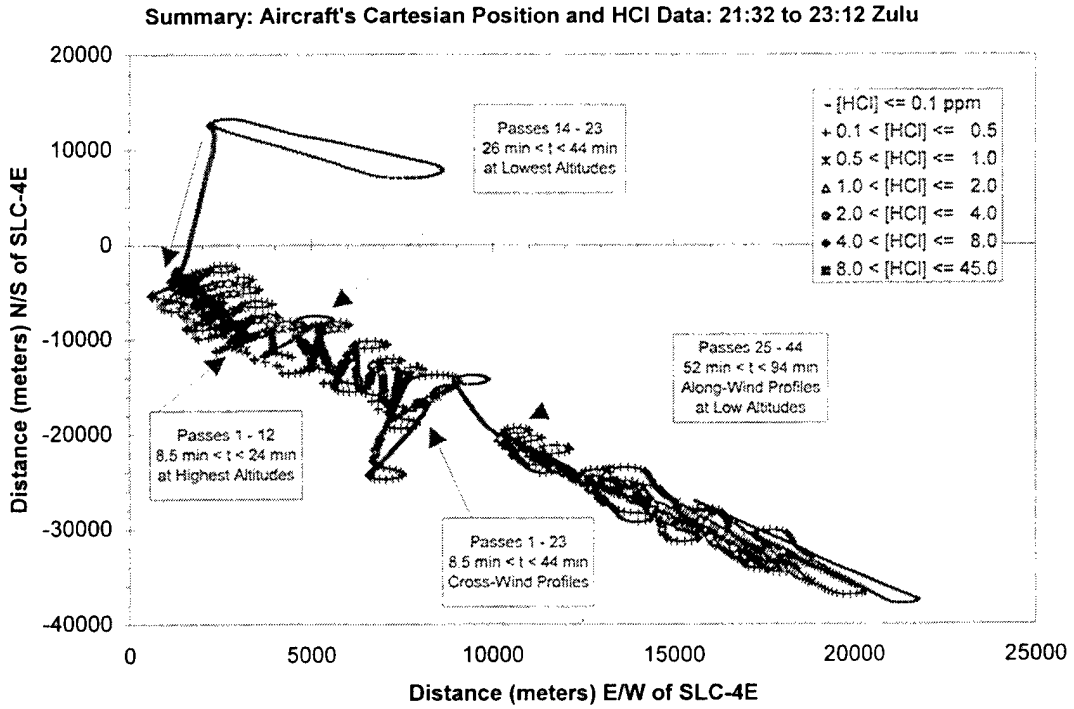

Figure 16. Cartesian plot documenting the aircraft's x-y position relative to SLC-4E and the measured HCl concentrations (based upon the Geomet detector) throughout the 100-min #K22 exhaust cloud sampling mission.

profiles during the first 44 min after launch (passes 1–23) and then shifted to along-wind sampling profiles from 52 to 94 min after launch (passes 25–44). Time (0–100 min), polar angle (0° to 360° in the rawinsonde convention), distance (0–40000 m), and altitude (0–1400 m MSL) are variables for the aircraft data and are documented in subsequent sections. The HCl concentration hits illustrated in Figure 16 can be interpreted in light of these other critical variables. During the first 12 passes (8.5 to 23 min), the aircraft sampled altitudes ranging from 700 to 1350 m MSL. These altitudes correspond to sampling slightly below to slightly above the imagery-derived middle (855 m MSL) of the ground cloud. At later times, the aircraft sampled altitudes ranging from 450 to 850 m MSL. These altitudes correspond to sampling below to sampling at the middle of the ground cloud. This shift in sampling altitude at 24 to 26 min after launch is coincident with the shift in the cloud bearing that is apparent in Figure 16.

3.3.1.3 Geomet Detector Response to Calibration Gases

Figure 17 and Figure 18 document pre-mission and post-mission calibration gas response curves for the Geomet as deployed for the #K22 mission. The Geomet's configuration was equivalent for the #K23, #K15, #K22, and #K16 missions. Prior to the #K22 mission, the Geomet reached 90% of its plateau in response within 30 s after the start of exposure to 1.1 ppm HCl vapor. After the #K22 sampling mission, the Geomet reached only 73% of its plateau in response within 30 s and required 112 s to reach 90% of its plateau in response to 1.0 ppm HCl vapor. In addition to the slower response time, the Geomet had only 91% of its pre-mission sensitivity (V/ppm). This behavior is consistent with the performance observed on previous Titan IV ground cloud sampling campaigns.

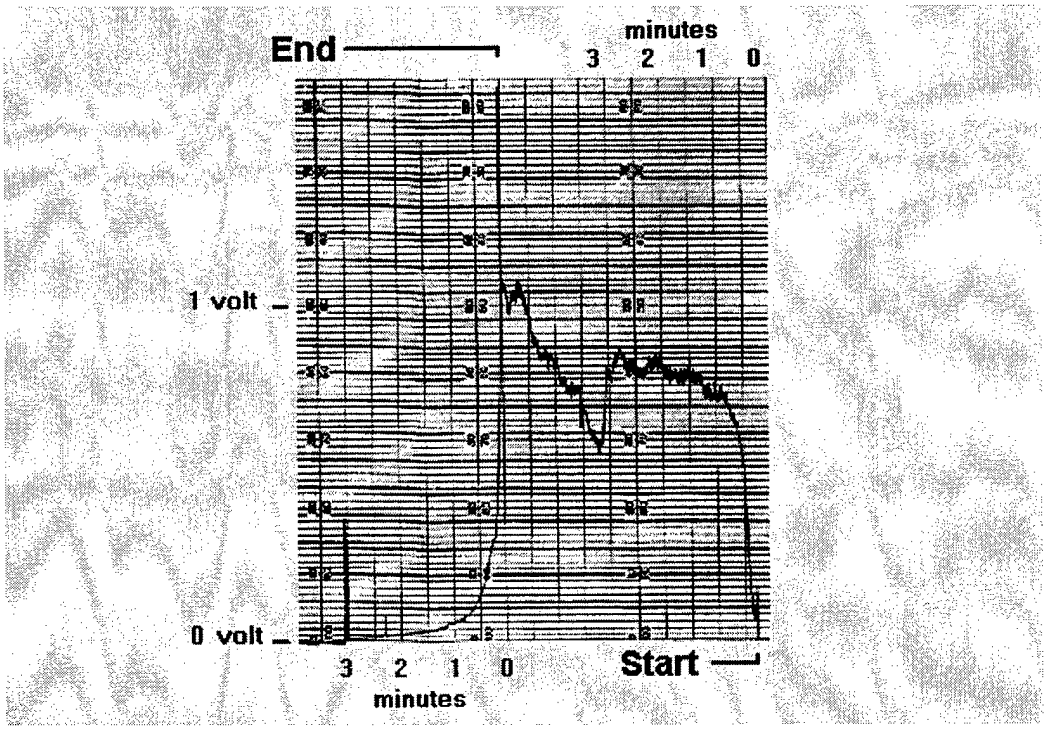

Figure 17. #K22 pre-flight raw response of the Geomet to 1.106 ppm HCl vapor. The operator adjusted the Geomet's plateau response to a V/ppm sensitivity during this period.

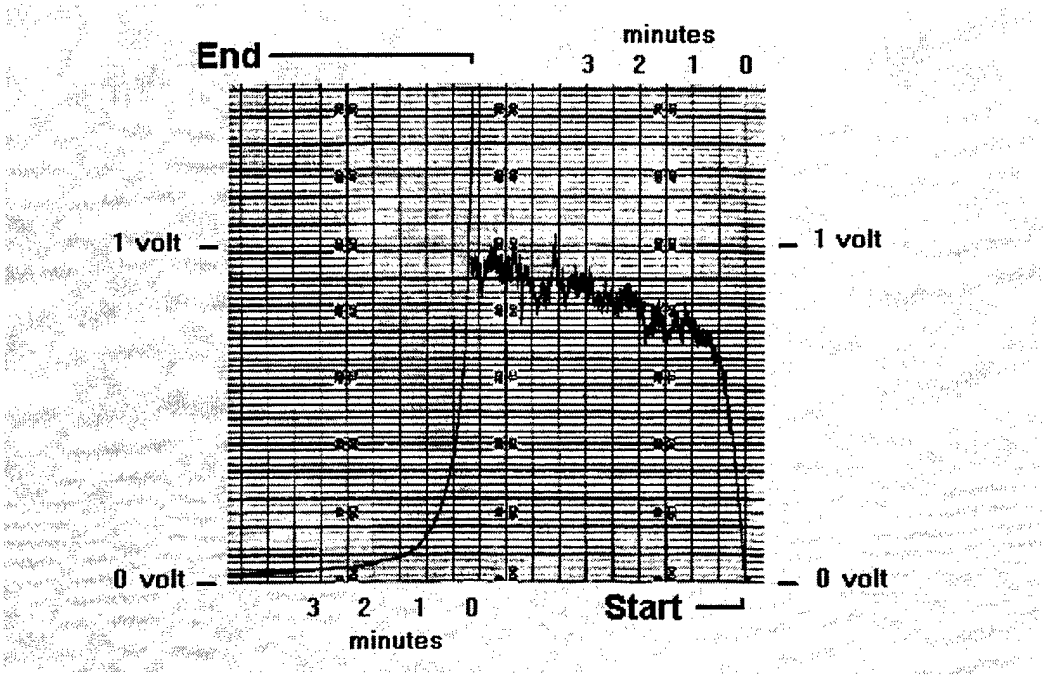

Figure 18. #K22 post–flight raw response of the Geomet to 1.035 ppm HCl vapor. This data documents a 0.91 V/ppm sensitivity for the Geomet with a reagent-depleted inlet.

The response characteristics of the Geomet detector make it useful, but not ideal, for aircraft sampling of Titan IV exhaust clouds. As configured for the Titan IV #K22 mission and as illustrated by Figures 17 and 18, the Geomet requires 30 s (or more) to reach 90% of its plateau in response. By comparing the data presented in Figures 17 and 18, one can see that the magnitude of the plateau in response as well as the time to reach it can worsen when the exposure times are extremely long (as in the #K22 mission, which sampled the launch cloud for 100 min). This is consistent with depletion of the reagent that coats the inlet. For all of the Titan IV missions (i.e., #K23, #K15, #K16, and #K22), the Geomet's inlet was coated with reagent once prior to the flight. Therefore, one would expect some systematic degradation in the Geomet's response characteristics during each sampling mission.

Since the aircraft is moving at more than 70 m/s and it takes 30 (or more) seconds for the Geomet to provide 90% response to the new HCl concentration, it is likely that the Geomet may underestimate the maximum HCl concentration for short encounters with the cloud. However, Figures 17 and 18 illustrate that the initial response to 10% of the plateau in response is extremely rapid. Thus, there should be little offset between the Geomet's first indication of change and the aircraft's encounter with the edge of the exhaust cloud. Therefore, we use the Geomet's HCl data to establish the position and relative strength of the exhaust cloud with the realization that the reported HCl concentration is an average value that depends upon the exposure history of the Geomet and the abruptness of HCl concentration changes.

In Section 3 of the #K16 report,[3] the Geomet's raw response and its integrated response were plotted against time for pre-flight and post-flight calibrations. Those plots documented that the Geomet accurately integrated the total HCl dose for those HCl vapor exposures. That analysis of the calibration curves was easy for the #K16 data since I-NET used a computer-based data logger for that calibration data rather than the strip chart recorder that they used for the #K22 calibration data. Since the Geomet's configuration was equivalent for the #K23, #K15, #K22, and #K16 missions, we can use the #K16 plots to establish this characteristic for the Geomet as deployed for all of these missions. In summary, the Geomet calibrations are HCl vapor challenges using constant concentration for long exposure times. These data illustrate that the Geomet has an almost instantaneous response to sudden large changes in HCl vapor concentration, and that the Geomet accurately measures the total HCl dose for each exposure. Therefore, the Geomet should accurately map not only the extent but also the average concentration (integrated dose divided by time) for each encounter with the Titan IV exhaust cloud.

3.3.1.4 Simultaneous Geomet and GFC Sampling of a Titan IV Exhaust Cloud

The temporal, relative, and absolute accuracy of the Geomet's response to a Titan IV exhaust cloud has been documented for the first few minutes after launch by comparison of the Geomet's cloud data to that of the Spectral Sciences gas filter correlation (GFC) spectrometer that flew on the same aircraft for the #K15 mission. The GFC spectrometer provided an instantaneous response to the exhaust cloud and was mounted beneath the aircraft. The inlet to the Geomet extended out of the front of the same aircraft. A GFC spectrometer was not flown on the #K22 mission so we will reference the #K15 data in this discussion.

Spectral Sciences provided a description of the GFC spectrometer setup, its calibration, and their analysis of the #K15 exhaust cloud data in Section 4 of the #K15 report.[4] In that section, they documented that the GFC spectrometer's optics were irreversibly coated with exhaust cloud aerosols every pass through the cloud. This resulted in a dramatic decrease in signal-to-noise ratio with every encounter with a cloud. However, the GFC technique, as deployed for #K15, had an almost instantaneous response to HCl vapor since there was no inlet to their GFC cell (i.e., that is why it was directly exposed to the exhaust cloud).

In Section 3 of the #K15 report, we compared the GFC data to the Geomet data to establish the significance of the Geomet's response characteristics for actual aircraft sampling of Titan IV #K15 exhaust cloud. This comparison documented excellent temporal agreement between the GFC spectrometer and the Geomet detector for actual exhaust cloud encounters. Therefore, the start of response upon entering the edge of the cloud and initial fall upon exiting the cloud should accurately map the extent of the cloud. This is consistent with the Geomet's rapid initial response to sudden changes in HCl concentration (i.e., the calibration data). These same comparisons documented excellent positional accuracy for the maximum concentration reported by the Geomet relative to that recorded by the GFC technique. Therefore, the Geomet's fast initial

response to significant changes makes it useful for mapping the position and shape of Titan IV launch clouds.

Section 3 of the #K15 report also investigated the effect of averaging time upon the comparison of GFC data to Geomet data. The analysis of that data is consistent with the Geomet's documented two-part response curve: (1) rapid initial response to a change in HCl concentration and (2) a slower rollover in response prior to reaching a plateau. The Geomet's fast component allows it to map the extent and position of the launch cloud as well as 3.85 s averaged GFC data. The GFC data had to be averaged with an 18-s period to equal the Geomet's maximum response, which is consistent with the longer times required for full Geomet response. Since the GFC technique only responds to vapor, while the Geomet responds to total (aerosol and vapor) HCl, this treatment could not provide quantitative rise characteristics for the Geomet. In summary, the Geomet not only provides quantitative integrated HCl for each pass through the cloud but also accurately maps the extent and position of the cloud by virtue of the fast component of its complicated response function.

3.3.2 HCl Concentration Hits as a Function of Bearing from SLC-4E

Figure 19 substantiates that the aircraft focused on a modest range of polar angles relative to the launch complex during its sampling of the #K22 ground cloud. In this report, the angles

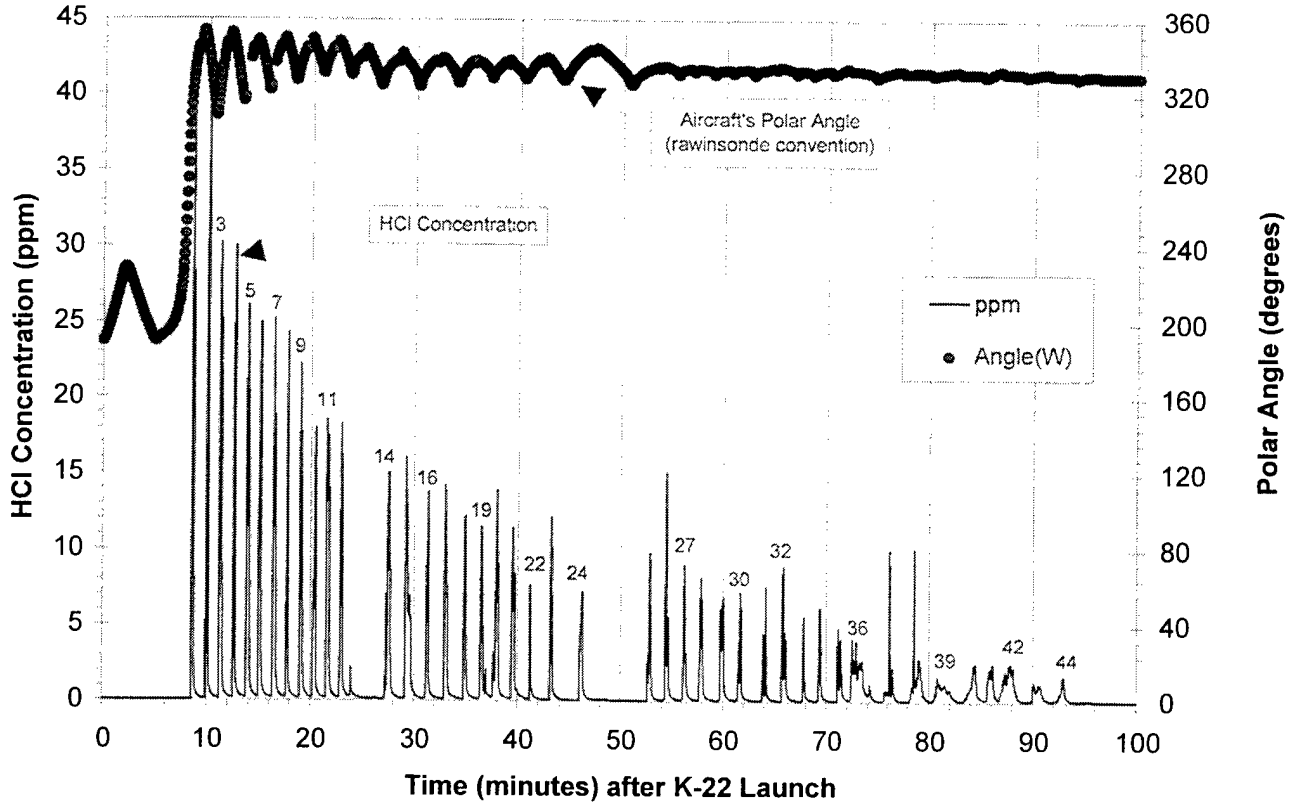

Figure 19. Summary of the aircraft's HCl concentration measurements and its polar angles (rawinsonde convention) plotted against time (minutes) after the Titan IV #K22 launch. This plot documents that the ground cloud moved along a southeasterly bearing.

reported will conform to the convention of rawinsonde wind vectors (the angle from which the wind originates that would push the cloud to the sampled position). Thus, the angles are related by

$$J = 180 + F \tag{3}$$

where ϑ is the equivalent rawinsonde wind angle, and Φ is the measured polar angle of the aircraft relative to SLC-4E and clockwise of true north. For example, when the aircraft is due east of SLC-4E, Φ is 90°, and ϑ is 270°. The nominal bearing of the ground cloud during the first 32 min after launch was shown by imagery to be 340° in previous report ***(Author: What report?)*** (Section 2) and in Figure 15. The T–0.25h rawinsonde wind vectors at the bottom, middle, and top of the observable ground cloud were 345°, 333°, and 351°, respectively, as documented in Figure 15. Referring to Figure 19, we will document that these data are consistent with the movement of the ground cloud along a bearing of 340° (based upon sampling at higher altitudes and early times) and along a bearing of 331° (based upon sampling at lower altitudes and later times). It is our conclusion that these HCl hits derive from sampling of the ground cloud as it is defined by REEDM and visualized by imagery.

3.3.3 HCl Concentration Hits as a Function of Radial Distance from SLC-4E

Figure 20 is a plot of the HCl concentration and of the aircraft's radial distance from SLC-4E against time after the #K22 launch. Figure 20 can be used to illustrate several logical conclusions

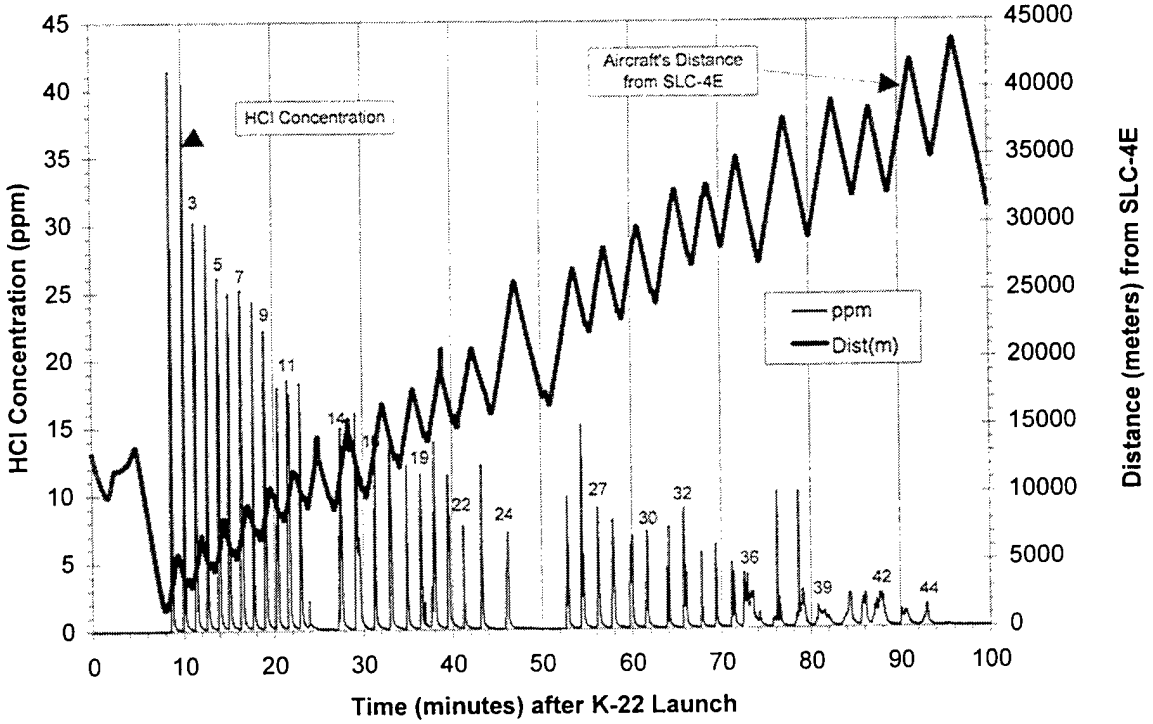

Figure 20. Summary of the aircraft's HCl concentration measurements and radial distances (m) from SLC-4E plotted against time (min) after the Titan IV #K22 launch.

regarding the aircraft's sampling campaign. The highest HCl concentrations are encountered at early times and close (<12 km) to the launch complex. As discussed previously and documented in later sections, the aircraft sampled at altitudes ranging from 700 to 1350 m MSL during this early period. Significant HCl concentrations (2–10 ppm) were observed at later times and at ranges of 12 to 40 km from SLC-4E. As discussed previously and documented in subsequent sections, the aircraft sampled at altitudes ranging from 450 to 850 m MSL during this later period. The most remote detection of the ground cloud occurred more than 94 min after launch and approximately 40 km from SLC-4E launch pad. All HCl hits, both initially and after down-wind dispersion, were observed to the southeast of SLC-4E, as discussed in the previous section. As documented in later sections, the bulk of the HCl hits was at altitudes between 500 and 1000 m MSL.

3.3.4 HCl Concentration Hits as a Function of Sampling Altitude

Figure 21 is a plot of the aircraft's HCl concentration data and of the aircraft's GPS altitude against time after the #K22 launch. Figure 21 documents that at early times (i.e., 0–23 min after launch) the HCl sampling was at altitudes between 700 and 1350 m MSL, which corresponds to the middle and upper half of the ground cloud as revealed by imagery during the first 32 min

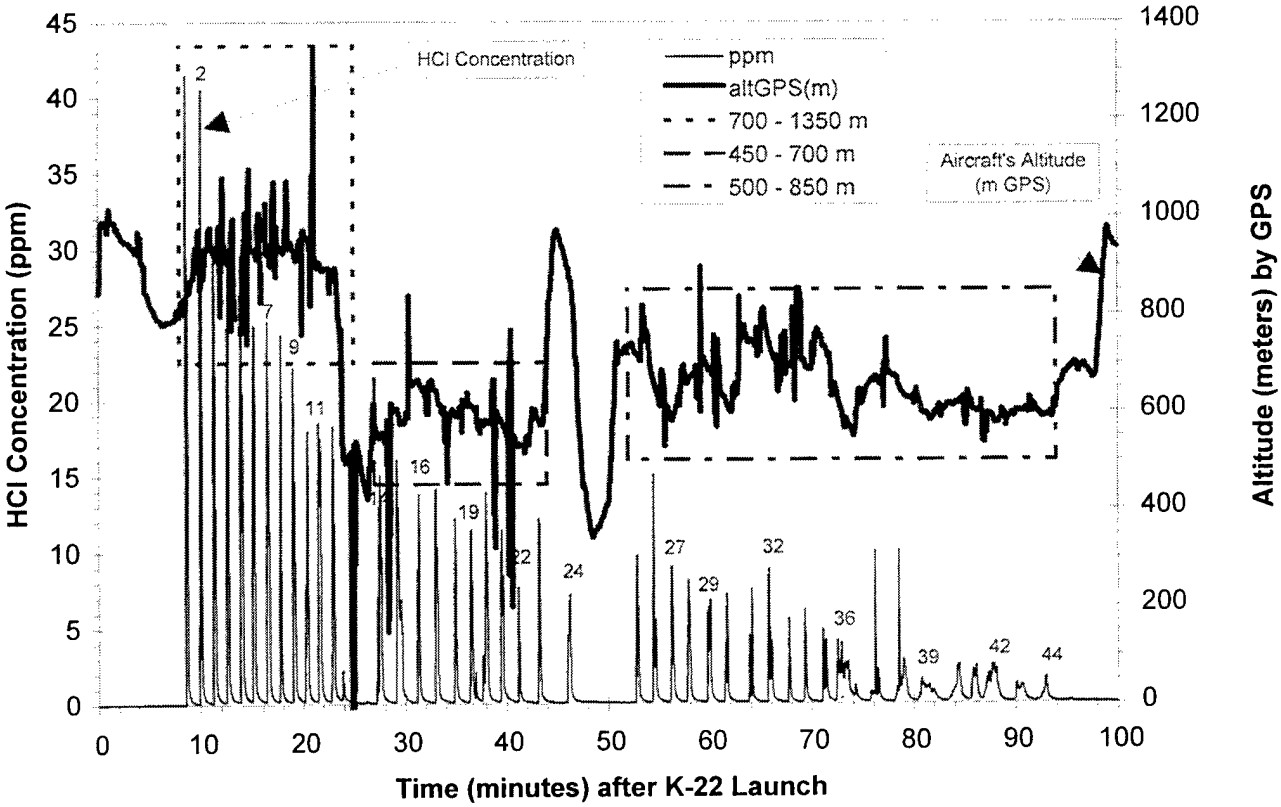

Figure 21. Summary of the aircraft's HCl concentration measurements and altitude (m) plotted against time (min) after the Titan IV #K22 launch.

after launch. Figure 21 documents that at later times (i.e., 27–94 min after launch) the HCl sampling was at altitudes between 450 and 850 m MSL, which corresponds to the middle and lower half of the ground cloud as revealed by imagery during the first 32 min after launch. Figure 16 documented a shift in the ground cloud's bearing coincident with this shift in the aircraft's sampling altitude. Therefore, these data suggest that the lower portion of the ground cloud moved on a more easterly bearing than the upper portion of the ground cloud or that the wind direction shifted at a time coincident with the aircraft's shift in sampling altitude.

3.3.5 HCl Concentration Hits as a Function of Aircraft Altitude and Position

This section will provide substantiation for observations made in previous portions of this overview of the aircraft's sampling data. The figures referenced in this section are subsets of the data presented in the Cartesian plot in Figure 16.

3.3.5.1 700 to 1350 m Altitudes and Cross-Wind Profiles at Early Times

Figure 22 is a Cartesian plot, centered at SLC-4E, of the aircraft's sampling data collected at altitudes between 700 and 1350 m MSL and at times between 8.5 and 23 min after the #K22 launch.

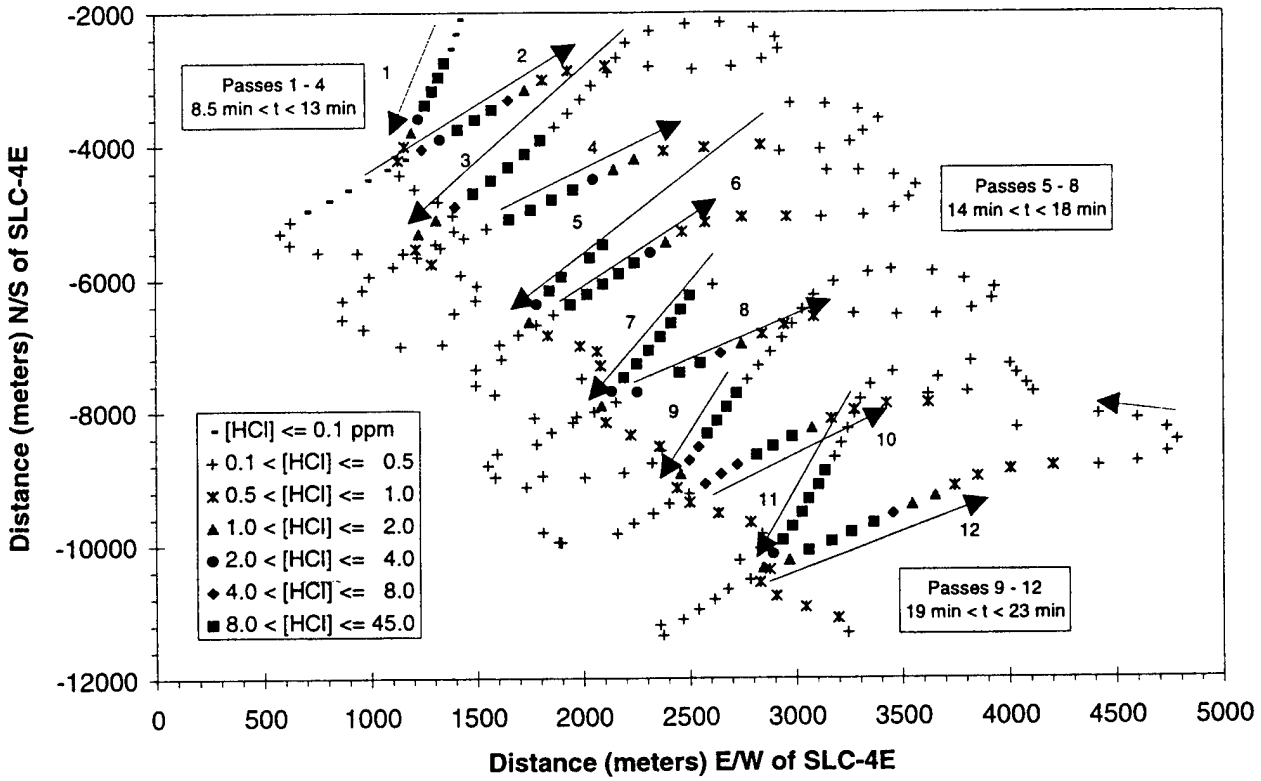

Figure 22. Summary Cartesian plot documenting the aircraft's position and measured HCl concentrations while sampling at altitudes between 700 and 1350 m MSL and at times between 8.5 and 23 min after the Titan IV #K22 Launch. These data document a southeasterly cloud bearing at altitudes within the middle and the top half of the ground cloud. For comparison, the imagery-derived altitudes were 317, 855, and 1393 m MSL for the bottom, middle, and top, respectively, of the stabilized cloud on a southeasterly bearing.

The aircraft's HCl concentration profiles document a southeasterly bearing for the cloud at these high altitudes. These early data can be directly compared to the imagery data collected during the first 32 min after launch. The imagery not only documented a southeasterly bearing for the cloud but also reported stabilization heights of 317, 855, and 1393 m MSL for the bottom, middle, and the top, respectively, for the ground cloud. Therefore, the aircraft's data presented in Figure 22 represent sampling in the middle and top half of the stabilized ground cloud (as defined by imagery).

3.3.5.2 450 to 700m Altitudes and Cross-Wind Profiles at Intermediate Times

Figure 23 is a Cartesian plot, centered at SLC-4E, of the aircraft's sampling data collected at altitudes between 450 and 700 m MSL and at times between 27 and 44 min after the #K22 launch. These HCl concentration profiles document a more easterly bearing than measured at earlier times by either the aircraft (i.e., Figure 22 covering 8.5 to 23 min) or by the imagery (Section 2 and Figure 15 covering the first 32 min after launch). Therefore, the data in Figure 23 document

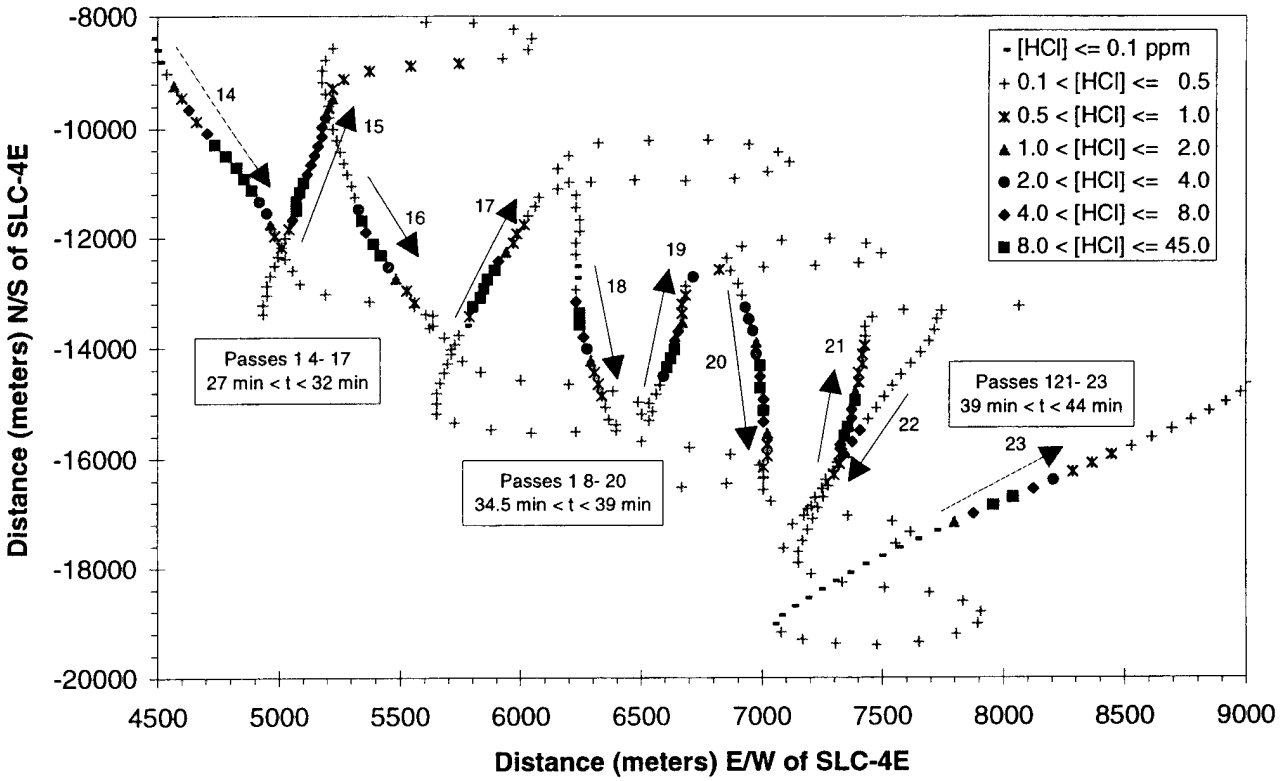

Figure 23. Summary Cartesian plot documenting the aircraft's position and measured HCl concentrations while sampling at altitudes between 450 and 700 m MSL between 27 and 44 min after the Titan IV #K22 Launch. These data document a shift in cloud bearing from earlier data. For comparison, the imagery-derived altitudes were 317, 855, and 1393 m MSL for the bottom, middle, and top, respectively, of the stabilized cloud on a southeasterly bearing (340° measured 4 to 32 min after launch). Therefore, these aircraft data are collected at altitudes within the lower half of the stabilized ground cloud.

a shift in the ground cloud's bearing that represents either lower altitudes or later times. The aircraft did not sample higher altitudes (i.e., Figure 22) at these distances. The imagery-derived altitudes (measured 4–32 min after launch) were 317, 855, and 1393 m MSL for the bottom, middle, and top of the stabilized ground cloud along a southeasterly bearing. Therefore, the aircraft data presented in Figure 23 represent sampling in the lower half of the ground cloud (as documented by quantitative imagery). The rawinsonde wind bearing near the bottom of the stabilized cloud was 345°, which would push the cloud to the southeast as observed at early times. At later times, the cloud moves in a more easterly direction closer to the 330° predicted by REEDM for the second transition layer. This bearing is closer to the rawinsonde wind bearing near the middle of the stabilized cloud, which was 333°. The rawinsonde data was from T–0.25h.

3.3.5.3 500 to 850m Altitudes and Along-Wind Profiles at Later Times

Figure 24 is a Cartesian plot, centered at SLC-4E, of the aircraft's sampling data collected at altitudes between 500 and 850 m MSL at times between 52 to 94 min after launch. The imagery-

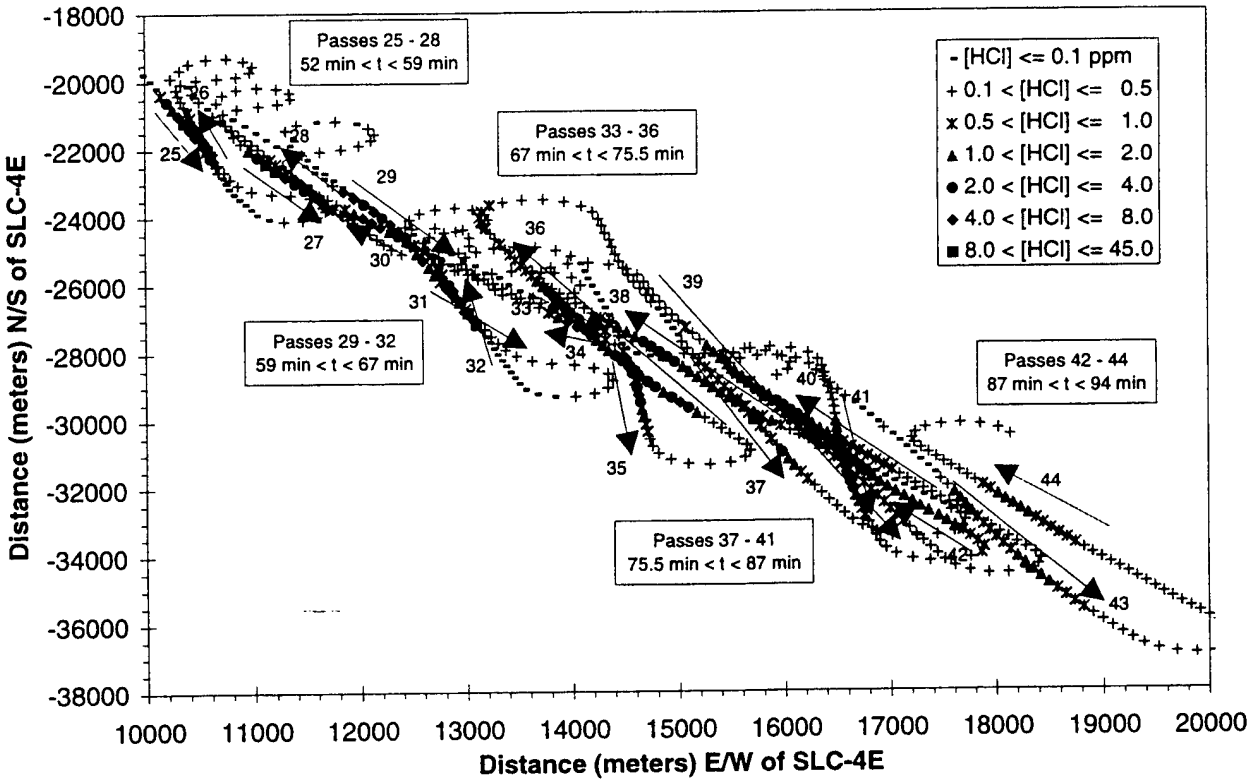

Figure 24. Summary Cartesian plot documenting the aircraft's position and measured HCl concentrations while sampling at altitudes between 500 and 850 m MSL between 52 and 94 min after the Titan IV #K22 Launch. The cloud bearing appears to be more easterly than documented by the aircraft data at higher altitudes and early times. For comparison, the imagery-derived altitudes were 317, 855, and 1393 m MSL for the bottom, middle, and top, respectively, of the stabilized cloud on a southeasterly bearing (340° measured 4 to 32 min after launch). Therefore, these aircraft data are collected at altitudes at the middle and lower half of the stabilized ground cloud.

derived altitudes (measured 4–32 min after launch) were 317, 855, and 1393 m MSL for the bottom, middle, and top, respectively, of the stabilized ground cloud along a southeasterly bearing. Therefore, Figure 24's along-wind HCl concentration profiles are at altitudes corresponding to the middle and lower half of the stabilized ground cloud. The cloud bearing is the same as documented by Figure 23 for lower altitudes and slightly earlier times. Therefore, the aircraft data documents that, at later times, the lower portion of the ground cloud moves along a more easterly bearing than observed, at early times, for the upper portion of the ground cloud.

3.3.5.3.1 500 to 850m Altitudes and Along-Wind Profiles at Later Times – Detail 1.

Figure 25 is a Cartesian plot, centered at SLC-4E, of the aircraft's sampling data collected at altitudes between 500 and 850 m MSL at times between 52 and 67 min after launch. Therefore, these data are a subset of the data plotted in Figure 24. Figure 25 allows the reader to review the aircraft data more carefully than is possible in Figure 24.

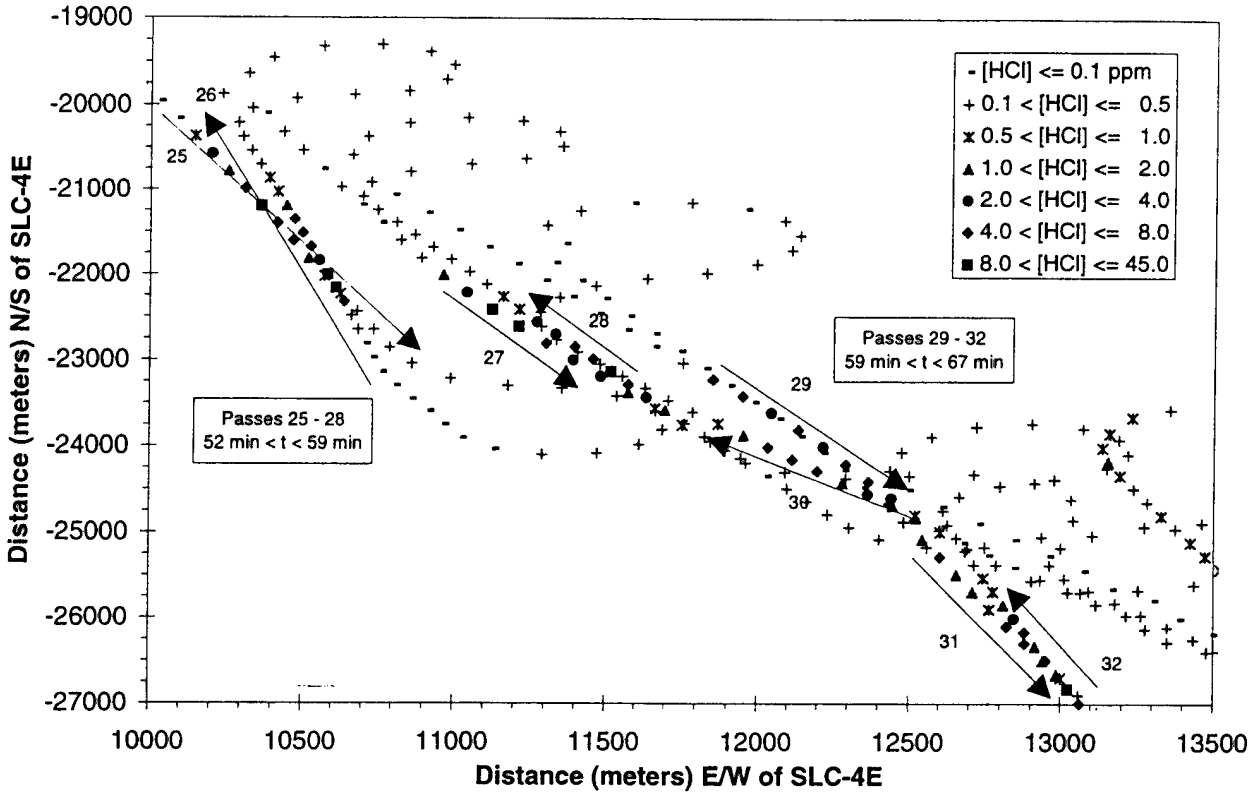

Figure 25. Summary Cartesian plot documenting the aircraft's position and measured HCl concentrations while sampling at altitudes between 500 and 850 m MSL between 52 and 67 min after the Titan IV #K22 launch (passes 25–32). The cloud bearing appears to be more easterly than documented by the aircraft data at higher altitudes and early times. For comparison, the imagery-derived altitudes were 317, 855, and 1393 m MSL for the bottom, middle, and top, respectively, of the stabilized cloud on a southeasterly bearing (340° measured 4 to 32 min after launch). Therefore, these aircraft data are collected at altitudes at the middle and lower half of the stabilized ground cloud.

3.3.5.3.2 500 to 850m Altitudes and Along-Wind Profiles at Later Times – Detail 2.

Figure 26 is a Cartesian plot, centered at SLC-4E, of the aircraft's sampling data collected at altitudes between 500 and 850 m MSL at times between 67 to 94 min after launch. Therefore, these data are a subset of the data plotted in Figure 24 and compliment the data presented in Figure 25. Figure 26 allows the reader to review the aircraft data more carefully than is possible in Figure 24.

3.3.6 Aircraft-Derived Cloud Bearing and Speed

As discussed previously, Figure 16 documented that the aircraft-derived bearing for the ground cloud shifted significantly when the aircraft dropped to lower altitudes (i.e., between 23 and 26 min after launch). In this section, we treat the early high-altitude aircraft data (i.e., Figure 27 and Figure 28) and the later lower-altitude data (i.e., Figure 29 and Figure 30) separately to quantify the cloud bearing and speed during each of these periods. Review of these figures reveals that at early times the higher-altitude portion of the ground cloud moved to the southeast along a bearing of 344° at an apparent speed of 8.3 m/s. In contrast, at later times, the lower-altitude portion

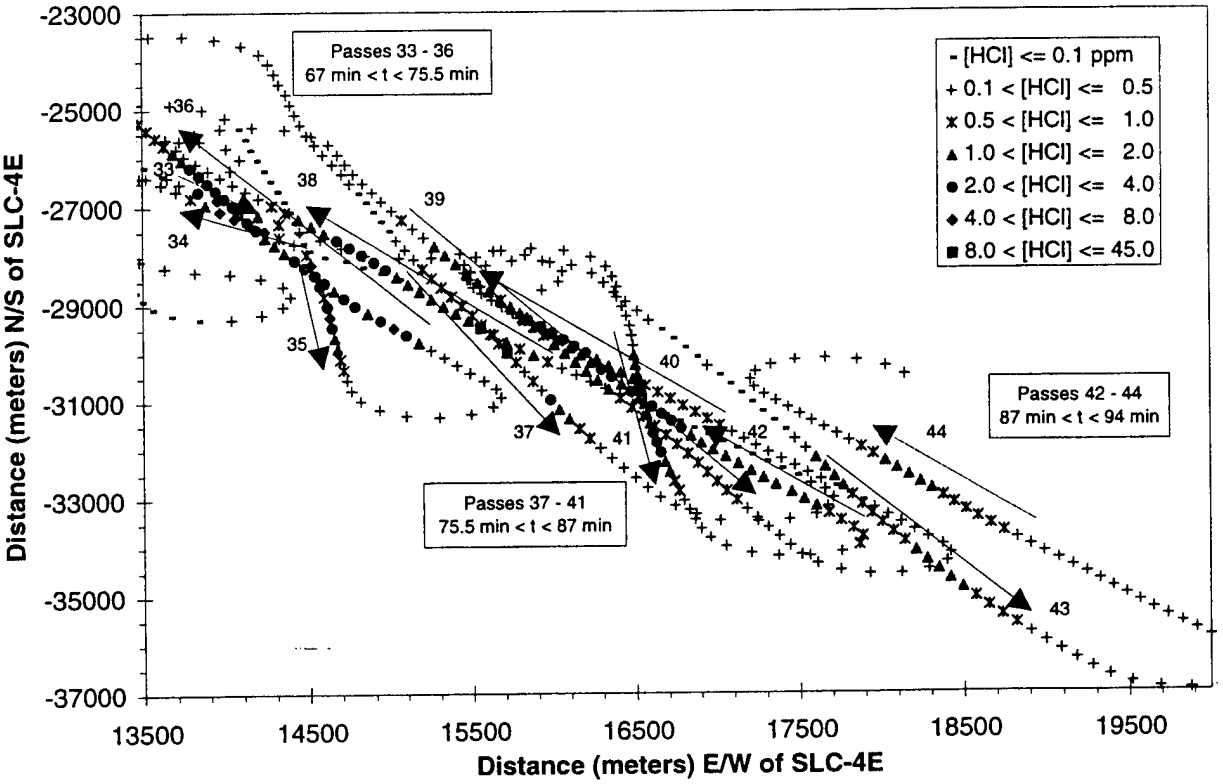

Figure 26. Summary Cartesian plot documenting the aircraft's position and measured HCl concentrations while sampling at altitudes between 500 and 850 m MSL between 67 and 94 min after the Titan IV #K22 launch (passes 33 to 44). The cloud bearing appears to be more easterly than documented by the aircraft data at higher altitudes and early times. For comparison, the imagery-derived altitudes were 317, 855, and 1393 m MSL for the bottom, middle, and top, respectively, of the stabilized cloud on a southeasterly bearing (340° measured 4 to 32 min after launch). Therefore, these aircraft data are collected at altitudes at the middle and lower half of the stabilized ground cloud.

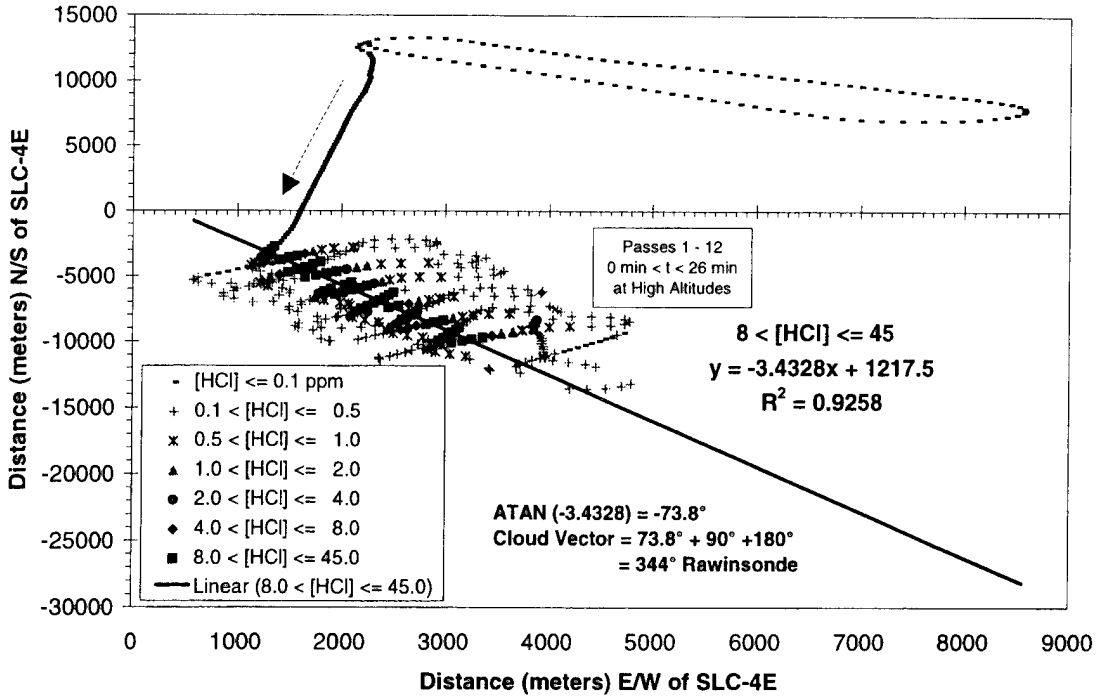

Figure 27. Aircraft-derived cloud bearing (344°) at early times (0–26 min for passes 1–12) and higher altitudes (700–1350 m). The aircraft flew only cross-wind profiles during this period.

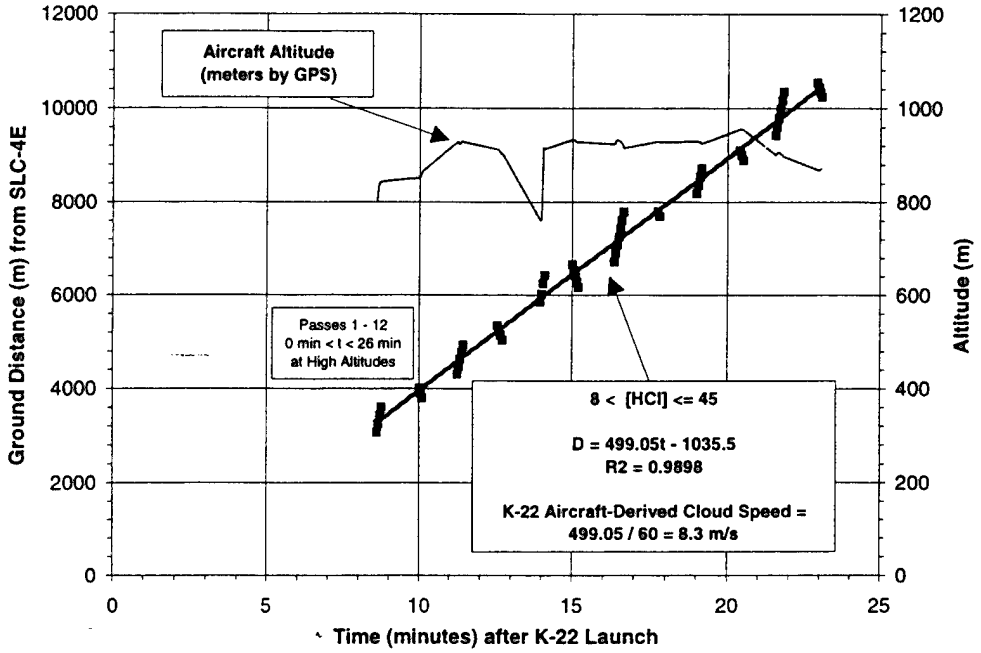

Figure 28. Aircraft-derived cloud speed (8.3 m/s) at early times (0–26 min for passes 1–12) and higher altitudes (700–1350 m). Since the aircraft did not necessarily fly through the center of the cloud, the aircraft-derived cloud speed can be biased by the flight pattern (i.e., high if the leading edge is sampled and low if the tailing edge is sampled).

of the ground cloud moved to the southeast along a bearing of 331° at an apparent speed of 7.7 m/s.

As mentioned previously, the aircraft concentrated on cross-wind profiles at early times (i.e., passes 1 through 23 at times between 8.5 to 44 min) and shifted to along-wind profiles at later times (i.e., passes 25 through 44 at times between 52 to 94 min). The data plotted in Figures 29 and 30 include both cross-wind and along-wind profiles that are fit by the same values of bearing and speed. Since the cross-wind profiles are best for measuring the bearing, while the along-wind profiles are better for measuring the speed, we are confident of both the bearing and the speed derived from the data presented in Figures 29 and 30, respectively. Since the aircraft does not necessarily sample the middle of the cloud, speeds derived solely from cross-wind profiles could be misleading (i.e., measured speed will be greater than the average if the leading edge is sampled or less than the average if the tailing edge is sampled). The data plotted in Figures 27 and 28 include only cross-wind profiles, and, therefore, we have more confidence in the ground cloud bearing than the ground cloud speed derived from these plots. Since the imagery data provides the outline of the ground cloud during the first 32 min after launch, one can interpret the aircraft's cross-wind profiles more accurately by review of the complimentary imagery data. Such an analysis is beyond the scope of this report.

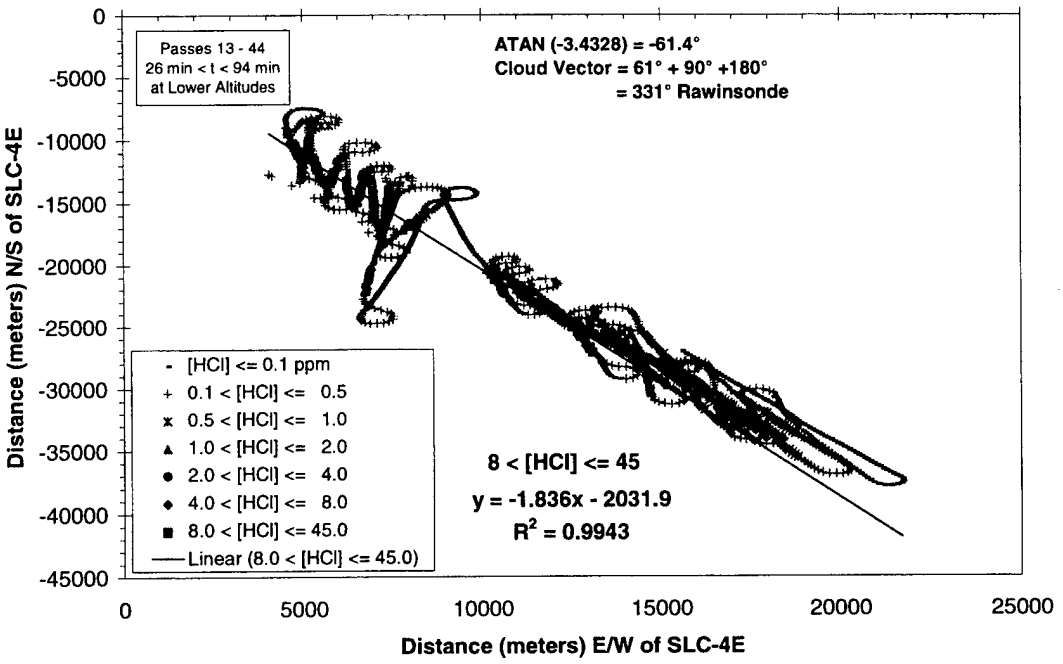

Figure 29. Aircraft-derived cloud bearing (331°) at later times (27–94 min for passes 13–44) and Lower Altitudes (450–850 m). Cross-wind for passes 13–23 and along-wind for passes 25–44.

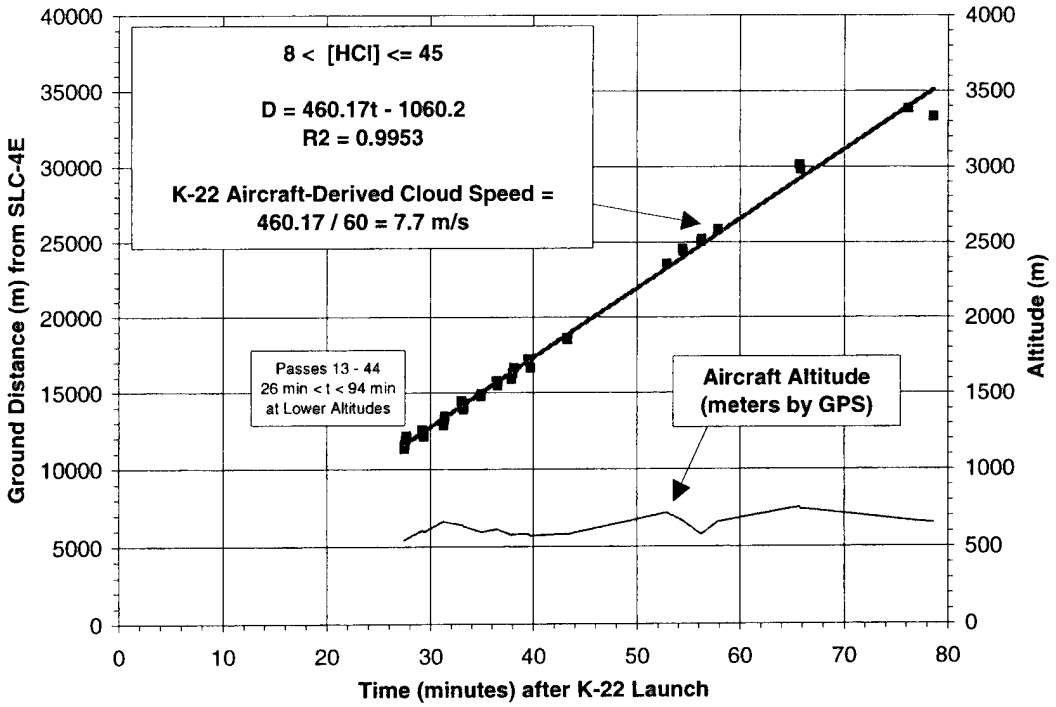

Figure 30. Aircraft-derived cloud speed (7.7 m/s) at later times (27–94 min for passes 14–44) and lower altitudes (450–850m). Since the aircraft flew both cross- and along-wind profiles during this period, we are more confident with the speed derived from these data than with the speed derived from the earlier higher-altitude data that included only cross-wind profiles.

3.3.7 Summary for Ground Cloud Characteristics and Comparison to REEDM

Table 6 summarizes the aircraft-derived, imagery-derived, rawinsonde-measured (T–0.25h), and REEDM-predicted (T–0h reconstruction based upon the T–0.25h rawinsonde sounding and T–0h DAS profiles) data for the #K22 ground cloud. Several conclusions are derived from review of the contents of this table:

(1) the imagery-derived stabilization height (702 m AGL, 855 m MSL) documents that the ground cloud rose 66% higher AGL than predicted by REEDM (424 m AGL, 577 m MSL);

(2) the imagery-derived stabilization time (5–7 min) is 150% to 250% longer than predicted by REEDM (2 min);

(3) the imagery-derived cloud bearing (340°) is bracketed by the rawinsonde-derived wind directions (330 to 351°) associated with the ground cloud;

(4) the early aircraft-derived cloud bearing (344° measured 8.5–23 min after launch and at altitudes at or slightly above the middle of the ground cloud) is closer to the imagery-derived bearing (340° measured 0–32 min after launch) than to REEDM prediction (330°);

(5) the later aircraft-derived cloud bearing (331° measured 27–94 min after launch and at altitudes at or slightly below the middle of the ground cloud) is closer to the REEDM prediction (330°) than to early aircraft-derived (344°) and imagery-derived (340°) bearings;

(6) the imagery-derived cloud speed (6.8 m/s) is almost identical to the rawinsonde-derived wind speed (6.9 m/s) at the height of the middle of the ground cloud;

(7) the imagery-derived cloud speed (6.8 m/s) is 127% faster than predicted by REEDM (3 m/s); and

(8) the aircraft-derived speed (7.7–8.3 m/s) is 157–177% faster than predicted by REEDM (3 m/s);

Table 6. Summary for #K22 Launch Cloud Data Derived from Aircraft HCl Sampling, Visible and Infrared Imagery, T–0.25h Rawinsonde Sounding Data, and T–0.25h REEDM Predictions (based upon T–0.25h rawinsonde and T–0h DAS data)

Attribute	Feature	Aircraft (HCl)	Imagery (IR only)	Imagery (Vis only)	Imagery (Mixed)	Rawinsonde (T–0.25h)	REEDM 7.07 (T–0.25h)
Height (m) Above SLC-4E (SLC-4E = 153 m MSL	Top	#N/A	#N/A	#N/A	1393	#N/A	#N/A
	Middle	#N/A	867	827	855	#N/A	424
	Bottom	#N/A	#N/A	#N/A	317	#N/A	#N/A
Time (min) After Launch	Top	#N/A	#N/A	#N/A	4–7	#N/A	#N/A
	Middle	#N/A	5–7	5–7	5–7	#N/A	2
	Bottom	#N/A	#N/A	#N/A	5–7	#N/A	#N/A
Bearing (deg) (Rawinsonde)	Top	344° early/upper	#N/A	#N/A	#N/A	351°	#N/A
	Middle	#N/A	#N/A	#N/A	340°	333°	330° (layer #2)
	Bottom	331° later/lower	#N/A	#N/A	#N/A	345°	#N/A
Speed (m/s) Away From SLC-4E	Top	8.3	#N/A	#N/A	#N/A	4.3	#N/A
	Middle	#N/A	#N/A	#N/A	6.8	6.9	3 (layer #2)
	Bottom	7.7	#N/A	#N/A	#N/A	3.4	#N/A

3.4 Conclusions

The aircraft's Geomet total HCl detector sampled the ground cloud from the Titan IV #K22 launch and obtained a large quantity of HCl concentration data as a function of time and aircraft position. The aircraft's HCl concentration data documented a shifting bearing for the launch's ground cloud. At early times (8.5–23 min), while sampling at higher altitudes (700–1350 m MSL), the aircraft documented a cloud bearing of 344° and speed of 8.3 m/s. At later times (27–94 min), while sampling at lower altitudes (450–850 m MSL), the aircraft documented a cloud bearing of 331° and speed of 7.7 m/s. For comparison, the imagery-derived cloud bearing was 340° at a speed of 6.8 m/s during the first 32 min after launch and at an average altitude of 855 m MSL. In contrast, REEDM's prediction for the stabilized ground cloud was a cloud bearing of 330° at a speed of 3 m/s with an average altitude of 577 m MSL. The aircraft sampled altitudes between 450 and 1350 m MSL while the imagery-derived altitudes for the bottom, middle, and top of the ground cloud were 317, 855, and 1393 m MSL, respectively. One should remember

two things when comparing the aircraft and imagery data: (1) the GPS altitude could be off by ±250 m and (2) the aircraft sampled for longer times than available by imagery.

The aircraft's data document measurable levels of HCl to altitudes as low as 500 m MSL. The aircraft's data include HCl detection at times greater than 94 min after the launch and as great as 40 km from SLC-4E. In a subsequent report, we will correlate the aircraft's HCl measurements with the imagery for the first 32 min after launch to document the dimensions and concentration distributions within the rising and the stabilized ground cloud. In a third report, we will provide a series of polar, Cartesian, and time plots for each 10-min increment in the aircraft's #K22 mission. In addition to cloud concentrations, one can extract angular spreads and along-wind cloud dimensions for favorable transects. These subsequent detailed data reviews will provide the data in a format that will facilitate direct comparison to individual dispersion model runs (i.e., for a specific time after launch, altitude above the pad, and distance from the pad). The intent of these reports is to document the #K22 exhaust cloud results in detail sufficient for validating dispersion models.

As discussed in this report, the Geomet detector is useful, but not ideal, for aircraft sampling of Titan IV launch clouds. We provide data that illustrate quantitative integrated response as well as excellent temporal and spatial accuracy for mapping the extent and position of Titan IV clouds. We also include data that document significant differences in the HCl concentrations reported by the Geomet and another detector that flew on the previous #K15 mission. These data illustrated that the concentration reported by both detectors is a strong function of their response functions (i.e., averaging time). These data suggest that the Geomet reports an HCl concentration that represents an average value for at least an 18-s period. In contrast, the temporal and spatial accuracy of the Geomet is consistent with an averaging time of only 3 to 4 seconds. The Geomet was configured identically for both the #K15 and the #K22 missions. Considering the available data, we recommend the use of caution when comparing measured HCl concentration to predicted HCl concentration since the averaging times associated with detectors are not necessarily the same as those used by default in dispersion models.

We document an error in the REEDM output. REEDM converts the height above ground level (AGL) to height above mean sea level (MSL) by using the height of the rawinsonde release site (100 m, 328 ft) instead of the height of launch pad (153 m, 501 ft). Therefore, the height MSL reported by REEDM in Appendix A is 53 m (173 ft) too low (i.e., 153m–100m). The magnitude of this correction will vary for each mission since the rawinsonde release site can vary (i.e., the #K15 rawinsonde was launched from building 900 while the #K22 rawinsonde was launched from building 1764).

4. Infrared Spectroscopy of the Titan IV #K22 Ground Cloud

[The material in this section was contributed by J. L. Hall of the Environmental Monitoring and Technology Department of The Aerospace Corporation's Space and Environment Technology Center]

4.1 Introduction

On 12 May 1996, the Titan IV #K22 vehicle was successfully launched from SLC-4E at Vandenberg Air Force Base at 14:32 PDT (21:32 GMT). This section describes the infrared spectroscopy measurements of the ground exhaust cloud, which were collected during the first 37 min following the launch. It includes a description of the infrared spectrometer platform used and the data calibration procedures.

An 8–12 μm Fourier transform infrared (FTIR) spectrometer was deployed for this launch to remotely determine the temperature history of the vehicle exhaust ground cloud by measuring the cloud's mid-infrared spectrum. The cloud temperature determines buoyancy of the cloud and is a major factor determining the ultimate cloud rise. Comparison of the measured cloud temperatures as a function of time with those predicted by the Rocket Exhaust Effluent Dispersion Model (REEDM) may shed light on why REEDM seems to be consistently underpredicting the cloud rise.[5,6] The spectrometer was deployed by personnel from The Aerospace Corporation at the Building 900 observation site, which is 2.9 mi NE of the SLC-4E launch pad. Alongside the spectrometer, a VIRIS (Visible and Infrared Imaging System) set-up containing an Agema 8–12 μm infrared camera was also deployed. Details of the deployment are given in Section 2 of this report. This site was chosen because it was closest to the launch pad but still outside the exclusion zone. Since the sensitivity of the infrared remote sensing method is a function of the integrated amount of atmospheric water along the instrument line-of-sight, close-in sites giving the highest possible elevation angles to the cloud are the most desirable.

Atmospheric conditions on the day of the test were almost perfect for these remote infrared measurements, with no low-altitude clouds or fog and a relatively low absolute humidity of ~12 g m^{-3}.

4.2 FTIR Spectrometer Description

The FTIR spectrometer used for these measurements is a compact instrument (10"H × 12"W × 18"L) manufactured by Block Engineering and configured to measure emission spectra. Its optical band pass is 750 to 1600 cm^{-1} (13 to 6.3 μm), which encompasses the 8–12 μm atmospheric transmission window. It uses an 8-in.-diam Cassegrain-type telescope as its front end and "coupled" interferometer (signal arm plus white-light-source arm) in the rear. The telescope gives the instrument a 1/4° field-of-view. The spectrometer is fitted with a closed-cycle cooler, which cools its HgCdTe detector to liquid N_2 temperature. The scan rate and nominal wave-

number resolution of the instrument are fixed at 3.3 Hz and 2 cm^{-1} (1.6 cm^{-1} FWHM*) respectively. For this deployment the noise equivalent spectral radiance (NESR) was 8×10^{-8} W cm^{-2} sr^{-1} $(cm^{-1})^{-1}$ (RMS) at 1000 cm^{-1} for a single scan. Figure 31 shows a plot of the noise measurement. This NESR is equivalent to a temperature difference of 0.5°C at 25°C and 1000 cm^{-1}. It is about a factor of 3 worse than normal for this spectrometer due to ground-loop noise pickup experienced during this deployment.

The spectrometer had been recently modified by installation of a thermally regulated insulated enclosure that surrounded the instrument and was sealed to the outside diameter of the telescope. Thermal control was achieved using a commercial Peltier device mounted at the top of the enclosure. The single device, manufactured by Thermoelectric Cooling America Corp., is capable of removing 35 W of heat from the enclosure at a temperature gradient of 20¡F between the inside of the enclosure and ambient air temperature outside. The spectrometer generates approximately 34 W of heat itself. The purpose of the enclosure is to minimize the drift in instrument temperature and hence calibration parameters during a set of measurements. This is of particular importance for field measurements where solar insolation and wind can induce significant drift.

The spectrometer enclosure is bolted to a base plate that also holds three co-aligned cameras. Two of these are CCD cameras operating in the visible spectrum to simplify pointing of the base plate at visible targets and to provide a record of the scene. One of the cameras has a motorized zoom lens plus a ×2 focal-length extender so that at its fully zoomed position it has a horizontal field-of-view (FOV) of 1.2° (i.e., only a few times that of the FTIR instrument to ensure accurate pointing). The second CCD camera has a motorized zoom lens, allowing its horizontal FOV to

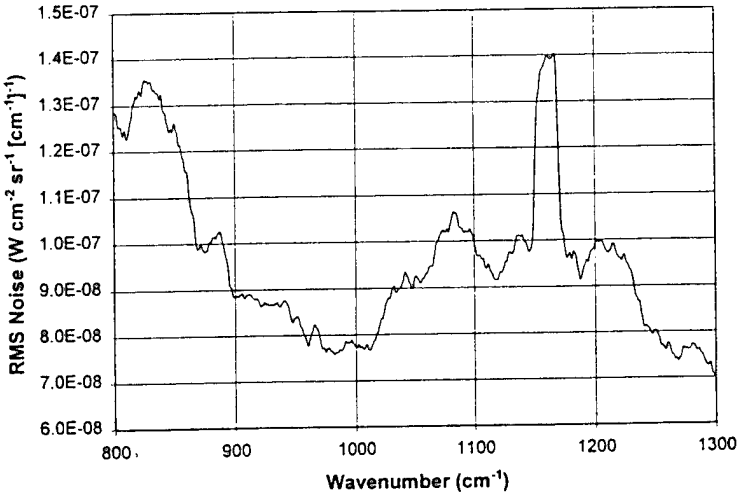

Figure 31. RMS noise measurement for the FTIR spectrometer for the #K22 launch ground cloud observations. The noise corresponds to a single scan of the spectrometer.

* The Full-Width-at-Half-Maximum (FWHM) specification is for interferogram data processed using a "medium" Norton-Beer apodization function. See R. H. Norton and R. Beer, "New Apodizing Functions for Fourier Spectrometry," *J. Opt. Soc. Am.*, 66(3), 1976, pp. 259-264.

be varied from 4.6° to 44°. Also mounted on the base plate is a 3–12 μm infrared camera (Inframetrics model 525) that can be fitted with standard 1-in-diam infrared optical filters. For this deployment, the infrared camera was used without an external lens, resulting in a FOV of 14° × 18° (vertically × horizontally). The camera is used to provide a real-time image of the integrated infrared radiance of the scene and is comparable to the Agema cameras of the VIRIS systems. For this deployment, the camera was operated without any optical filters since the primary contributor to the infrared emission of the ground launch cloud in the 8–12 μm window is water, which emits over the entire wavelength region.

The base plate on which all of the cameras are mounted is attached to a Samson QSH-25 tripod fluid head. We have constructed our own elevation and azimuth mount for this head using rotary optical encoders purchased from Tangent Instruments (2048 lines/rev) and appropriate anti-backlash spur gears. Each axis has a resolution of 0.07°, although its accuracy is somewhat less due to non-repeatability in the fluid head.

The visible camera signals are first fed through an IRIG B time inserter module manufactured by Xybion on which the angle encoder readout of azimuth and elevation position are both edge-encoded and superimposed as a character string on the bottom of the video image. The signals are then sent through a video crosshairs generator and a "picture-in-picture" unit that positions one of the camera views into the top left–hand quarter of the other camera view. This composite picture is recorded onto VHS tape to give a time-tagged video record of the spectrometer view during the measurement. IRIG B timing is recorded on the HIFI audio tracks of a second VCR that records the infrared camera video. For this test, IRIG B timing was derived from a portable GOES satellite receiver. All of the support electronics are housed in two separate transport cases.

The base plate cameras and FTIR spectrometer are all co-aligned before the measurement to a hot infrared source (a camper's propane heating unit) placed far enough away from the tripod to minimize parallax errors at the expected distances of interest during the measurement.

The azimuth-elevation angle readout on the tripod mount was calibrated before the launch using the calculated azimuth angle from the spectrometer site to the SLC-4E launch pad.

4.3 Data Acquisition

Interferograms from the FTIR spectrometer were recorded using a Dell 486/66 computer configured with timing and 16-bit A/D boards. The data acquisition program was written in-house to enable contiguous interferogram recording and storage at the operational scan rate of the spectrometer (3.3 Hz). Each interferogram consists of 2048 data points. The optical retardation in the interferometer is measured using a HeNe laser, and each data point is acquired on every fourth HeNe laser fringe at a rate of 8.5 kHz.

Data can be processed in real time and displayed on the computer screen, enabling tracking of the cloud using the spectrometer signal even when the cloud is invisible in all of the co-aligned camera views. For post-launch data analysis back at the laboratory, numerous background

datasets were acquired by viewing regions of sky at the same elevation angle as the cloud datasets but to either side of the cloud.

4.4 Dataset Calibration

Accurate calibration of the recorded spectra is important for quantitative interpretation of these spectra. Each spectral dataset is converted into radiance units using calibration factors calculated from three-temperature calibration runs acquired during the course of the measurement. We use a large-area blackbody source consisting of a 1/4" × 12" × 12" aluminum plate spray painted with Krylon Ultra Flat Black Enamel paint and heated on the rear side with Kapton heaters under proportional control. The average emissivity of the surface of the source is 0.94 across the spectral region of interest.[7] Typically, the calibration temperatures span the range from ambient temperature to 60°C. After the test, this laboratory-constructed unit was calibrated back in the laboratory against a blackbody standard source (emissivity > 0.99, with NIST** -traceable temperature calibration) purchased from The Eppley Laboratory.

Two calibration runs were acquired during the course of these measurements. The first was acquired approximately 1 h before launch time and the other approximately 30 min after the launch, interleaved with exhaust cloud spectra. The calibration factors determined from these two runs showed remarkable consistency. Figure 32 shows a comparison of the slope terms.

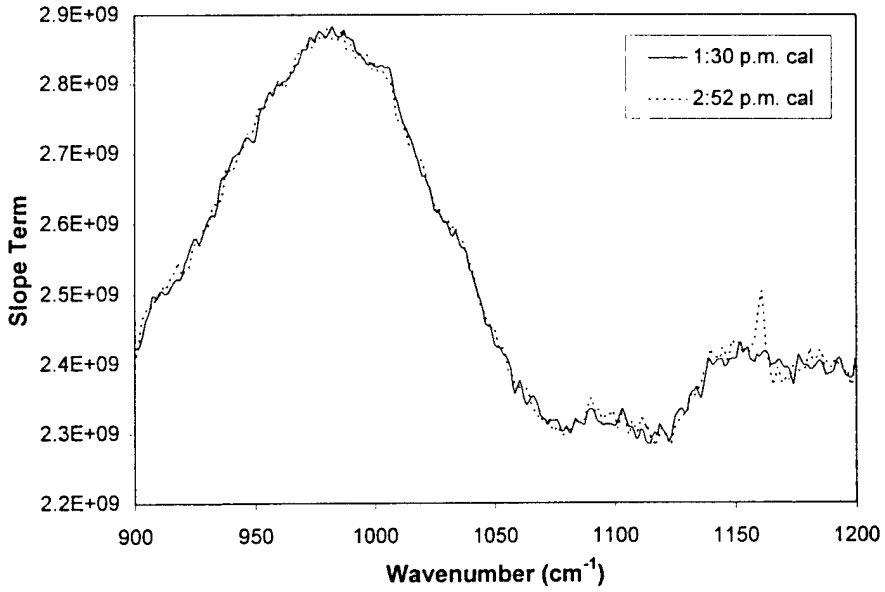

Figure 32. Slope terms calculated from the two calibration runs at 1:30 pm and 2:52 pm (local) on the day of the #K22 measurements. The wavenumber scale of this plot was expanded to see the differences between the two curves. The peak near 1160 cm^{-1} is a known transient noise feature (see Figure 4.1).

** National Institute of Standards and Technology

We have written our own software to perform the spectral calibration and analysis procedures. Non-standard calibration routines were required for this set of measurements because the cloud was viewed against the cold sky infrared background. Under these circumstances, the internal radiometric signature of the spectrometer, which is out of phase with the radiation from the scene, is significant.[8]

As discussed in 4.2, the spectrometer tripod was fitted with angle encoders providing an angular resolution of 0.07° in both azimuth and elevation directions. The tripod and spectrometer base-plate were leveled using bubble levels before the event. We calculated the true azimuth angle to the SLC-4E launch pad structure from the spectrometer site using differential GPS coordinates for both sites (see Section 2). The tripod azimuth angle readout was then adjusted to this value when the mount was pointed at the launch pad. Each spectrum is time-tagged as it is acquired by the computer. The azimuth and elevation angles of the instrument mount that correspond to these times is interpolated from a log of IRIG B time versus mount angles. This log is created by replay of the visible CCD videotape through a VED-100 video inserter operating in decode mode.

4.5 Observations and Analysis

Spectral data were acquired from just after launch to approximately 37 min later, at which time the ground exhaust cloud was barely perceptible in the camera views. During this period, data was acquired at 3 or 4 separate regions of the cloud along a horizontal line at 2 or 3 different altitudes within the cloud. The cloud traveled away from the spectrometer site during the entire observation period.

Figure 33 shows an example exhaust cloud spectrum acquired at 53 s after launch and compares it with a sky background spectrum taken at the same elevation angle and a calculated blackbody spectrum at 25°C. The blackbody spectrum represents the limit of an optically thick cloud at the given temperature. (The one shown does not account for the absorption of radiation by the intervening atmosphere.) Both the ground cloud and sky spectra show numerous sharp spectral features that are due to atmospheric water. The broad emission feature in the sky spectrum

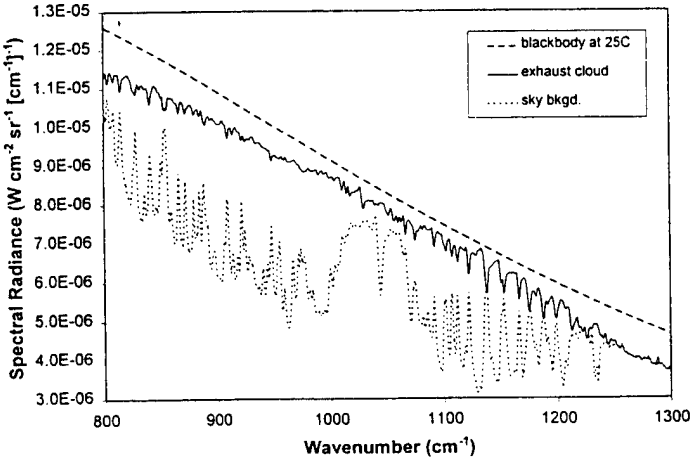

Figure 33. Spectra of the exhaust ground cloud acquired 53 s after launch and a sky background at the same elevation angle (4°). The cloud spectrum is an average of 5 scans. A blackbody spectrum at 25°C is shown for comparison.

between 1000 and 1075 cm^{-1} is due to ozone in the stratosphere. It does not appear in the exhaust cloud spectrum because the cloud is optically thick, so all radiation from the atmosphere beyond it is absorbed.

Figure 34 shows exhaust cloud and sky background spectra acquired at 2.5 min after launch. Now the ozone feature is readily apparent in the cloud spectrum, indicating that the exhaust cloud has already become optically thin.

Analysis of selected datasets shows good consistency between the spectral radiance of the ground exhaust cloud measured by the spectrometer and the integrated radiance measured by the co-located Agema camera. Comparisons have been made for selected Agema images acquired separately with both an 8–12 μm bandpass filter and a narrowband filter centered at 10.6 μm.

The measured spectra cannot be directly converted into true cloud temperatures for two reasons. First, the atmosphere has significant absorption between the spectrometer and the cloud because of the large distance separating them, and thus even if the cloud is optically thick, the apparent temperature is reduced. Second, when the cloud starts to become optically thin, there is a contri

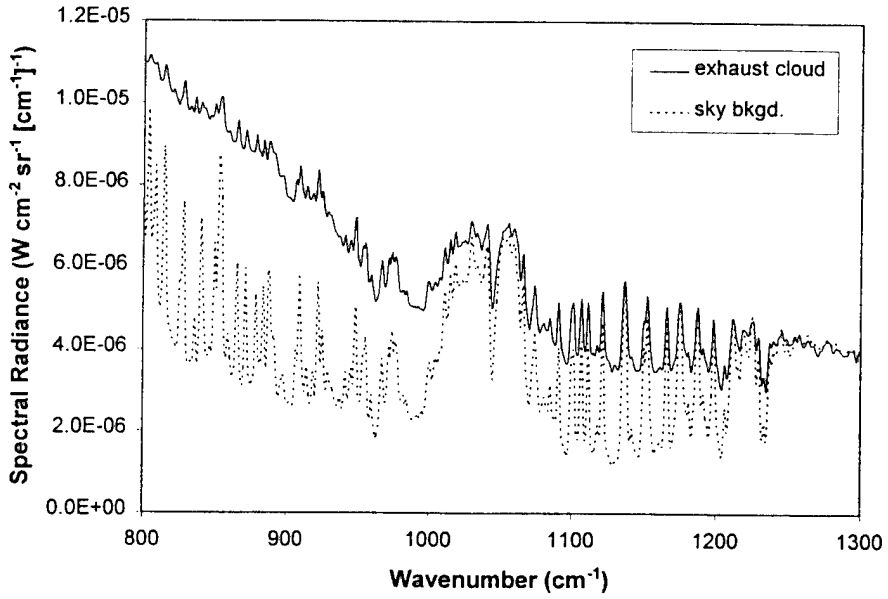

Figure 34. Spectra of the exhaust ground cloud acquired 2.5 min after launch and a sky background at the same elevation angle (11.5°). The cloud spectrum is an average of 4 scans. The exhaust cloud is now optically thin.

bution to the measured radiance spectrum from the "cold" sky background beyond the cloud. The effect of this is also a reduced apparent temperature for the cloud. The following radiative transfer equation describes the various radiance contributions that sum to give the spectral radiance observed by the spectrometer, L_{obs} :

$$L_{obs} = L_{near} + \tau_{near}\, \varepsilon_{cloud}\, L_{cloud} + (1 - \varepsilon_{cloud})\, L_{far}\, \tau_{near}$$

where,

L_{near} is the spectral radiance from the atmosphere between the spectrometer and the cloud

τ_{near} is the transmission of the same intervening atmosphere

ε_{cloud} is the cloud's emittance

L_{cloud} is the spectral radiance of a blackbody at the cloud temperature

L_{far} is the spectral radiance from the atmosphere extending from the back of the cloud to space

In the first two minutes, when the cloud is optically thick ($\varepsilon_{cloud} = 1$), the temperature of the cloud can be obtained by modeling the near-field atmospheric transmission and radiance. Extracting the cloud temperature at longer times, when the cloud is not optically thick, is a more difficult problem. This will require the development of new modeling software and, therefore, will be time consuming. Because of manpower constraints, this should only be undertaken if it can be shown that the cloud temperature is a useful diagnostic for the cloud rise algorithm testing and validation.

4.6 Summary

An FTIR spectrometer has been successfully deployed to measure 8–12 μm spectra of the ground exhaust cloud from the Titan IV #K22 vehicle at Vandenberg Air Force Base on 12 May 1996. Calibrated data on the cloud were acquired for a duration of 37 min following the launch. Preliminary analysis of the data showed that the cloud became optically thin in this wavelength region within the first 2 min after launch. Detailed analysis of the data to extract the true ground cloud temperatures as a function of time will require sophisticated modeling of the radiance contributions from the intervening atmosphere as well as the atmosphere beyond the cloud.

5. Ground HCl Sampling

5.1 Introduction

The NASA Kennedy Space Center's Toxic Vapor Detection and Contamination Monitoring Laboratory supported the exhaust plume measurements for the #K22 launch in several ways. The Geomet HCl monitors were prepared and calibrated in support of the aircraft sampling described and reported in Section 3. In support of planned mobile ground sampling, Interscan monitors were prepared and calibrated. Finally, ground HCl dosimeters were prepared, deployed, recovered, and read to determine the ground deposition of HCl resulting from the ground cloud movement. These efforts were carried out under the leadership of Paul Yocum, sponsored by the 45th Space Wing Bioenvironmental Engineering Branch under LtCol Rusden, and are all covered in this section of the report.

5.2 Lab Standard Preparation

All chemicals, test equipment, glassware, tubing, clamps, three Geomet HCl monitors, and three Interscan HCl monitors were shipped out to Vandaenberg AFB for setup in the lab in the 30 AMDS Bioenvironmental Engineering shop. The 50 ppm HCl gas mixture ordered for the 5 Dec 95 launch monitoring was sufficient for use during the May launch monitoring. A mojor change during this trip was that the BEE shop was able to obtain the use of a 10,000 ft^3 tube-bank. This was used instead of the vane-type breathing air pump from the December trip. The tube-bank was coupled to a Miller Nelson Flow-Temperature-Humidity control system. The combination of Miller Nelson and tube-bank made it possible to produce a consistent and very accurate HCl output.

5.3 Equipment Preparation

Prior to the airborne launch monitoring at Vandenberg AFB, a voltage divider built by the TVD/CM lab was incorporated into the Geomet HCl monitor to divide the output voltage by 4 without affecting the autoranging system built into the unit. The Interscan HCl monitoring equipment used external 2.0 L/min sample pumbs to increase flow rate through the test cell and decrease response time. The Geomet and Interscan HCl monitors were calibrated the day before the launch as well as 6 h prior to launch and were used to monitor the HCl output of the lab standard. This was done to verify consistency of measurement by the Interscans.

5.4 Mobile Ground Monitoring

Two Interscan real-time HCl monitors were provided to the Air Force mobile HCl monitoring teams. The mobile monitoring teams could not obtain access into the area of the HCl plume so the Interscans were not used.

5.5 Dosimeter Monitoring

The primary goal for HCl dosimeter monitoring during this Titan IV launch was collection of ground-level data from around the launch facility. Dosimeters were fabricated on 7 May 96 at the TVD laboratory on CCAS, FL and shipped out to Vandenberg. Dosimeters were provided to Air Force personnel for near-field placement around the southwestern side of the launch complex. Dosimeters were also placed along the projected plume track in a southwwesterly direction from Complex 4E the morning of the launch. Seventeen dosimeters (identified as A1–A21 in Figure 36) were placed southeast of the launch complex in a 25° arc 5 ft above ground level from 700 to 1600 ft from the vehicle. Ten dosimeters (identified as B1–B10) in Figure 36) were placed SSW to SE along Tank Road, 2800–3400 ft from the launch complex. Ten dosimeters (identified as C1–C10 in Figure 37) were placed SSE to SE along the ridge access road between the end of Avery Road and Spring Canyon Road, 7000–8000 ft from the launch complex. The remaining ten dosimeters (identified as D1–D10 in Figure 38) were placed SSW to SE along the ridge access road and Honda Road between Alvado and the "500" area at the end of Perry Road, 10,500–13,500 ft from the launch complex. Of the 47 dosimeters placed in the field, only one could not be recovered. The plume track went in a southwesterly direction as projected, with a large percentage of the dosimeters indicating the presence of HCl. Dosages by dosimeter number in ppm minutes is shown in Table 7. Dosimeter placement and dosages obtained are indicated in Figures 35 through 38.

5.6 Airborne Sampling

At the request of the 30 AMDS Bioenvironmental Engineering office at Vandenberg AFB, CA, one Geomet model 401B HCl detector modified and calibrated for airborne effluent plume sampling was sent out to California for use during the 5 Dec 95 Titan IV launch. Two additional unmodified Geomet HCl monitors were also sent along as backup units. The instrument was calibrated one day prior to the launch at the field lab set up in the BEE office on Vandenberg AFB using a verified vapor sample of 1.1 ppm HCl at approximately 40% RH and 78°F. The unit was functioning properly and responded as expected during these prelaunch tests. The instrument was energized and allowed to stabilize while sampling HCl-free air. The unit calibration stability was then evaluated by alternately sampling HCl-free and 1.1 ppm HCl vapor. The instrument responded within 5% of the calibrated value during prelaunch calibration testing. The ceramic sample tube was then rinsed with deiionized water, and a coating solution was applied. The day of the launch, the Geomet HCl monitoring instrument was calibrated at the field lab using the verified vapor sample of 1.1 ppm HCl at approximately 40% RH and 78°F. The instrument was then delivered and mounted into the aircraft. After the instrument was installed, some verivication tests were performed to confirm unit operation and response while mounted in the flight monitoring position. The unit was functioning properly and responded as expected during these pre-flight tests. The aircraft was flown into the launch plume nemerous times over a 90-min period with the Geomet taking air samples during transit to monitor HCl levels. The instrument was returned to the field lab after the flight for post-flight calibration. The instrument was energized and allowed to stabilize while sampleing HCl-free air. A baseline shift of less than 0.05 ppm was noted. The unit calibration stability was then evaluated by alternately sampling HCl-free and 1.1 ppm HCl vapor. The instrument responded within 5% of the calibrated value during post–calibration testing. The ceramic sample tube was then rinsed with deionized water, and a coating solution was applied. After rinsing and recoating the sample tube, the Geomet read

the Geomet read the HCl level coming out of the standard (1.1 ppm), and the the unit was returned to zero upon removal.

The implementation of Geomet test and calibration procedures, as well as the establishement of a good working relationship with the other Titan IV plume monitoring program contractors, has laid the foundation for future airborne monitoring activities in California, if required. The credibility of the data collected will only increase with the routine executiion of the procedures established for this flight.

Table 7. Dosimeter Results

Number	LOS	ppm min	Number	LOS	ppm min
A1	No change		B6	0.375	15.62
A2	No change		B7	0.360	14.37
A3	0.420	19.67	B8	0.521	30.45
A4	0.129	1.72	B9	0.529	31.41
A5	Blown Away		B10	0.516	29.86
A6	1.821	378.80	C1	No Change	
A7	0.648	47.35	C2	No Change	
A8	1.824	380.05	C3	0.051	0.22
A9	1.847	389.73	C4	0.557	34.87
A10	1.139	147.56	C5	0.585	38.50
A11	0.298	9.77	C6	0.634	45.30
A12	0.277	8.42	C7	0.918	95.48
A13	1.840	386.77	C8	0.682	52.50
A14	Not Placed		C9	1.021	118.41
A15	Not Placed		C10	0.729	60.06
A16	Not Placed		D1	No Change	
A17	0.224	5.41	D2	No Change	
A18	Not Placed		D3	No Change	
A19	0.454	23.04	D4	No Change	
A20	0.036	0.10	D5	No Change	
A21	0.280	8.60	D6	No Change	
B1	No Change		D7	Unmeasurable	0
B2	No Change		D8	Unmeasurable	0
B3	No Change		D9	Unmeasurable	0
B4	No Change		D10	0.224	5.44
B5	No Change		F1	Not Placed	

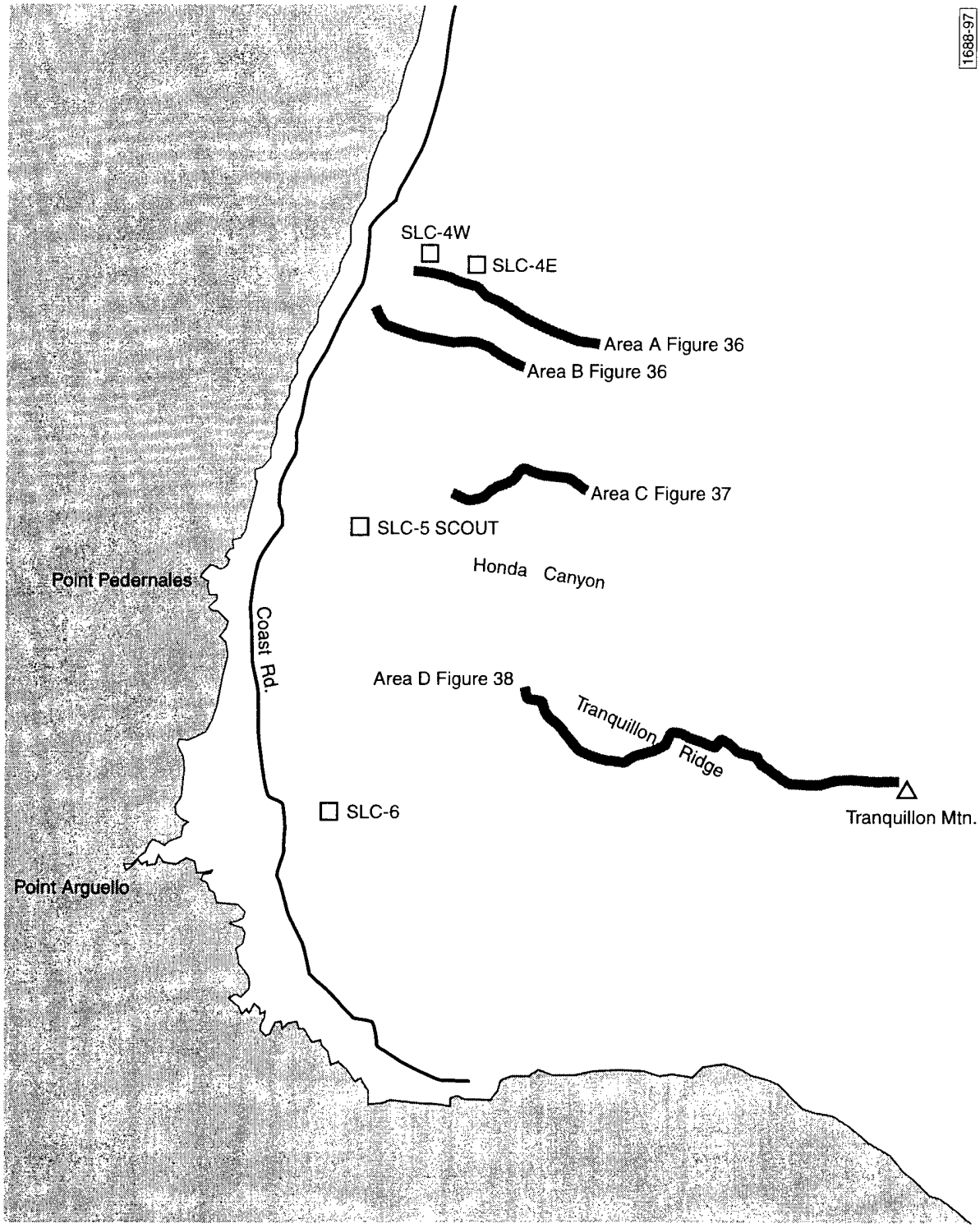

Figure 35. General area map.

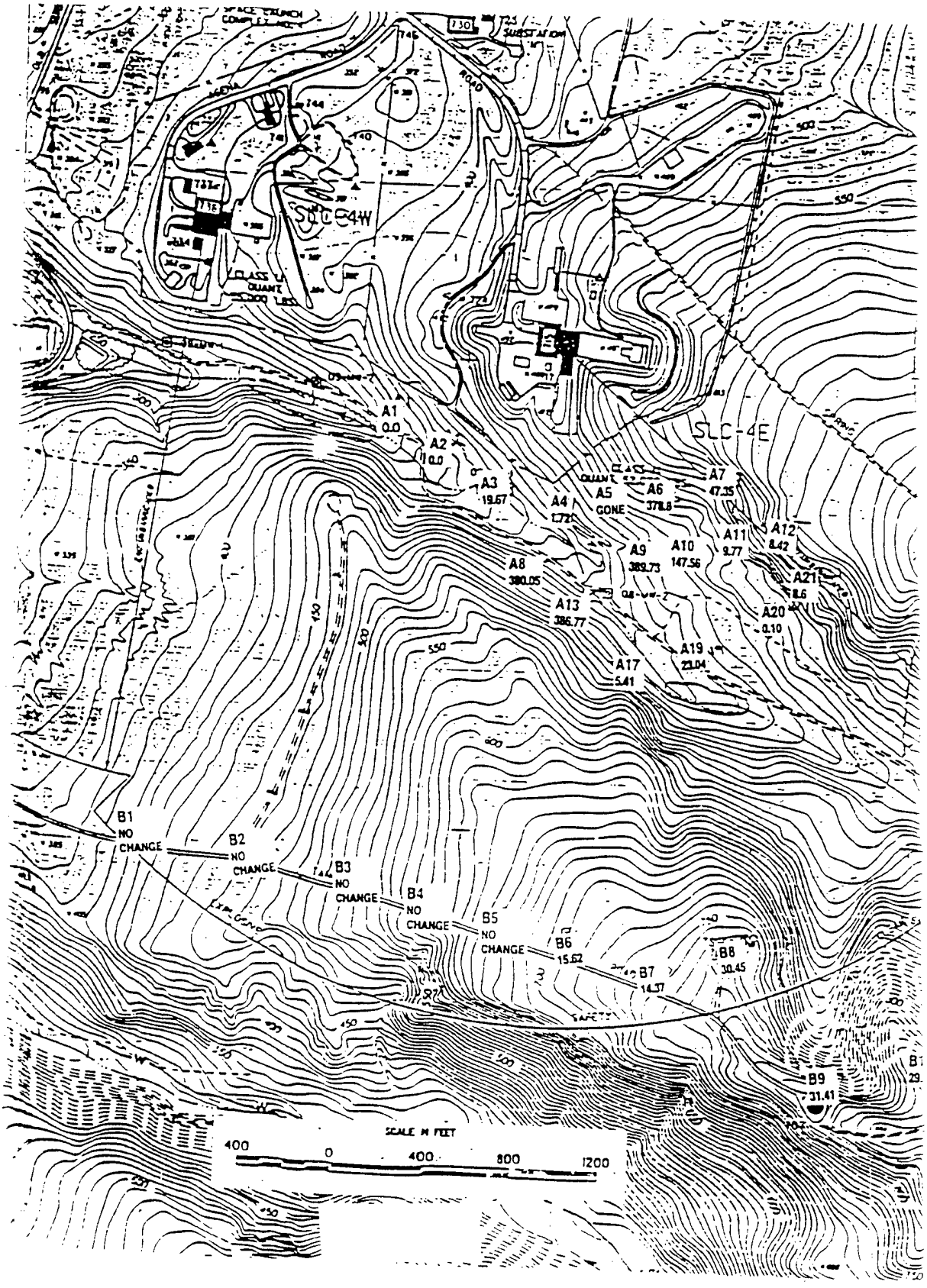

Figure 36. Dosimeter deployment and results—SLC-4 and Tank Road area.

(1)

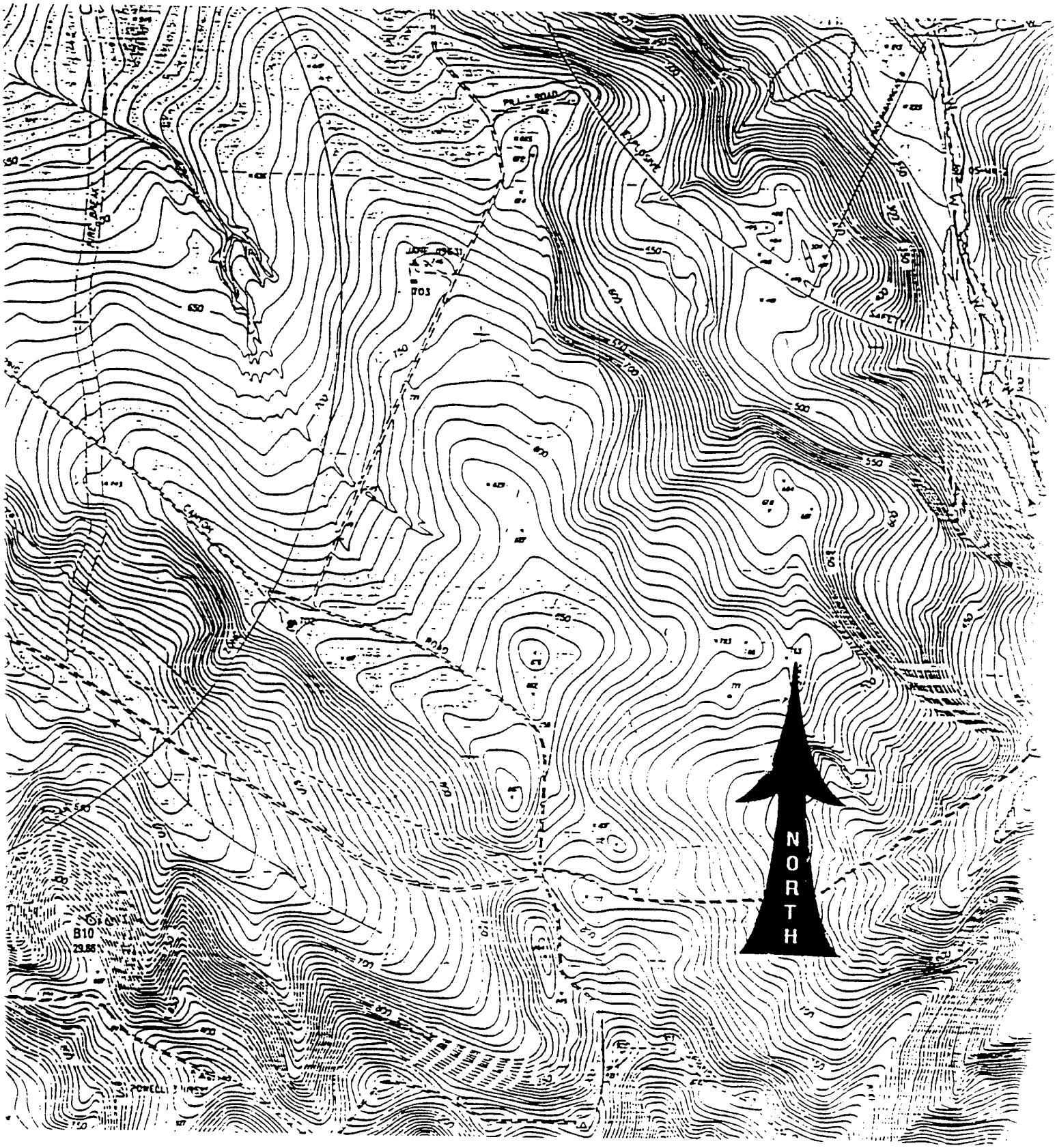

(2)

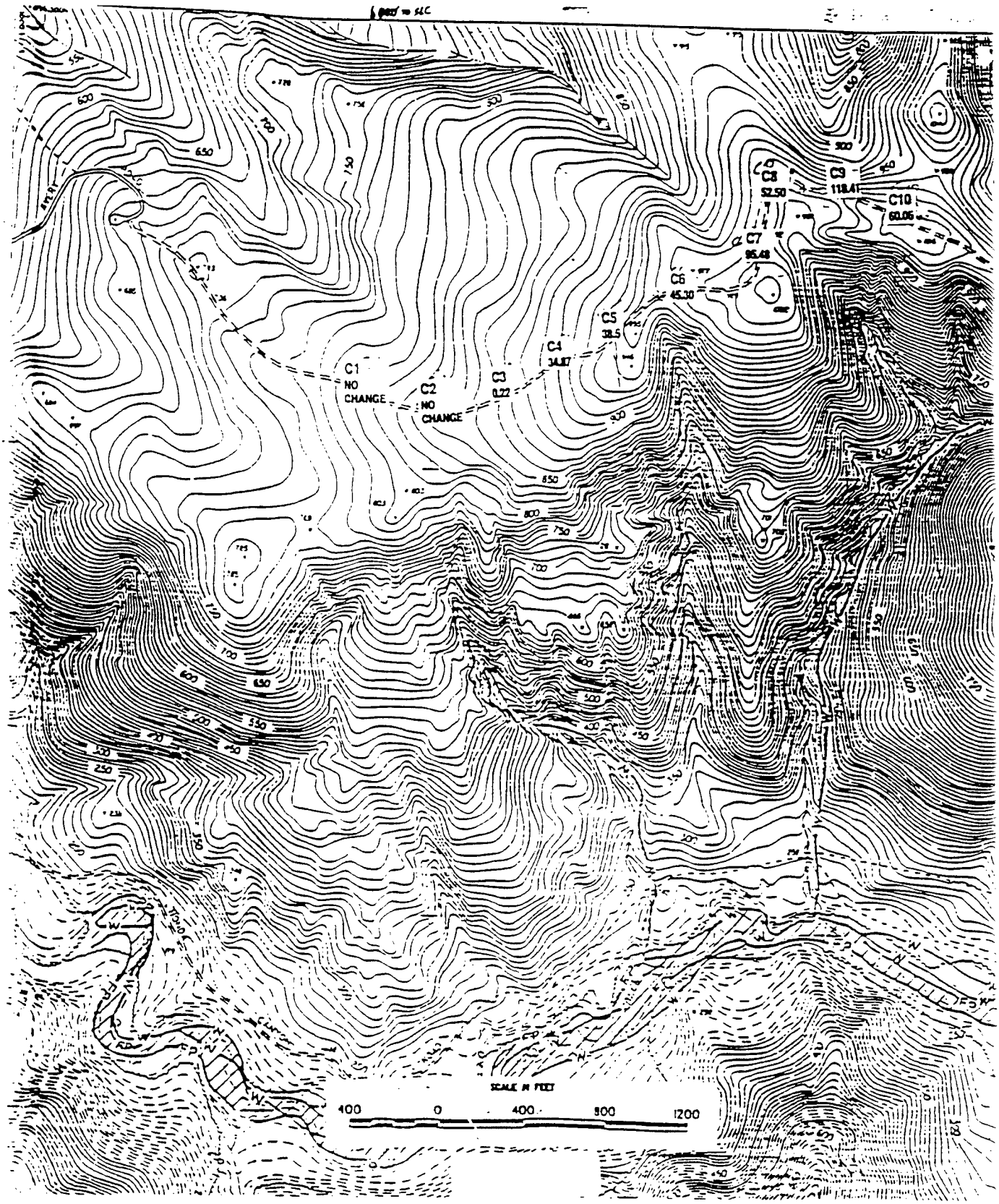

Figure 37. Dosimeter deployment and results—Avery/Spring Canyon Road area.

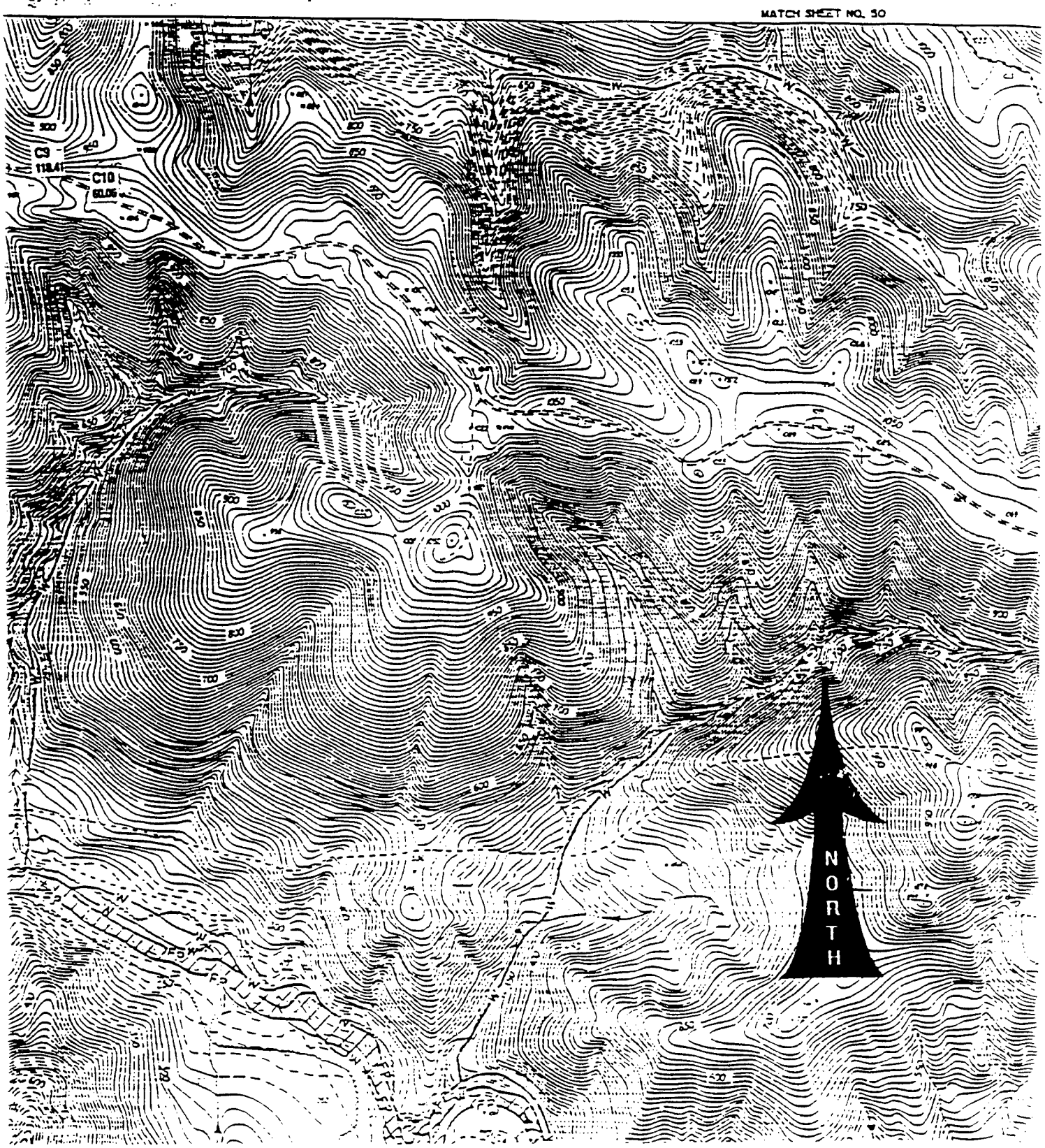

2

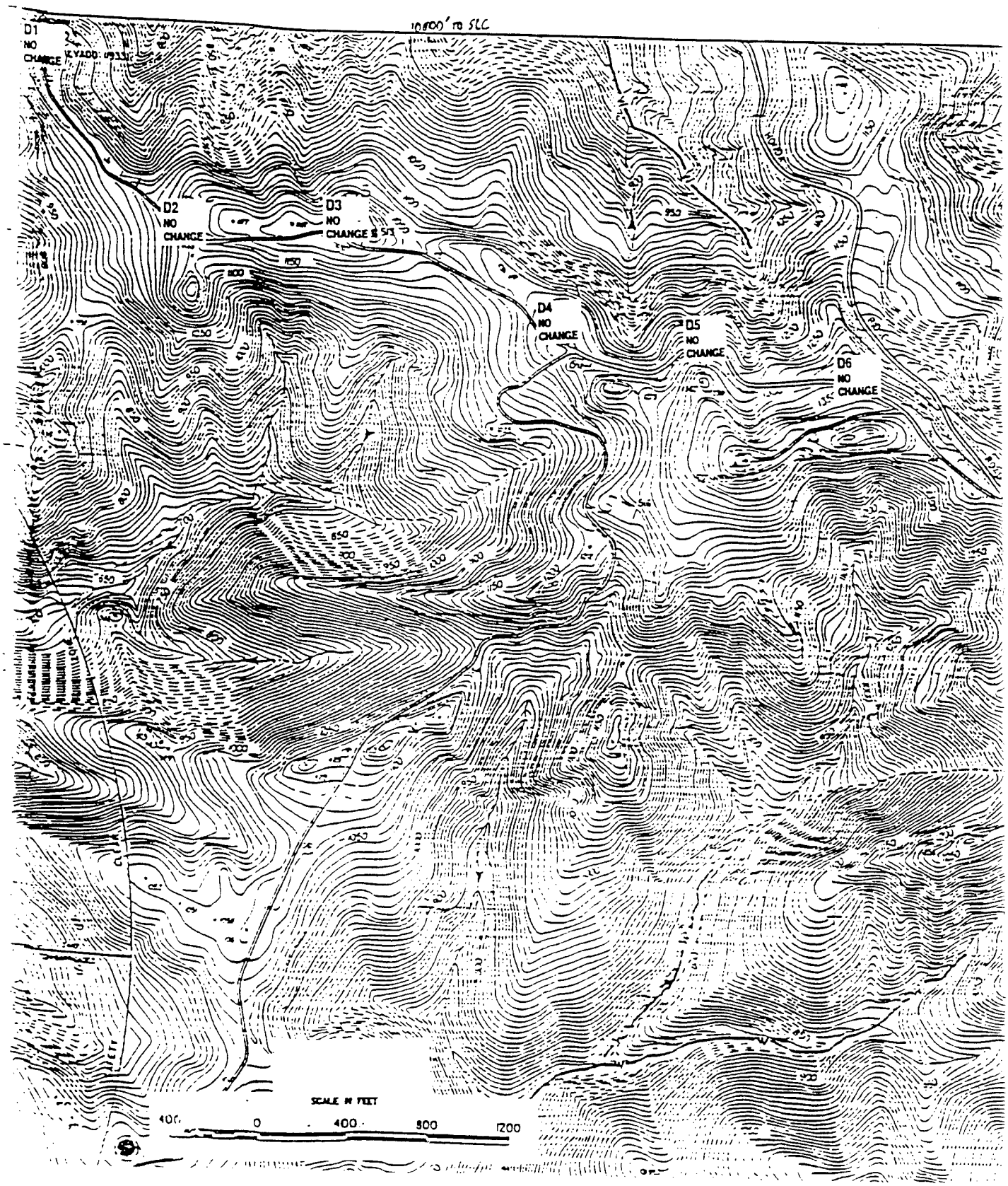

Figure 38. Dosimeter deployment and results—Honda Ridge area.

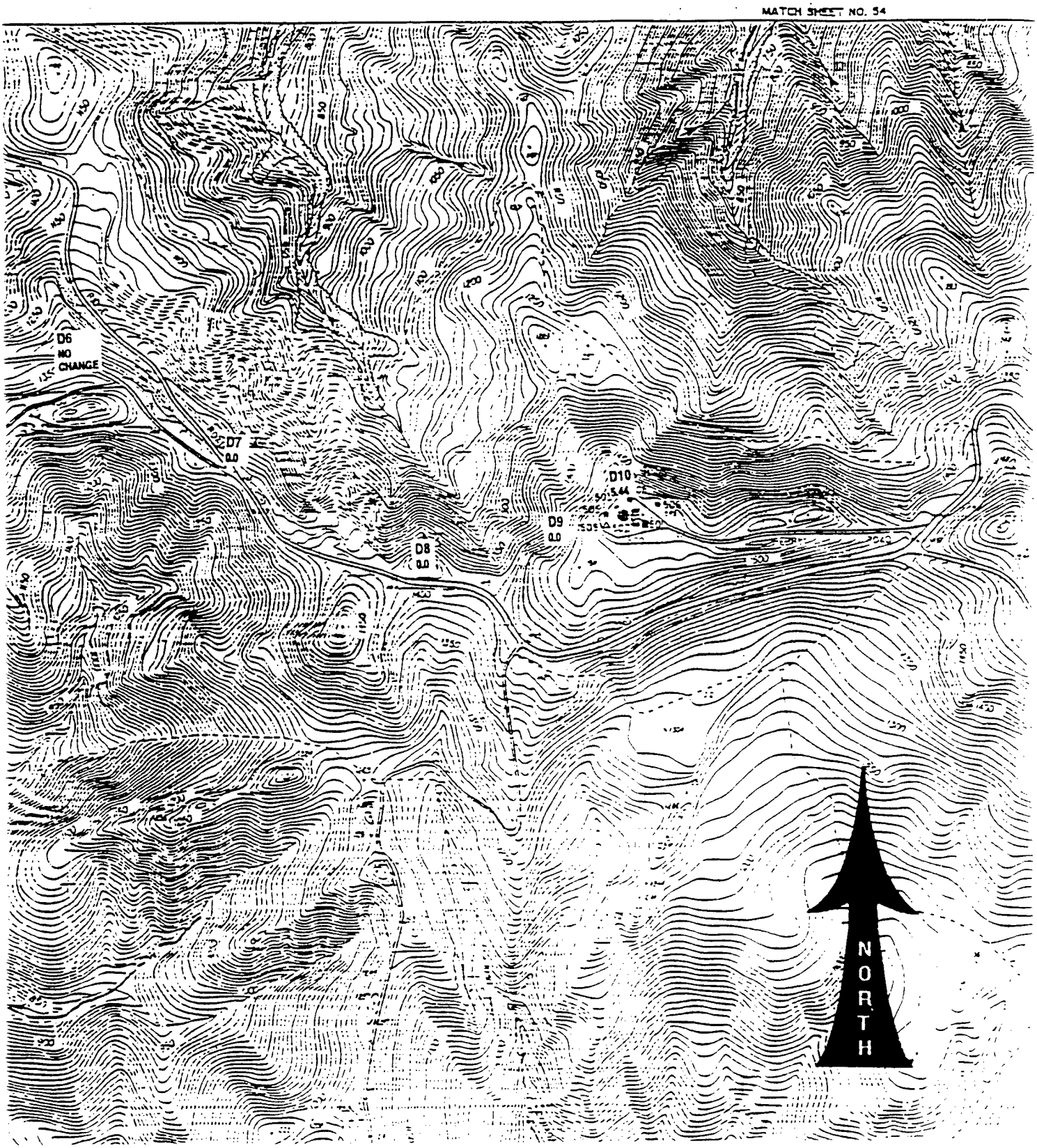

(2)

References

1. Bjorklund, J. R., "User's Manual for the REEDM Version 7 (Rocket Exhaust Effluent Diffusion Model) Computer Program, Vol. I," TR-90-157-01, AF Systems Command, Patrick AFB, FL (April 1990).

2. Womack, J. M., "Rocket Exhaust Effluent Diffusion Model Sensitivity Study," TOR-95(5448)-3, The Aerospace Corporation, El Segundo, CA (May 1995).

3. Ground Cloud Dispersion Measurements During the Titan IV Mission #K16 (24 April 1996) at Cape Canaveral Air Station,"TR-97(1410)-4, The Aerospace Corporation, El Segundo, CA (31 March 1997).

4. Ground Cloud Dispersion Measurements During the Titan IV Mission #K15 (5 December 1995) at Vandenberg Air Force Base,"TR-97(1410)-3, The Aerospace Corporation, El Segundo, CA (10 February 1997).

5. "Ground Cloud Dispersion Measurements During the Titan IV Mission #K19 (10 July 1995) at Cape Canaveral Air Station," Aerospace report no. TR-96(1410)-3 (1996).

6. "Ground Cloud Dispersion Measurements During the Titan IV Mission #K15 (5 December 1995) at Vandenberg Air Force Base," Aerospace report no. TR-97(1410)-3 (1997).

7. "Spectral Emission Signatures of Ambient Temperature Objects," R. J. Brown and B. G. Young, *Applied Optics* 14, 2927 (1975).

8. "Radiometric Calibration of IR Fourier Transform Spectrometers: Solution to a Problem with the High-Resolution Interferometer Sounder," H. E. Revercomb et al., *Applied Optics* 27, 3210 (1988).

Appendix A—REEDM Version 7.07 Predictions for the #K22 Mission

This Appendix includes REEDM version 7.07 runs for impact at both the surface (0 m AGL) and stabilization height (predicted by REEDM). We include the plots of the rawinsonde meteorological data, the predicted maximum concentration versus downwind distance, and the predicted concentration isopleths overlayed on a range map. These plots are followed by the detailed REEDM report for that run.

Stabilization Height Predictions

The following figures and table are the REEDM version 7.07 output for the stabilization height run. These predictions were compared with actual #K22 ground cloud observations in Section 2 for the quantitative imagery and with the aircraft's HCl measurements in Section 3.

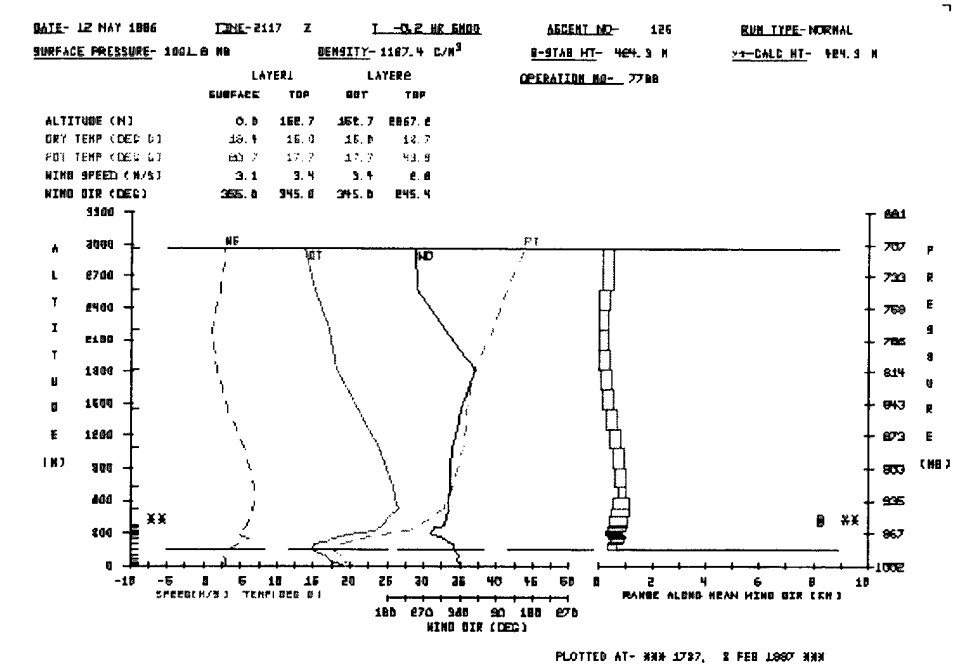

Figure A1. Meteorological Output Plot from REEDM Version 7.07 for K-22 Mission Using T-0.25h Rawinsonde for T-0.0h Reconstruction.

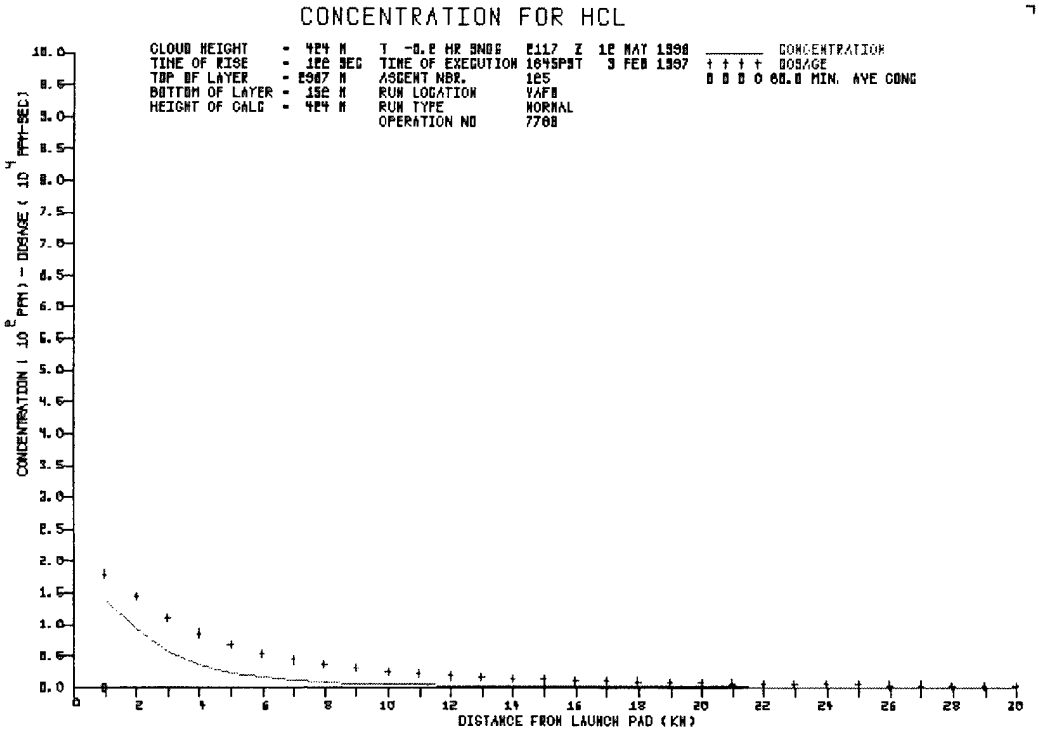

Figure A2. HCl Concentration Predictions from REEDM Version 7.07 for K-22 Mission Using T-0.25h Rawinsonde for T-0.0h Reconstruction.

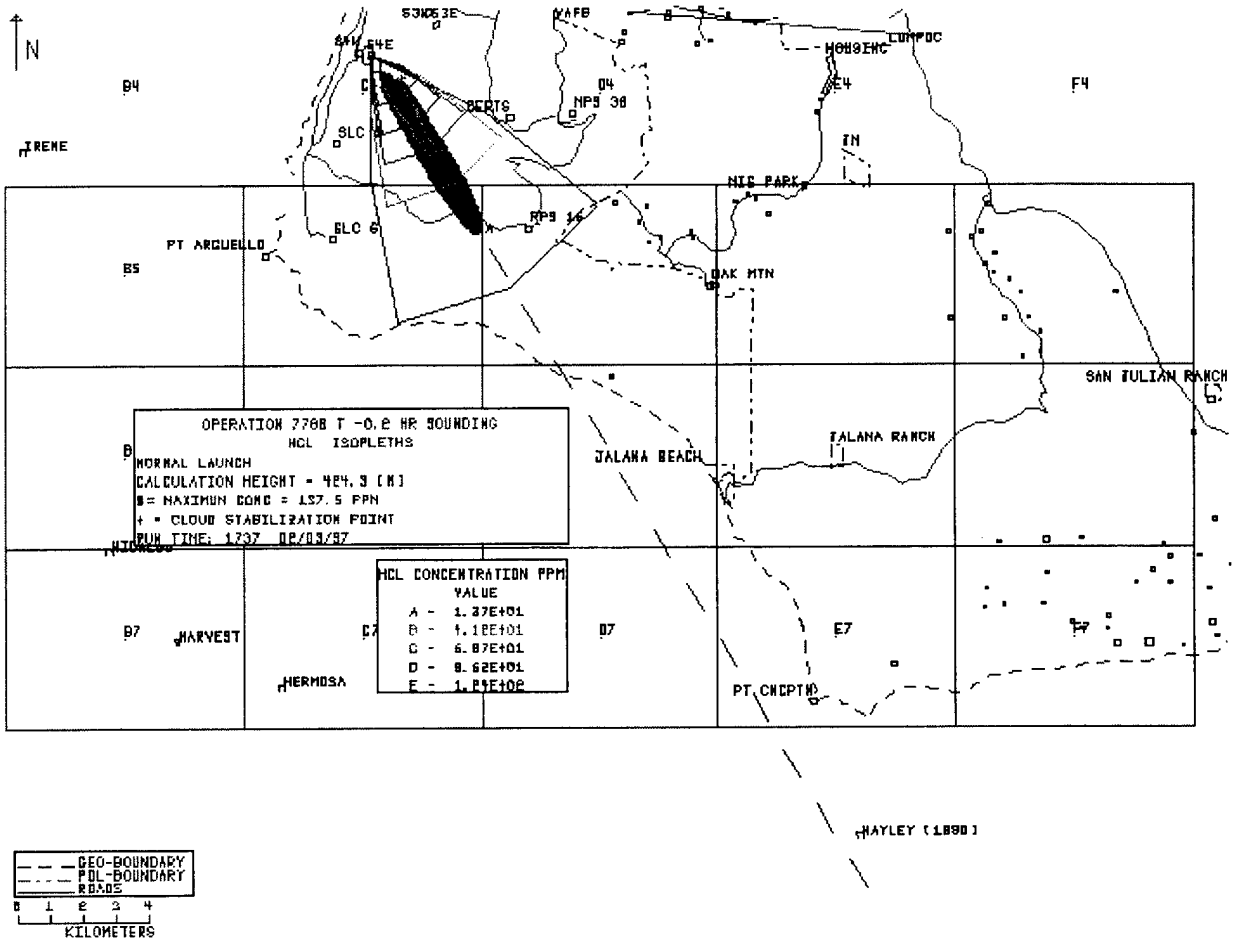

Figure A3. HCl Concentration Isopleth Predictions from REEDM Version 7.07 for K-22 Mission Using T-0.25h Rawinsonde for T-0.0h Reconstruction.

1**********

ROCKET EXHAUST EFFLUENT DIFFUSION MODEL REEDM PAGE 01
VERSION 7.07 AT VAFB
OPERATION NUMBER 7788, 1129 PDT 17 MAY 1996
launch time: 1432 PDT 12 MAY 1996
RAWINSONDE ASCENT NUMBER 125, 2117 Z 12 MAY 1996 T +0.0 HR

****

----- PROGRAM OPTIONS -----

MODEL		CONCENTRATION
RUN TYPE		OPERATIONAL
WIND-FIELD TERRAIN EFFECTS MODEL		NONE
LAUNCH VEHICLE		TITAN IV
LAUNCH TYPE		NORMAL
LAUNCH COMPLEX NUMBER		4E
TURBULENCE PARAMETERS ARE DETERMINED FROM		DOPPLER & TOWER DATA
SURFACE CHEMISTRY MODEL		absorption coefficient
SPECIES SURFACE FACTOR	HCL	0.000
CLOUD SHAPE		ELLIPTICAL
CALCULATION HEIGHT		STABILIZATION
PROPELLANT TEMPERATURE (DEG. C)		12.56
CONCENTRATION AVERAGING TIME (SEC.)		3600.00
mixing layer reflection coefficient (RNG- 0 TO 1,no reflection=0)		1.0000
DIFFUSION COEFFICIENTS	LATERAL	1.0000
	VERTICAL	1.0000
VEHICLE AIR ENTRAINMENT PARAMETER	GAMMAE	0.6400
DOWNWIND EXPANSION DISTANCE (METERS)	LATERAL	100.00
	VERTICAL	100.00

----- DATA FILES -----

INPUT FILES

RAWINSONDE FILE	op7788.t0
DATA BASE FILE	rdmbase.mas

OUTPUT FILES

PRINT FILE	op7788.cld
PLOT FILE	op7788t0.plt

1**********

ROCKET EXHAUST EFFLUENT DIFFUSION MODEL REEDM PAGE 02
VERSION 7.07 AT VAFB
OPERATION NUMBER 7788, 1129 PDT 17 MAY 1996
launch time: 1432 PDT 12 MAY 1996
RAWINSONDE ASCENT NUMBER 125, 2117 Z 12 MAY 1996 T +0.0 HR

****

----- METEOROLOGICAL RAWINSONDE DATA -----

TEST NBR SITE: 1764 OP NO: W7788 ASC NO: 125
RAWINSONDE MSS/WIN
TIME- 2117 Z DATE- 12 MAY 1996
ASCENT NUMBER 125

----- T +0.0 HR SOUNDING -----

MET. LEV. NO.	ALTITUDE MSL (FT)	ALTITUDE GND (FT)	GND (M)	WIND DIR (DEG)	WIND SPEED (M/S)	WIND SPEED (KTS)	AIR TEMP (DEG C)	AIR PTEMP (DEG C)	AIR DPTEMP (DEG C)	AIR PRESS (MB)	AIR RH (%)	H M	INT-ERP
1	328	0.0	0.0	355	3.1	6.0	19.4	20.7	10.7	1001.8	57.0		
2	383	54.9	16.7	0	3.1	6.0	18.7	20.1	9.9	999.9	56.7		
3	431	102.9	31.4	355	3.1	6.0	18.1	19.6	9.2	998.2	56.4		
4	472	143.9	43.9	355	3.1	6.0	17.5	19.1	8.6	996.7	55.7		**
5	513	184.9	56.4	354	3.1	6.0	17.0	18.6	8.0	995.3	56.0		
6	567	238.4	72.7	357	2.8	5.5	16.9	18.7	9.1	993.4	60.5		**
7	620	291.9	89.0	359	2.6	5.0	16.7	18.8	10.3	991.5	66.0		
8	725	396.4	120.8	352	3.0	5.8	15.9	18.2	9.9	987.8	67.5		**
9	829	500.9	152.7	345	3.4	6.6	15.0	17.7	9.4	984.1	69.0	*	
10	984	655.9	199.9	343	4.8	9.3	15.2	18.4	9.8	978.6	70.0		
11	1067	738.4	225.1	332	5.4	10.5	16.5	20.0	9.6	975.8	63.6		**
12	1149	820.9	250.2	320	6.0	11.7	17.9	21.6	9.4	972.9	58.1		
13	1206	877.4	267.4	308	5.5	10.6	18.9	22.7	9.3	970.9	53.7		**
14	1262	933.9	284.7	296	4.9	9.6	19.8	23.8	9.1	969.0	50.0		
15	1313	984.9	300.2	285	4.5	8.7	21.3	25.6	9.9	967.3	48.3		
16	1384	1055.9	321.8	289	5.0	9.7	23.4	28.0	11.1	964.8	46.0		
17	1477	1148.9	350.2	295	5.6	10.9	23.9	28.8	10.3	961.7	42.5		
18	1515	1186.9	361.8	309	5.7	11.1	24.1	29.0	10.0	960.4	41.1		**
19	1553	1224.9	373.4	323	5.9	11.4	24.3	29.3	9.7	959.2	39.6		
20	1806	1477.9	450.5	326	6.3	12.2	25.4	31.1	8.1	950.8	33.5		**
21	2059	1730.9	527.6	329	6.7	13.1	26.5	32.8	6.5	942.5	28.0		
22	2380	2051.4	625.3	331	6.8	13.2	26.1	33.4	5.5	932.1	26.9		**
23	2700	2371.9	723.0	333	6.9	13.4	25.8	34.0	4.5	921.8	25.3		
24	3292	2963.9	903.4	337	6.2	12.0	24.9	34.7	2.6	903.0	23.8		**
25	3884	3555.9	1083.8	340	5.5	10.7	23.9	35.4	0.7	884.6	21.6		
26	4478	4149.9	1264.9	351	4.3	8.4	22.4	35.7	-0.3	866.4	22.6		**
27	5072	4743.9	1445.9	2	3.1	6.1	20.9	35.9	-1.2	848.5	22.7		
28	5681	5352.9	1631.6	18	2.4	4.7	19.5	36.4	-1.5	830.4	24.7		**
29	6290	5961.9	1817.2	34	1.7	3.3	18.1	36.8	-1.9	812.7	25.5		
30	6914	6585.9	2007.4	359	1.3	2.6	17.6	38.1	-5.1	794.8	21.5		**
31	7538	7209.9	2197.6	323	1.0	1.9	17.1	39.4	-8.3	777.3	16.8		
32	8146	7817.9	2382.9	287	1.6	3.1	16.1	40.4	-9.2	760.6	17.5		**
33	8754	8425.9	2568.2	251	2.2	4.3	15.2	41.3	-10.0	744.2	16.6		
34	10063	9734.9	2967.2	245	2.8	5.5	13.7	43.9	-11.0	709.9	16.9		

* - INDICATES THE CALCULATED TOP OF THE SURFACE MIXING LAYER
** - INDICATES THAT DATA IS LINEARLY INTERPOLATED FROM INPUT METEOROLOGY

```
1*************************************************************************
                ROCKET EXHAUST EFFLUENT DIFFUSION MODEL REEDM        PAGE   03
                          VERSION 7.07 AT VAFB
                  OPERATION NUMBER   7788, 1129 PDT 17 MAY 1996
                      launch time:  1432 PDT 12 MAY 1996
       RAWINSONDE ASCENT NUMBER    125, 2117   Z 12 MAY 1996  T  +0.0 HR
*************************************************************************

                  ----- METEOROLOGICAL RAWINSONDE DATA -----


 SURFACE AIR DENSITY (GM/M**3)                                      1187.36
 MIXING LAYER HEIGHT   152.68 (M) SPECIFIED BY PRESSURE LEVEL (MB)   984.09
 CLOUD COVER IN TENTHS OF CELESTIAL DOME                               0.0
 CLOUD CEILING (M)                                                  9999.0

***REEDM  WARNING 09, END OF FILE READ, DATA MAY BE TRUNCATED, FILE =
                    op7788.t0
                     THE ERROR OCCURRED AT RECORD   60.00

***REEDM  ERROR 09, INCOMPLETE DATA - DOPPLER
                     THE ERROR OCCURRED AT RECORD   60.00
                         ----- PLUME RISE DATA -----

EXHAUST RATE OF MATERIAL INTO GRN CLD-   (GRAMS/SEC)          4.13939E+06
TOTAL GROUND CLD MATERIAL-               (GRAMS)              3.89607E+07
HEAT OUTPUT PER GRAM-                    (CALORIES)                1555.6
VEHICLE RISE HEIGHT DEFINING GROUND CLD- (M)                        199.9
VEHICLE RISE TIME PARAMETERS-            (TK=(A*Z**B)+C)  A=       0.8677
                                                          B=       0.4500
                                                          C=       0.0000
EXHAUST RATE OF MATERIAL INTO CONTRAIL-  (GRAMS/SEC)          4.13939E+06
CONTRAIL HEAT OUTPUT PER GRAM-           (CALORIES)                1555.6
```

1**********

ROCKET EXHAUST EFFLUENT DIFFUSION MODEL REEDM PAGE 04
VERSION 7.07 AT VAFB
OPERATION NUMBER 7788, 1129 PDT 17 MAY 1996
launch time: 1432 PDT 12 MAY 1996
RAWINSONDE ASCENT NUMBER 125, 2117 Z 12 MAY 1996 T +0.0 HR

****

----- EXHAUST CLOUD -----

MET. LAYER NO.	TOP OF LAYER (METERS)	CLOUD RISE TIME (SECONDS)	CLOUD RISE RANGE (METERS)	CLOUD RISE BEARING (DEGREES)	STABILIZED CLOUD RANGE (METERS)	STABILIZED CLOUD BEARING (DEGREES)
1	16.7	2.9	4.5	176.2	0.0	0.0
2	31.4	4.4	11.3	177.8	0.0	0.0
3	43.9	5.7	15.6	177.2	0.0	0.0
4	56.4	7.0	19.6	176.7	0.0	0.0
5	72.7	8.7	24.2	176.3	0.0	0.0
6	89.0	10.6	29.3	176.3	0.0	0.0
7	120.8	14.5	37.0	176.6	0.0	0.0
8	152.7	19.0	49.6	175.3	0.0	0.0
9	199.9	26.9	71.4	172.2	462.4	165.3
10	225.1	31.7	100.3	169.2	561.6	159.4
11	250.2	37.0	126.6	165.4	609.5	149.7
12	267.4	41.0	151.6	161.0	608.2	140.5
13	284.7	45.3	170.9	156.9	551.7	132.2
14	300.2	49.5	187.2	152.8	499.1	125.1
15	321.8	55.8	204.8	147.9	489.9	123.0
16	350.2	65.5	237.8	141.9	522.8	125.2
17	361.8	70.0	273.2	138.3	566.0	129.8
18	373.4	75.1	300.2	137.5	576.1	136.9
19	450.5	122.6 *	599.7	140.8	599.7	140.8
20	527.6	122.6 *	599.7	140.8	599.7	140.8
21	625.3	122.6 *	599.7	140.8	599.7	140.8
22	723.0	122.6 *	599.7	140.8	599.7	140.8
23	903.4	122.6 *	599.7	140.8	599.7	140.8
24	1083.8	122.6 *	599.7	140.8	599.7	140.8
25	1264.9	122.6 *	599.7	140.8	599.7	140.8
26	1445.9	122.6 *	599.7	140.8	599.7	140.8
27	1631.6	122.6 *	599.7	140.8	599.7	140.8
28	1817.2	122.6 *	599.7	140.8	599.7	140.8
29	2007.4	122.6 *	599.7	140.8	599.7	140.8
30	2197.6	122.6 *	599.7	140.8	599.7	140.8
31	2382.9	122.6 *	599.7	140.8	599.7	140.8
32	2568.2	122.6 *	599.7	140.8	599.7	140.8
33	2967.2	122.6 *	599.7	140.8	599.7	140.8

* - INDICATES CLOUD STABILIZATION TIME WAS USED

1**********

ROCKET EXHAUST EFFLUENT DIFFUSION MODEL REEDM PAGE 05
VERSION 7.07 AT VAFB
OPERATION NUMBER 7788, 1129 PDT 17 MAY 1996
launch time: 1432 PDT 12 MAY 1996
RAWINSONDE ASCENT NUMBER 125, 2117 Z 12 MAY 1996 T +0.0 HR

****

----- EXHAUST CLOUD -----

CHEMICAL SPECIES = HCL

MET. LAYER NO.	TOP OF LAYER (METERS)		LAYER SOURCE STRENGTH (GRAMS)	CLOUD UPDRAFT VELOCITY (M/S)	CLOUD RADIUS (METERS)	STD. DEVIATION MATERIAL DIST. ALONGWIND (METERS)	CROSSWIND (METERS)
1	16.7		0.00000E+00	9.0	0.0	0.0	0.0
2	31.4		0.00000E+00	9.9	0.0	0.0	0.0
3	43.9		0.00000E+00	9.9	0.0	0.0	0.0
4	56.4		0.00000E+00	9.6	0.0	0.0	0.0
5	72.7		0.00000E+00	9.1	0.0	0.0	0.0
6	89.0		0.00000E+00	8.6	0.0	0.0	0.0
7	120.8		0.00000E+00	7.5	0.0	0.0	0.0
8	152.7		0.00000E+00	6.6	0.0	0.0	0.0
9	199.9		2.25740E+05	5.5	138.1	64.3	64.3
10	225.1		2.92170E+05	5.0	213.8	99.6	99.6
11	250.2		3.94924E+05	4.5	248.5	115.8	115.8
12	267.4		3.23047E+05	4.2	271.5	126.5	126.5
13	284.7		3.60990E+05	3.9	287.0	133.7	133.7
14	300.2		3.54970E+05	3.6	299.5	139.6	139.6
15	321.8		5.34228E+05	3.2	311.5	145.1	145.1
16	350.2		7.57666E+05	2.7	324.2	151.1	151.1
17	361.8		3.24610E+05	2.4	331.8	154.6	154.6
18	373.4		3.31449E+05	2.2	335.3	156.2	156.2
19	450.5	*	2.58344E+06	0.0	342.5	159.6	159.6
20	527.6	*	2.97908E+06	0.0	332.9	155.1	155.1
21	625.3	*	2.91684E+06	0.0	283.7	132.2	132.2
22	723.0	*	1.36187E+06	0.0	132.4	61.7	61.7
23	903.4	*	1.44906E+06	0.0	199.9	93.2	93.2
24	1083.8	*	1.29706E+06	0.0	199.9	93.2	93.2
25	1264.9	*	1.18675E+06	0.0	199.9	93.2	93.2
26	1445.9	*	1.09652E+06	0.0	199.9	93.2	93.2
27	1631.6	*	1.04831E+06	0.0	199.9	93.2	93.2
28	1817.2	*	9.84553E+05	0.0	199.9	93.2	93.2
29	2007.4	*	9.52955E+05	0.0	199.9	93.2	93.2
30	2197.6	*	9.04473E+05	0.0	199.9	93.2	93.2
31	2382.9	*	8.40729E+05	0.0	199.9	93.2	93.2
32	2568.2	*	8.05479E+05	0.0	199.9	93.2	93.2
33	2967.2	*	1.63184E+06	0.0	199.9	93.2	93.2

* - INDICATES CLOUD STABILIZATION TIME WAS USED

1**********

ROCKET EXHAUST EFFLUENT DIFFUSION MODEL REEDM PAGE 06
VERSION 7.07 AT VAFB
OPERATION NUMBER 7788, 1129 PDT 17 MAY 1996
launch time: 1432 PDT 12 MAY 1996
RAWINSONDE ASCENT NUMBER 125, 2117 Z 12 MAY 1996 T +0.0 HR

****

----- CLOUD STABILIZATION -----

CALCULATION HEIGHT	(METERS)		424.25
STABILIZATION HEIGHT	(METERS)		424.25
STABILIZATION TIME	(SECS)		122.64
FIRST MIXING LAYER HEIGHT-	(METERS)	TOP =	152.68
		BASE=	0.00
SECOND SELECTED LAYER HEIGHT-	(METERS)	TOP =	2967.20
		BASE=	152.68
SIGMAR(AZ) AT THE SURFACE	(DEGREES)		11.0536
SIGMER(EL) AT THE SURFACE	(DEGREES)		1.2023

MET. LAYER NO.	WIND SPEED (M/SEC)	WIND SPEED SHEAR (M/SEC)	WIND DIRECTION (DEG)	WIND DIRECTION SHEAR (DEG)	SIGMA OF AZI ANG (DEG)	SIGMA OF ELE ANG (DEG)
1	3.09	0.00	357.50	5.00	9.3169	3.4922
2	3.09	0.00	357.50	-5.00	8.8304	7.9312
3	3.09	0.00	354.83	-0.35	11.8804	11.8804
4	3.09	0.00	354.47	-0.35	15.4805	15.4805
5	2.96	-0.26	355.47	2.35	19.6305	19.6305
6	2.70	-0.26	357.83	2.35	24.2902	24.2902
7	2.78	0.41	355.50	-7.00	25.4004	25.4004
8	3.19	0.41	348.50	-7.00	12.6004	12.6004
9	4.09	1.39	344.00	-2.00	1.0000	1.0000
10	5.09	0.62	337.25	-11.50	1.0000	1.0000
11	5.71	0.62	325.75	-11.50	1.0000	1.0000
12	5.75	-0.54	313.98	-12.05	1.0000	1.0000
13	5.21	-0.54	301.92	-12.05	1.0000	1.0000
14	4.71	-0.46	290.45	-10.90	1.0000	1.0000
15	4.73	0.51	287.15	4.30	1.0000	1.0000
16	5.30	0.62	292.15	5.70	1.0000	1.0000
17	5.67	0.13	302.10	14.20	1.0000	1.0000
18	5.80	0.13	316.30	14.20	1.0000	1.0000
19	6.08	0.44	324.72	2.65	1.0000	1.0000
20	6.52	0.44	327.38	2.65	1.0000	1.0000
21	6.78	0.08	329.88	2.35	1.0000	1.0000
22	6.85	0.08	332.22	2.35	1.0000	1.0000
23	6.55	-0.69	335.08	3.35	1.0000	1.0000
24	5.85	-0.69	338.42	3.35	1.0000	1.0000
25	4.91	-1.18	345.55	10.90	1.0000	1.0000
26	3.73	-1.18	356.45	10.90	1.0000	1.0000
27	2.78	-0.72	10.00	16.20	1.0000	1.0000
28	2.06	-0.72	26.20	16.20	1.0000	1.0000
29	1.52	-0.35	16.41	-35.77	1.0000	1.0000
30	1.17	-0.35	340.64	-35.77	1.0000	1.0000

1**********

ROCKET EXHAUST EFFLUENT DIFFUSION MODEL REEDM PAGE 07
VERSION 7.07 AT VAFB
OPERATION NUMBER 7788, 1129 PDT 17 MAY 1996
launch time: 1432 PDT 12 MAY 1996
RAWINSONDE ASCENT NUMBER 125, 2117 Z 12 MAY 1996 T +0.0 HR

****

----- CALCULATED METEOROLOGICAL LAYER PARAMETERS -----

MET. LAYER NO.	WIND SPEED (M/SEC)	WIND SPEED SHEAR (M/SEC)	WIND DIRECTION (DEG)	WIND DIRECTION SHEAR (DEG)	SIGMA OF AZI ANG (DEG)	SIGMA OF ELE ANG (DEG)
31	1.30	0.61	304.86	-35.78	1.0000	1.0000
32	1.91	0.61	269.09	-35.77	1.0000	1.0000
33	2.52	0.62	248.30	-5.80	1.0000	1.0000

ALTITUDE RANGE USED IN COMPUTING TRANSITION LAYER AVERAGES
IS 152.7 TO 2967.2 METERS.

TRANSITION LAYER NUMBER- 1

VALUE AT	HEIGHT (METERS)	TEMP. (DEG K)	WIND SPEED (M/SEC)	WIND SPEED SHEAR (M/SEC)	WIND DIR. (DEG)	WIND DIR. SHEAR (DEG)	SIGMA AZI. (DEG)	SIGMA ELE. (DEG)
TOP-	152.68	290.80	3.40		345.00		1.0000	1.0000
LAYER-			0.00	0.00	360.00	0.00	0.0000	0.0000
BOTTOM-	0.00	293.83	3.09		355.00		11.0536	1.2023

TRANSITION LAYER NUMBER- 2

VALUE AT	HEIGHT (METERS)	TEMP. (DEG K)	WIND SPEED (M/SEC)	WIND SPEED SHEAR (M/SEC)	WIND DIR. (DEG)	WIND DIR. SHEAR (DEG)	SIGMA AZI. (DEG)	SIGMA ELE. (DEG)
TOP-	2967.20	317.05	2.83		245.40		1.0000	1.0000
LAYER-			3.04	1.70	329.85	19.49	1.0000	1.0000
BOTTOM-	152.68	290.80	3.40		345.00		1.0000	1.0000

----- MAXIMUM CENTERLINE CALCULATIONS -----

** DECAY COEFFICIENT (1/SEC) = 0.00000E+00 **

CONCENTRATION OF HCL AT A HEIGHT OF 424.3 METERS
DOWNWIND FROM A TITAN IV NORMAL LAUNCH
CALCULATIONS APPLY TO THE LAYER BETWEEN 152.7 AND 2967.2 METERS

RANGE FROM PAD (METERS)	BEARING FROM PAD (DEGREES)	PEAK CONCEN-TRATION (PPM)	CLOUD ARRIVAL TIME (MIN)	CLOUD DEPARTURE TIME (MIN)
1000.0001	144.4145	137.4595	1.7470	6.1752
2000.0000	147.1348	93.6437	6.3818	12.0371
3000.0000	147.8898	57.2287	11.1360	18.1458
4000.0000	148.2231	35.5221	15.8074	24.3806
5000.0000	148.5056	23.1894	20.4368	30.6800
6000.7637	148.9350	15.8530	25.0500	37.0213
7000.5977	149.1005	11.2778	29.6450	43.3745
8000.9561	148.9633	8.2970	34.2327	49.7406
9000.5576	149.2113	6.2835	38.8155	56.1153
10000.7939	149.1270	4.8823	43.3950	62.4960
11000.3145	149.4157	3.8831	47.9720	68.8811
12000.4385	149.3592	3.1537	52.5474	75.2694
13000.5723	149.3114	2.6067	57.1213	81.6603
14000.7139	149.2703	2.1881	61.6943	88.0531
15000.1465	149.5959	1.8625	66.2664	94.4474
16000.1963	149.5654	1.6045	70.8378	100.8430
17000.2500	149.5384	1.3958	75.4086	107.2397
18000.3066	149.5145	1.2246	79.9790	113.6371
19000.3672	149.4930	1.0824	84.5491	120.0353
20000.4297	149.4737	0.9627	89.1188	126.4342
21000.4941	149.4563	0.8611	93.6882	132.8335
22000.5605	149.4404	0.7741	98.2574	139.2333
23000.6270	149.4259	0.6989	102.8263	145.6335
24000.0195	149.7775	0.6336	107.3951	152.0340
25000.0273	149.7655	0.5766	111.9638	158.4348
26000.0352	149.7544	0.5265	116.5323	164.8359
27000.0449	149.7442	0.4821	121.1007	171.2372
28000.0566	149.7346	0.4428	125.6689	177.6387
29000.0664	149.7258	0.4077	130.2371	184.0404
30000.0781	149.7175	0.3762	134.8052	190.4423

	RANGE	BEARING
137.460 IS THE MAXIMUM PEAK CONCENTRATION	1000.0	144.4

1**********

ROCKET EXHAUST EFFLUENT DIFFUSION MODEL REEDM PAGE 09
VERSION 7.07 AT VAFB
OPERATION NUMBER 7788, 1129 PDT 17 MAY 1996
launch time: 1432 PDT 12 MAY 1996
RAWINSONDE ASCENT NUMBER 125, 2117 Z 12 MAY 1996 T +0.0 HR

****

----- MAXIMUM CENTERLINE CALCULATIONS -----

** DECAY COEFFICIENT (1/SEC) = 0.00000E+00 **

CONCENTRATION OF HCL AT A HEIGHT OF 424.3 METERS
DOWNWIND FROM A TITAN IV NORMAL LAUNCH
CALCULATIONS APPLY TO THE LAYER BETWEEN 152.7 AND 2967.2 METERS

RANGE FROM PAD (METERS)	BEARING FROM PAD (DEGREES)	60.0 MIN. MEAN CONCEN-TRATION (PPM)	CLOUD ARRIVAL TIME (MIN)	CLOUD DEPARTURE TIME (MIN)
1000.0001	144.4145	5.1244	1.7470	6.1752
2000.0000	147.1348	4.1400	6.3818	12.0371
3000.0000	147.8898	3.2163	11.1360	18.1458
4000.0000	148.2231	2.5119	15.8074	24.3806
5000.0000	148.5056	2.0051	20.4368	30.6800
6000.7637	148.9350	1.6315	25.0500	37.0213
7000.5977	149.1005	1.3506	29.6450	43.3745
8000.9561	148.9633	1.1356	34.2327	49.7406
9000.5576	149.2113	0.9686	38.8155	56.1153
10000.7939	149.1270	0.8376	43.3950	62.4960
11000.3145	149.4157	0.7341	47.9720	68.8811
12000.4385	149.3592	0.6517	52.5474	75.2694
13000.5723	149.3114	0.5846	57.1213	81.6603
14000.7139	149.2703	0.5293	61.6943	88.0531
15000.1465	149.5959	0.4835	66.2664	94.4474
16000.1963	149.5654	0.4449	70.8378	100.8430
17000.2500	149.5384	0.4118	75.4086	107.2397
18000.3066	149.5145	0.3830	79.9790	113.6371
19000.3672	149.4930	0.3577	84.5491	120.0353
20000.4297	149.4737	0.3352	89.1188	126.4342
21000.4941	149.4563	0.3150	93.6882	132.8335
22000.5605	149.4404	0.2968	98.2574	139.2333
23000.6270	149.4259	0.2802	102.8263	145.6335
24000.0195	149.7775	0.2650	107.3951	152.0340
25000.0273	149.7655	0.2511	111.9638	158.4348
26000.0352	149.7544	0.2381	116.5323	164.8359
27000.0449	149.7442	0.2261	121.1007	171.2372
28000.0566	149.7346	0.2149	125.6689	177.6387
29000.0664	149.7258	0.2044	130.2371	184.0404
30000.0781	149.7175	0.1946	134.8052	190.4423

	RANGE	BEARING
5.124 IS THE MAXIMUM 60.0 MIN. MEAN CONCENTRATION	1000.0	144.4

```
1*********************************************************************************
                ROCKET EXHAUST EFFLUENT DIFFUSION MODEL REEDM          PAGE   10
                          VERSION 7.07 AT VAFB
                   OPERATION NUMBER   7788, 1129 PDT 17 MAY 1996
                       launch time:  1432 PDT 12 MAY 1996
        RAWINSONDE ASCENT NUMBER    125, 2117   Z 12 MAY 1996  T  +0.0 HR
 *********************************************************************************

                   ----- hazard box coordinates -----


 HAZARD BOX COORDINATES FOR HCL          CONCENTRATION
        SCENARIO =          NORMAL          MET PROFILE = T  +0.0 HR
        DIRECTIONAL UNCERTAINTY =    25.0  RANGE EXTENSTION FACTOR =     1.3
        SOURCE LOCATION =  34 37 55  120 36 45

 ISOPLETH # 1 VALUE = 1.0000E+01  PPM
 CRASH GRID COORDINATES:
 17 BU   30 BN   43 BD   33 AT   32 AT   19 AP   16 BG   17 BU
 RANGE(NMI) AND BEARING(DEG), LAT(DMS) AND LONG(DMS) :
      2.5  117.       5.1  123.       5.1  148.
      2.4  180.       5.1  175.       5.1  150.
    34 36 46  120 34  7    34 35  1  120 31 37    34 33 29  120 33 36
    34 35 28  120 36 49    34 32 48  120 36 22    34 33 25  120 33 45

 ISOPLETH # 2 VALUE = 5.0000E+01  PPM
 CRASH GRID COORDINATES:
 17 BU   21 BT   28 BN   24 BJ   18 BH   17 BQ   17 BU
 RANGE(NMI) AND BEARING(DEG), LAT(DMS) AND LONG(DMS) :
      0.7  110.       2.2  122.       2.2  147.
      0.7  181.       2.2  174.       2.2  149.
    34 37 39  120 35 56    34 36 42  120 34 27    34 36  0  120 35 19
    34 37 13  120 36 47    34 35 41  120 36 32    34 35 58  120 35 24


 *** REEDM  HAS TERMINATED
```

Surface Impact Predictions

This section includes the REEDM version 7.07 output for the surface impact run. For the stabilization height run, we included the plots of the rawinsonde meteorological data, the predicted maximum concentration versus downwind distance, and the predicted concentration isopleths overlayed on a range map. Since REEDM predicts zero HCl concentration at the ground level, we include no plots for the surface run. The rawinsonde meteorological data is identical to the data plotted in Figure A1 for the stabilization height run. Therefore, this section includes only the detailed REEDM report for this run. The first page of the REEDM output is its listing of errors and is not included in this appendix.

1**********

ROCKET EXHAUST EFFLUENT DIFFUSION MODEL REEDM PAGE 2
VERSION 7.07 AT VAFB
OPERATION NUMBER 7788, 1123 PDT 17 MAY 1996
launch time: 1432 PDT 12 MAY 1996
RAWINSONDE ASCENT NUMBER 125, 2117 Z 12 MAY 1996 T +0.0 HR

****

----- PROGRAM OPTIONS -----

MODEL		CONCENTRATION
RUN TYPE		OPERATIONAL
WIND-FIELD TERRAIN EFFECTS MODEL		NONE
LAUNCH VEHICLE		TITAN IV
LAUNCH TYPE		NORMAL
LAUNCH COMPLEX NUMBER		4E
TURBULENCE PARAMETERS ARE DETERMINED FROM		DOPPLER & TOWER DATA
SURFACE CHEMISTRY MODEL		deposition velocity
SPECIES SURFACE FACTOR	HCL	3.000
CLOUD SHAPE		ELLIPTICAL
CALCULATION HEIGHT		SURFACE
PROPELLANT TEMPERATURE (DEG. C)		12.56
CONCENTRATION AVERAGING TIME (SEC.)		3600.00
mixing layer reflection coefficient (RNG- 0 TO 1,no reflection=0)		1.0000
DIFFUSION COEFFICIENTS	LATERAL	1.0000
	VERTICAL	1.0000
VEHICLE AIR ENTRAINMENT PARAMETER	GAMMAE	0.6400
DOWNWIND EXPANSION DISTANCE (METERS)	LATERAL	100.00
	VERTICAL	100.00

----- DATA FILES -----

INPUT FILES

RAWINSONDE FILE	op7788.t0
DATA BASE FILE	rdmbase.mas

OUTPUT FILES

PRINT FILE	op7788t0.out
PLOT FILE	op7788t0.plt

----- METEOROLOGICAL RAWINSONDE DATA -----

TEST NBR SITE: 1764 OP NO: W7788 ASC NO: 125
RAWINSONDE MSS/WIN
TIME- 2117 Z DATE- 12 MAY 1996
ASCENT NUMBER 125

----- T +0.0 HR SOUNDING -----

MET. LEV. NO.	ALTITUDE MSL (FT)	ALTITUDE GND (FT)	GND (M)	WIND DIR (DEG)	WIND SPEED (M/S)	WIND SPEED (KTS)	AIR TEMP (DEG C)	AIR PTEMP (DEG C)	AIR DPTEMP (DEG C)	AIR PRESS (MB)	AIR RH (%)	H M	INT-ERP
1	328	0.0	0.0	355	3.1	6.0	19.4	20.7	10.7	1001.8	57.0		
2	383	54.9	16.7	0	3.1	6.0	18.7	20.1	9.9	999.9	56.7		
3	431	102.9	31.4	355	3.1	6.0	18.1	19.6	9.2	998.2	56.4		
4	472	143.9	43.9	355	3.1	6.0	17.5	19.1	8.6	996.7	55.7		**
5	513	184.9	56.4	354	3.1	6.0	17.0	18.6	8.0	995.3	56.0		
6	567	238.4	72.7	357	2.8	5.5	16.9	18.7	9.1	993.4	60.5		**
7	620	291.9	89.0	359	2.6	5.0	16.7	18.8	10.3	991.5	66.0		
8	725	396.4	120.8	352	3.0	5.8	15.9	18.2	9.9	987.8	67.5		**
9	829	500.9	152.7	345	3.4	6.6	15.0	17.7	9.4	984.1	69.0	*	
10	984	655.9	199.9	343	4.8	9.3	15.2	18.4	9.8	978.6	70.0		
11	1067	738.4	225.1	332	5.4	10.5	16.5	20.0	9.6	975.8	63.6		**
12	1149	820.9	250.2	320	6.0	11.7	17.9	21.6	9.4	972.9	58.1		
13	1206	877.4	267.4	308	5.5	10.6	18.9	22.7	9.3	970.9	53.7		**
14	1262	933.9	284.7	296	4.9	9.6	19.8	23.8	9.1	969.0	50.0		
15	1313	984.9	300.2	285	4.5	8.7	21.3	25.6	9.9	967.3	48.3		
16	1384	1055.9	321.8	289	5.0	9.7	23.4	28.0	11.1	964.8	46.0		
17	1477	1148.9	350.2	295	5.6	10.9	23.9	28.8	10.3	961.7	42.5		
18	1515	1186.9	361.8	309	5.7	11.1	24.1	29.0	10.0	960.4	41.1		**
19	1553	1224.9	373.4	323	5.9	11.4	24.3	29.3	9.7	959.2	39.6		
20	1806	1477.9	450.5	326	6.3	12.2	25.4	31.1	8.1	950.8	33.5		**
21	2059	1730.9	527.6	329	6.7	13.1	26.5	32.8	6.5	942.5	28.0		
22	2380	2051.4	625.3	331	6.8	13.2	26.1	33.4	5.5	932.1	26.9		**
23	2700	2371.9	723.0	333	6.9	13.4	25.8	34.0	4.5	921.8	25.3		
24	3292	2963.9	903.4	337	6.2	12.0	24.9	34.7	2.6	903.0	23.8		**
25	3884	3555.9	1083.8	340	5.5	10.7	23.9	35.4	0.7	884.6	21.6		
26	4478	4149.9	1264.9	351	4.3	8.4	22.4	35.7	-0.3	866.4	22.6		**
27	5072	4743.9	1445.9	2	3.1	6.1	20.9	35.9	-1.2	848.5	22.7		
28	5681	5352.9	1631.6	18	2.4	4.7	19.5	36.4	-1.5	830.4	24.7		**
29	6290	5961.9	1817.2	34	1.7	3.3	18.1	36.8	-1.9	812.7	25.5		
30	6914	6585.9	2007.4	359	1.3	2.6	17.6	38.1	-5.1	794.8	21.5		**
31	7538	7209.9	2197.6	323	1.0	1.9	17.1	39.4	-8.3	777.3	16.8		
32	8146	7817.9	2382.9	287	1.6	3.1	16.1	40.4	-9.2	760.6	17.5		**
33	8754	8425.9	2568.2	251	2.2	4.3	15.2	41.3	-10.0	744.2	16.6		
34	10063	9734.9	2967.2	245	2.8	5.5	13.7	43.9	-11.0	709.9	16.9		

* - INDICATES THE CALCULATED TOP OF THE SURFACE MIXING LAYER
** - INDICATES THAT DATA IS LINEARLY INTERPOLATED FROM INPUT METEOROLOGY

----- METEOROLOGICAL RAWINSONDE DATA -----

SURFACE AIR DENSITY (GM/M**3)	1187.36
MIXING LAYER HEIGHT 152.68 (M) SPECIFIED BY PRESSURE LEVEL (MB)	984.09
CLOUD COVER IN TENTHS OF CELESTIAL DOME	0.0
CLOUD CEILING (M)	9999.0

***REEDM WARNING 09, END OF FILE READ, DATA MAY BE TRUNCATED, FILE = op7788.t0
THE ERROR OCCURRED AT RECORD 60.00

***REEDM ERROR 09, INCOMPLETE DATA - DOPPLER
THE ERROR OCCURRED AT RECORD 60.00

----- PLUME RISE DATA -----

EXHAUST RATE OF MATERIAL INTO GRN CLD-	(GRAMS/SEC)		4.13939E+06
TOTAL GROUND CLD MATERIAL-	(GRAMS)		3.89607E+07
HEAT OUTPUT PER GRAM-	(CALORIES)		1555.6
VEHICLE RISE HEIGHT DEFINING GROUND CLD-	(M)		199.9
VEHICLE RISE TIME PARAMETERS-	(TK=(A*Z**B)+C)	A=	0.8677
		B=	0.4500
		C=	0.0000
EXHAUST RATE OF MATERIAL INTO CONTRAIL-	(GRAMS/SEC)		4.13939E+06
CONTRAIL HEAT OUTPUT PER GRAM-	(CALORIES)		1555.6

----- EXHAUST CLOUD -----

MET. LAYER NO.	TOP OF LAYER (METERS)	CLOUD RISE TIME (SECONDS)	CLOUD RISE RANGE (METERS)	CLOUD RISE BEARING (DEGREES)	STABILIZED CLOUD RANGE (METERS)	STABILIZED CLOUD BEARING (DEGREES)
1	16.7	2.9	4.5	176.2	0.0	0.0
2	31.4	4.4	11.3	177.8	0.0	0.0
3	43.9	5.7	15.6	177.2	0.0	0.0
4	56.4	7.0	19.6	176.7	0.0	0.0
5	72.7	8.7	24.2	176.3	0.0	0.0
6	89.0	10.6	29.3	176.3	0.0	0.0
7	120.8	14.5	37.0	176.6	0.0	0.0
8	152.7	19.0	49.6	175.3	0.0	0.0
9	199.9	26.9	71.4	172.2	462.4	165.3
10	225.1	31.7	100.3	169.2	561.6	159.4
11	250.2	37.0	126.6	165.4	609.5	149.7
12	267.4	41.0	151.6	161.0	608.2	140.5
13	284.7	45.3	170.9	156.9	551.7	132.2
14	300.2	49.5	187.2	152.8	499.1	125.1
15	321.8	55.8	204.8	147.9	489.9	123.0
16	350.2	65.5	237.8	141.9	522.8	125.2
17	361.8	70.0	273.2	138.3	566.0	129.8
18	373.4	75.1	300.2	137.5	576.1	136.9
19	450.5	122.6 *	599.7	140.8	599.7	140.8
20	527.6	122.6 *	599.7	140.8	599.7	140.8
21	625.3	122.6 *	599.7	140.8	599.7	140.8
22	723.0	122.6 *	599.7	140.8	599.7	140.8
23	903.4	122.6 *	599.7	140.8	599.7	140.8
24	1083.8	122.6 *	599.7	140.8	599.7	140.8
25	1264.9	122.6 *	599.7	140.8	599.7	140.8
26	1445.9	122.6 *	599.7	140.8	599.7	140.8
27	1631.6	122.6 *	599.7	140.8	599.7	140.8
28	1817.2	122.6 *	599.7	140.8	599.7	140.8
29	2007.4	122.6 *	599.7	140.8	599.7	140.8
30	2197.6	122.6 *	599.7	140.8	599.7	140.8
31	2382.9	122.6 *	599.7	140.8	599.7	140.8
32	2568.2	122.6 *	599.7	140.8	599.7	140.8
33	2967.2	122.6 *	599.7	140.8	599.7	140.8

* - INDICATES CLOUD STABILIZATION TIME WAS USED

----- EXHAUST CLOUD -----

CHEMICAL SPECIES = HCL

MET. LAYER NO.	TOP OF LAYER (METERS)		LAYER SOURCE STRENGTH (GRAMS)	CLOUD UPDRAFT VELOCITY (M/S)	CLOUD RADIUS (METERS)	STD. DEVIATION MATERIAL DIST. ALONGWIND (METERS)	CROSSWIND (METERS)
1	16.7		0.00000E+00	9.0	0.0	0.0	0.0
2	31.4		0.00000E+00	9.9	0.0	0.0	0.0
3	43.9		0.00000E+00	9.9	0.0	0.0	0.0
4	56.4		0.00000E+00	9.6	0.0	0.0	0.0
5	72.7		0.00000E+00	9.1	0.0	0.0	0.0
6	89.0		0.00000E+00	8.6	0.0	0.0	0.0
7	120.8		0.00000E+00	7.5	0.0	0.0	0.0
8	152.7		0.00000E+00	6.6	0.0	0.0	0.0
9	199.9		2.25740E+05	5.5	138.1	64.3	64.3
10	225.1		2.92170E+05	5.0	213.8	99.6	99.6
11	250.2		3.94924E+05	4.5	248.5	115.8	115.8
12	267.4		3.23047E+05	4.2	271.5	126.5	126.5
13	284.7		3.60990E+05	3.9	287.0	133.7	133.7
14	300.2		3.54970E+05	3.6	299.5	139.6	139.6
15	321.8		5.34228E+05	3.2	311.5	145.1	145.1
16	350.2		7.57666E+05	2.7	324.2	151.1	151.1
17	361.8		3.24610E+05	2.4	331.8	154.6	154.6
18	373.4		3.31449E+05	2.2	335.3	156.2	156.2
19	450.5	*	2.58344E+06	0.0	342.5	159.6	159.6
20	527.6	*	2.97908E+06	0.0	332.9	155.1	155.1
21	625.3	*	2.91684E+06	0.0	283.7	132.2	132.2
22	723.0	*	1.36187E+06	0.0	132.4	61.7	61.7
23	903.4	*	1.44906E+06	0.0	199.9	93.2	93.2
24	1083.8	*	1.29706E+06	0.0	199.9	93.2	93.2
25	1264.9	*	1.18675E+06	0.0	199.9	93.2	93.2
26	1445.9	*	1.09652E+06	0.0	199.9	93.2	93.2
27	1631.6	*	1.04831E+06	0.0	199.9	93.2	93.2
28	1817.2	*	9.84553E+05	0.0	199.9	93.2	93.2
29	2007.4	*	9.52955E+05	0.0	199.9	93.2	93.2
30	2197.6	*	9.04473E+05	0.0	199.9	93.2	93.2
31	2382.9	*	8.40729E+05	0.0	199.9	93.2	93.2
32	2568.2	*	8.05479E+05	0.0	199.9	93.2	93.2
33	2967.2	*	1.63184E+06	0.0	199.9	93.2	93.2

* - INDICATES CLOUD STABILIZATION TIME WAS USED

----- CLOUD STABILIZATION -----

CALCULATION HEIGHT	(METERS)		0.00
STABILIZATION HEIGHT	(METERS)		424.25
STABILIZATION TIME	(SECS)		122.64
FIRST MIXING LAYER HEIGHT-	(METERS)	TOP =	152.68
		BASE=	0.00
SECOND SELECTED LAYER HEIGHT-	(METERS)	TOP =	2967.20
		BASE=	152.68
SIGMAR(AZ) AT THE SURFACE	(DEGREES)		11.0536
SIGMER(EL) AT THE SURFACE	(DEGREES)		1.2023

MET. LAYER NO.	WIND SPEED (M/SEC)	WIND SPEED SHEAR (M/SEC)	WIND DIRECTION (DEG)	WIND DIRECTION SHEAR (DEG)	SIGMA OF AZI ANG (DEG)	SIGMA OF ELE ANG (DEG)
1	3.09	0.00	357.50	5.00	9.3169	3.4922
2	3.09	0.00	357.50	-5.00	8.8304	7.9312
3	3.09	0.00	354.83	-0.35	11.8804	11.8804
4	3.09	0.00	354.47	-0.35	15.4805	15.4805
5	2.96	-0.26	355.47	2.35	19.6305	19.6305
6	2.70	-0.26	357.83	2.35	24.2902	24.2902
7	2.78	0.41	355.50	-7.00	25.4004	25.4004
8	3.19	0.41	348.50	-7.00	12.6004	12.6004
9	4.09	1.39	344.00	-2.00	1.0000	1.0000
10	5.09	0.62	337.25	-11.50	1.0000	1.0000
11	5.71	0.62	325.75	-11.50	1.0000	1.0000
12	5.75	-0.54	313.98	-12.05	1.0000	1.0000
13	5.21	-0.54	301.92	-12.05	1.0000	1.0000
14	4.71	-0.46	290.45	-10.90	1.0000	1.0000
15	4.73	0.51	287.15	4.30	1.0000	1.0000
16	5.30	0.62	292.15	5.70	1.0000	1.0000
17	5.67	0.13	302.10	14.20	1.0000	1.0000
18	5.80	0.13	316.30	14.20	1.0000	1.0000
19	6.08	0.44	324.72	2.65	1.0000	1.0000
20	6.52	0.44	327.38	2.65	1.0000	1.0000
21	6.78	0.08	329.88	2.35	1.0000	1.0000
22	6.85	0.08	332.22	2.35	1.0000	1.0000
23	6.55	-0.69	335.08	3.35	1.0000	1.0000
24	5.85	-0.69	338.42	3.35	1.0000	1.0000
25	4.91	-1.18	345.55	10.90	1.0000	1.0000
26	3.73	-1.18	356.45	10.90	1.0000	1.0000
27	2.78	-0.72	10.00	16.20	1.0000	1.0000
28	2.06	-0.72	26.20	16.20	1.0000	1.0000
29	1.52	-0.35	16.41	-35.77	1.0000	1.0000
30	1.17	-0.35	340.64	-35.77	1.0000	1.0000

----- CALCULATED METEOROLOGICAL LAYER PARAMETERS -----

MET. LAYER NO.	WIND SPEED (M/SEC)	WIND SPEED SHEAR (M/SEC)	WIND DIRECTION (DEG)	WIND DIRECTION SHEAR (DEG)	SIGMA OF AZI ANG (DEG)	SIGMA OF ELE ANG (DEG)
31	1.30	0.61	304.86	-35.78	1.0000	1.0000
32	1.91	0.61	269.09	-35.77	1.0000	1.0000
33	2.52	0.62	248.30	-5.80	1.0000	1.0000

ALTITUDE RANGE USED IN COMPUTING TRANSITION LAYER AVERAGES
IS 0.0 TO 723.0 METERS.

TRANSITION LAYER NUMBER- 1

VALUE AT	HEIGHT (METERS)	TEMP. (DEG K)	WIND SPEED (M/SEC)	WIND SPEED SHEAR (M/SEC)	WIND DIR. (DEG)	WIND DIR. SHEAR (DEG)	SIGMA AZI. (DEG)	SIGMA ELE. (DEG)
TOP-	152.68	290.80	3.40		345.00		1.0000	1.0000
LAYER-			2.98	0.16	354.42	3.77	16.7745	16.0834
BOTTOM-	0.00	293.83	3.09		355.00		11.0536	1.2023

TRANSITION LAYER NUMBER- 2

VALUE AT	HEIGHT (METERS)	TEMP. (DEG K)	WIND SPEED (M/SEC)	WIND SPEED SHEAR (M/SEC)	WIND DIR. (DEG)	WIND DIR. SHEAR (DEG)	SIGMA AZI. (DEG)	SIGMA ELE. (DEG)
TOP-	2967.20	317.05	2.83		245.40		1.0000	1.0000
LAYER-			5.82	0.76	324.58	8.05	1.0000	1.0000
BOTTOM-	152.68	290.80	3.40		345.00		1.0000	1.0000

1**********

ROCKET EXHAUST EFFLUENT DIFFUSION MODEL REEDM PAGE 9
VERSION 7.07 AT VAFB
OPERATION NUMBER 7788, 1123 PDT 17 MAY 1996
launch time: 1432 PDT 12 MAY 1996
RAWINSONDE ASCENT NUMBER 125, 2117 Z 12 MAY 1996 T +0.0 HR

****

----- MAXIMUM CENTERLINE CALCULATIONS -----

** DECAY COEFFICIENT (1/SEC) = 0.00000E+00 **

CONCENTRATION OF HCL AT A HEIGHT OF 0.0 METERS
DOWNWIND FROM A TITAN IV NORMAL LAUNCH
CALCULATIONS APPLY TO THE LAYER BETWEEN 0.0 AND 152.7 METERS

RANGE FROM PAD (METERS)	BEARING FROM PAD (DEGREES)	PEAK CONCEN-TRATION (PPM)	CLOUD ARRIVAL TIME (MIN)	CLOUD DEPARTURE TIME (MIN)
** NO HCL FOUND **				

----- MAXIMUM CENTERLINE CALCULATIONS -----

** DECAY COEFFICIENT (1/SEC) = 0.00000E+00 **

CONCENTRATION OF HCL AT A HEIGHT OF 0.0 METERS
DOWNWIND FROM A TITAN IV NORMAL LAUNCH
CALCULATIONS APPLY TO THE LAYER BETWEEN 0.0 AND 152.7 METERS

RANGE FROM PAD (METERS)	BEARING FROM PAD (DEGREES)	60.0 MIN. MEAN CONCEN-TRATION (PPM)	CLOUD ARRIVAL TIME (MIN)	CLOUD DEPARTURE TIME (MIN)

** NO HCL FOUND **

Appendix B—Meteorological Data for the #K22 Mission

7) T-ZERO RECONSTRUCTION

$ 05/13/96 16:04:26
2130Z 05 12 96 10

TWR	LVL	HMSL	SPD	DIR	TEMP	RH	TD	SOSD	SOSM	PRESS	SIG-A	SIG-E
300	1	99.0	99.0	99.0	99.0	99.0	99.0	99.0	99.0	999.0	15.4	1.0
300	54	99.0	99.0	99.0	99.0	99.0	99.0	99.0	99.0	999.0	10.4	5.7
300	102	99.0	99.0	99.0	99.0	99.0	99.0	99.0	99.0	999.0	11.1	10.0
300	184	99.0	99.0	99.0	99.0	99.0	99.0	99.0	99.0	999.0	12.4	17.2
300	291	99.0	99.0	99.0	99.0	99.0	99.0	99.0	99.0	999.0	13.2	26.6
300	500	99.0	99.0	99.0	99.0	99.0	99.0	99.0	99.0	999.0	1.0	1.0
300	655	99.0	99.0	99.0	99.0	99.0	99.0	99.0	99.0	999.0	1.0	1.0
300	820	99.0	99.0	99.0	99.0	99.0	99.0	99.0	99.0	999.0	1.0	1.0
300	933	99.0	99.0	99.0	99.0	99.0	99.0	99.0	99.0	999.0	1.0	1.0
300	984	99.0	99.0	99.0	99.0	99.0	99.0	99.0	99.0	999.0	1.0	1.0
300	1055	99.0	99.0	99.0	99.0	99.0	99.0	99.0	99.0	999.0	1.0	1.0
300	1148	99.0	99.0	99.0	99.0	99.0	99.0	99.0	99.0	999.0	1.0	1.0
300	1224	99.0	99.0	99.0	99.0	99.0	99.0	99.0	99.0	999.0	1.0	1.0
300	1730	99.0	99.0	99.0	99.0	99.0	99.0	99.0	99.0	999.0	1.0	1.0
300	2371	99.0	99.0	99.0	99.0	99.0	99.0	99.0	99.0	999.0	1.0	1.0
300	3555	99.0	99.0	99.0	99.0	99.0	99.0	99.0	99.0	999.0	1.0	1.0
300	4743	99.0	99.0	99.0	99.0	99.0	99.0	99.0	99.0	999.0	1.0	1.0
300	5961	99.0	99.0	99.0	99.0	99.0	99.0	99.0	99.0	999.0	1.0	1.0
300	7209	99.0	99.0	99.0	99.0	99.0	99.0	99.0	99.0	999.0	1.0	1.0
300	8425	99.0	99.0	99.0	99.0	99.0	99.0	99.0	99.0	999.0	1.0	1.0
300	9734	99.0	99.0	99.0	99.0	99.0	99.0	99.0	99.0	999.0	1.0	1.0

$ 05/13/96 16:04:31
UNINTERPOLATED DATA

TEST NBR SITE: 1764 OP NO: W7788 ASC NO: 125
1764
BLDG 1764, VANDENBERG AFB, CALIF.
RAWINSONDE MSS/WIN 6.0 4.9 21
2117Z 12 MAY 1996 984.09 0
ASCENT NBR 125

ALT	DIR	SPD	TEMP	DEWPT	PRESS	RH	ABH	DENSITY	IR	SOS	S	I
329.0	355.0	6.0	19.4	10.7	1001.80	57.0	0.0	1192.94	0.0	0.0	1	9
383.0	0.0	6.0	18.7	9.9	999.88	56.7	0.0	1193.32	0.0	0.0	1	0
431.0	355.0	6.0	18.1	9.2	998.17	56.4	0.0	1193.66	0.0	0.0	1	0
513.0	354.3	6.0	17.0	8.0	995.26	56.0	0.0	1194.23	0.0	0.0	1	9
620.0	359.0	5.0	16.7	10.3	991.45	66.0	0.0	1185.93	0.0	0.0	1	9
829.0	345.0	6.6	15.0	9.4	984.09	69.0	0.0	1184.39	0.0	0.0	2	9
984.0	343.0	9.3	15.2	9.8	978.62	70.0	0.0	1176.82	0.0	0.0	2	9
1149.0	320.0	11.7	17.9	9.4	972.89	58.1	0.0	1159.09	0.0	0.0	2	0
1262.0	295.9	9.6	19.8	9.1	968.98	50.0	0.0	1147.11	0.0	0.0	2	9
1313.0	285.0	8.7	21.3	9.9	967.25	48.3	0.0	1138.90	0.0	0.0	2	0
1384.0	289.3	9.7	23.4	11.1	964.84	46.0	0.0	1127.58	0.0	0.0	2	9
1477.0	295.0	10.9	23.9	10.3	961.72	42.5	0.0	1122.33	0.0	0.0	2	0
1553.0	323.4	11.4	24.3	9.7	959.17	39.6	0.0	1118.05	0.0	0.0	4	9
2059.0	328.7	13.1	26.5	6.5	942.50	28.0	0.0	1091.50	0.0	0.0	4	9
2700.0	333.4	13.4	25.8	4.5	921.80	25.3	0.0	1070.51	0.0	0.0	4	9

```
  3884.0 340.1  10.7   23.9    0.7  884.64  21.6 0.0 1034.65 0.0 0.0 4 9
  5072.0   1.9   6.1   20.9   -1.2  848.53  22.7 0.0 1002.79 0.0 0.0 4 9
  6290.0  34.3   3.3   18.1   -1.9  812.72  25.5 0.0  969.74 0.0 0.0 4 9
  7538.0 287.0   0.8   17.1   -8.3  777.33  16.8 0.0  931.52 0.0 0.0 4 9
  8754.0 251.2   4.3   15.2  -10.0  744.18  16.6 0.0  897.79 0.0 0.0 4 9
 10063.0 245.4   5.5   13.7  -11.0  709.86  16.9 0.0  860.90 0.0 0.0 4 9
#EOR
#EOI
```

Appendix C—Description of Sampling Aircraft

Cloud sampling was performed using a Piper Seminole aircraft Model PA-44-180. The following pages present a photo of this model, with performance specification data, downloaded from the New Piper Aircraft Inc. Internet Web page and used by permission. Also presented are sketches of the installation of the Geomet instrument probe. These sketches were prepared to document the external aircraft modifications for FAA approval. Note that the external length of the probe is 18 in. The end of the probe is 6 in. forward of the aircraft's nose, 11.5 in. to the starboard side of the aircraft centerline, and 8 in. from the nearest aircraft surface.

Piper Seminole

Piper Seminole - PA-44-180

Performance Specifications

Engine

Manufacturer: Lycoming
Model: 0-360-A1H6/LO-360-A1H6
Horsepower: 180 hp

Weights

Gross Weight: 3800 lbs/1724 kgs
Standard Empty/Equipped Weight (*b,c): 2586 lbs/1173 kgs
Standard Useful Load (*a): 1230 lbs/558 kgs

Dimensions

Wing Span: 38.6 feet/11.8 meters
Length: 27.6 feet/8.4 meters
Height: 8.5 feet/2.6 meters
Wing Area: 183.8 square feet/17.08 square meters

Fuel Capacity

Usable Fuel: 108 gallons/409 litres

Maximum Speed

TAS at Gross Weight: 168 kts/311 kmh

Cruising Speeds

Normal Cruise Speed: 162 kts/300 kmh

Cruising Range

Cruising Range: 610 nm/1130 km
(45 minute reserves at 75% power)

Stall Speed

Flaps Down Full 40 degrees: IAS 55 kts/IAS 102 kmh

Service Ceiling

Twin Engine (100 fpm): 15,000 feet/4572 meters
Single Engine (50 fpm): 3,800 feet/1158 meters

Take-Off Distance

Total over 50-foot obstacle: 2200 feet/671 meters

Landing Distance

Total over 50-foot obstacle: 1490 feet/454 meters

*a. Standard Useful load is ramp weight minus standard equipped weight.
*b. The standard empty weight and standard equipped weight are the same.
*c. Standard aircraft per marketing.

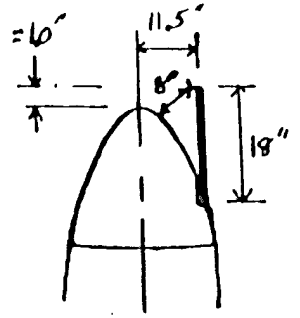

GEOMET .
Probe Location

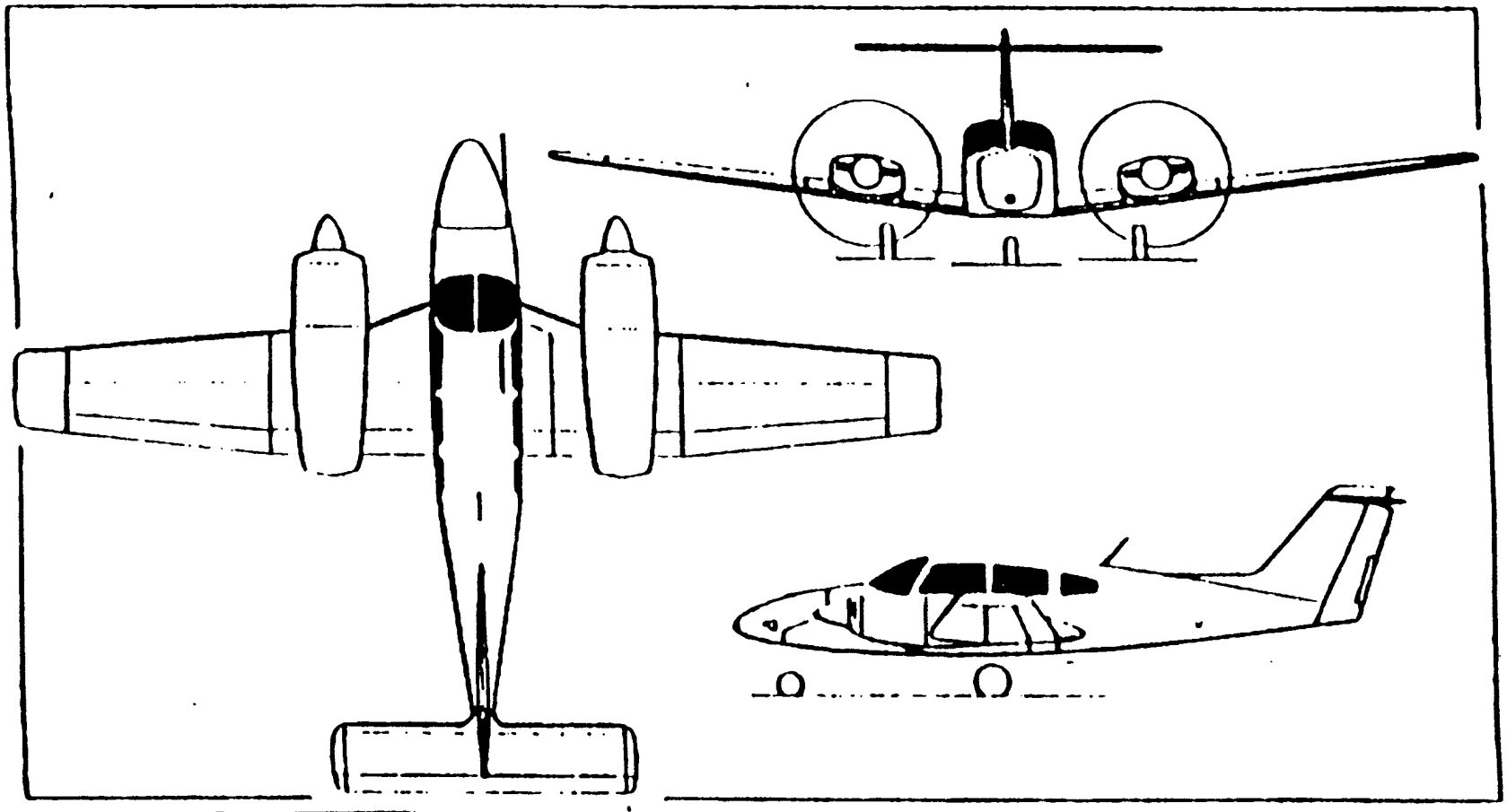

Piper Seminole lightweight twin-engined four-seat cabin monoplane *(Pilot Press)*